AD632126

USAAVLABS TECHNICAL REPORT 66-18

STEADY-STATE THRUST AUGMENTORS AND JET PUMPS

By

Peter R. Payne

March 1966

U. S. ARMY AVIATION MATERIEL LABORATORIES

FORT EUSTIS, VIRGINIA

CONTRACT DA 44-177-AMC-337(T)
PETER R. PAYNE, INC.
ROCKVILLE, MARYLAND

DEPARTMENT OF THE ARMY
U. S. ARMY AVIATION MATERIEL LABORATORIES
FORT EUSTIS. VIRGINIA 23604

This report represents a consolidation of the author's efforts
under various contractual studies in the area of steady-state
augmentors, eductors, and ejectors, and is offered for the
exchange and dissemination of information.

STEADY-STATE THRUST AUGMENTORS

AND JET PUMPS

by

Peter R. Payne

Prepared by

Peter R. Payne, Inc.
12221 Parklawn Drive
Rockville, Maryland

for

U. S. ARMY AVIATION MATERIEL LABORATORIES
FORT EUSTIS, VIRGINIA

ABSTRACT

The state of the art in steady-state augmentors and jet pumps is briefly re-
viewed and a general performance theory developed. Generalized charts are
presented giving the augmentation ratio obtainable from an optimized eductor,
together with the associated geometrical and fluid-dynamic parameters. This
theory is shown to give good agreement with experiment. Experimental mea-
surements made by various investigators in the past do not achieve the pre-
dicted optimum performance, however, because of various deviations from
optimum design in their test eductors.

The performance of eductors in an axial stream and the total head rise obtain-
able through an eductor are both investigated theoretically. The report con-
cludes with a brief survey of various unconventional eductors, including multi-
stage units, Coanda eductors and crypto-steady flow devices.

FOREWORD

The work herein reported was carried out by Peter R. Payne, Inc., Rockville, Maryland, in compliance with U. S. Army Aviation Materiel Laboratories Contract No. DA 44-177-AMC-337(T).

The principal investigator and report author was Mr. Peter R. Payne. Important contributions were made by Messrs. James O. Justice and Alastair Anthony.

CONTENTS

ILLUSTRATIONS

TABLES

SYMBOLS

The prefix Δ denotes an increment of the appropriate quantity. When it prefixes a pressure, it usually denotes that the pressure is "gauge"; that is, the pressure is measured relative to ambient static pressure p_a . For example,

$$\Delta P = P - p_a$$
$$\Delta p = p - p_a$$

Where special symbols are defined and used in only one place in the report, they do not appear in the following list.

A an area

A_j primary jet area

A_2 eductor exit area

b width of a mixing zone

C_f skin friction drag coefficient

C_p static pressure coefficient

     $= \Delta p / \tfrac{1}{2}\rho\, u_0^2$

D_{SF} skin friction drag force

ΔH a total head rise

J_a momentum flux of primary jet when exhausting to ambient

     static pressure

J_0 momentum flux of primary jet

J_2 momentum flux of eductor exhaust

ℓ Prandtl's mixing length

ℓ_m mixing length

$\dot{n}$ air mass flow

$\dot{n}_j$ primary jet mass flow

$\dot{n}_{ja}$ primary jet mass flow exhausting to ambient static pressure

n ratio of secondary to primary air mass flow

p_a ambient static pressure

P a total pressure

$\Delta\bar{p}$ $\Delta p/\tfrac{1}{2}\rho\,u_j^2$, a non-dimensional static pressure

$\Delta\bar{P}$ $\Delta P/\tfrac{1}{2}\rho\,u_j^2$, a non-dimensional total pressure

R universal gas constant

R_e Reynolds number

S_{WET} wetted area

t jet thickness

T thrust force

T total temperature

u a velocity parallel to the x-axis

u_j primary jet velocity

u_{ja} primary jet velocity when exhausting to ambient static pressure

u_n mean velocity at the end of the mixing chamber, assumed

       coincidental with the diffuser throat

u_o free-stream velocity

u_1 velocity of secondary entrained air, before mixing

u_2 average exhaust velocity

v velocity parallel to the y- axis

x horizontal ordinate

y vertical ordinate

ε virtual kinetic viscosity

η eductor efficiency

or η a non-dimensional ordinate ratio

η_D diffuser efficiency

μ coefficient of fluid viscosity

ν kinematic viscosity

ξ ratio of total head recovery in a recirculating eductor

ρ mass density of the fluid

ρ_o mass density of the free-stream

ϕ thrust augmentation ratio

INTRODUCTION

This re, rt is concerned with reviewing the state of the art in jet augmentation. An augmentor is broadly defined as a device which in some way augments a jet – usually referred to as the primary jet – by allowing ambient fluid to mix with it to achieve a desired result. Since there appears to be no universally accepted terminology, the following definitions are used in this report.

Eductor (or occasionally, Inductor)

A generic term describing devices in which a primary fluid or gaseous jet gives up energy to a secondary flow. The exit flow thus has a lower velocity than the primary jet, but the mass flow is increased. The primary and secondary fluids are not necessarily the same.

Injector (for which an alternative is Jet Pump)

An injector is an eductor used to pump fluid against a back-pressure, such as feed water to a steam boiler, for example, or air into the plenum chamber of a GEM. An injector generally has a larger diffuser area ratio than the equivalent thrust augmentor of the same mass flow ratio.

Augmentor

A thrust augmentor is an eductor which is optimized for maximum thrust increase; a mass flow augmentor is designed for maximum mass flow increase. In practice there is little difference between the two.

Ejector

An ejector may be defined as an eductor which exhausts air to ambient from a region of lower pressure, as in "pumping out" a vacuum chamber, for example. Although closely analogous to an injector, it has significant geometrical differences if the mixing section pressure is very low.

The basic geometry common to all such devices is shown in Figure 1.
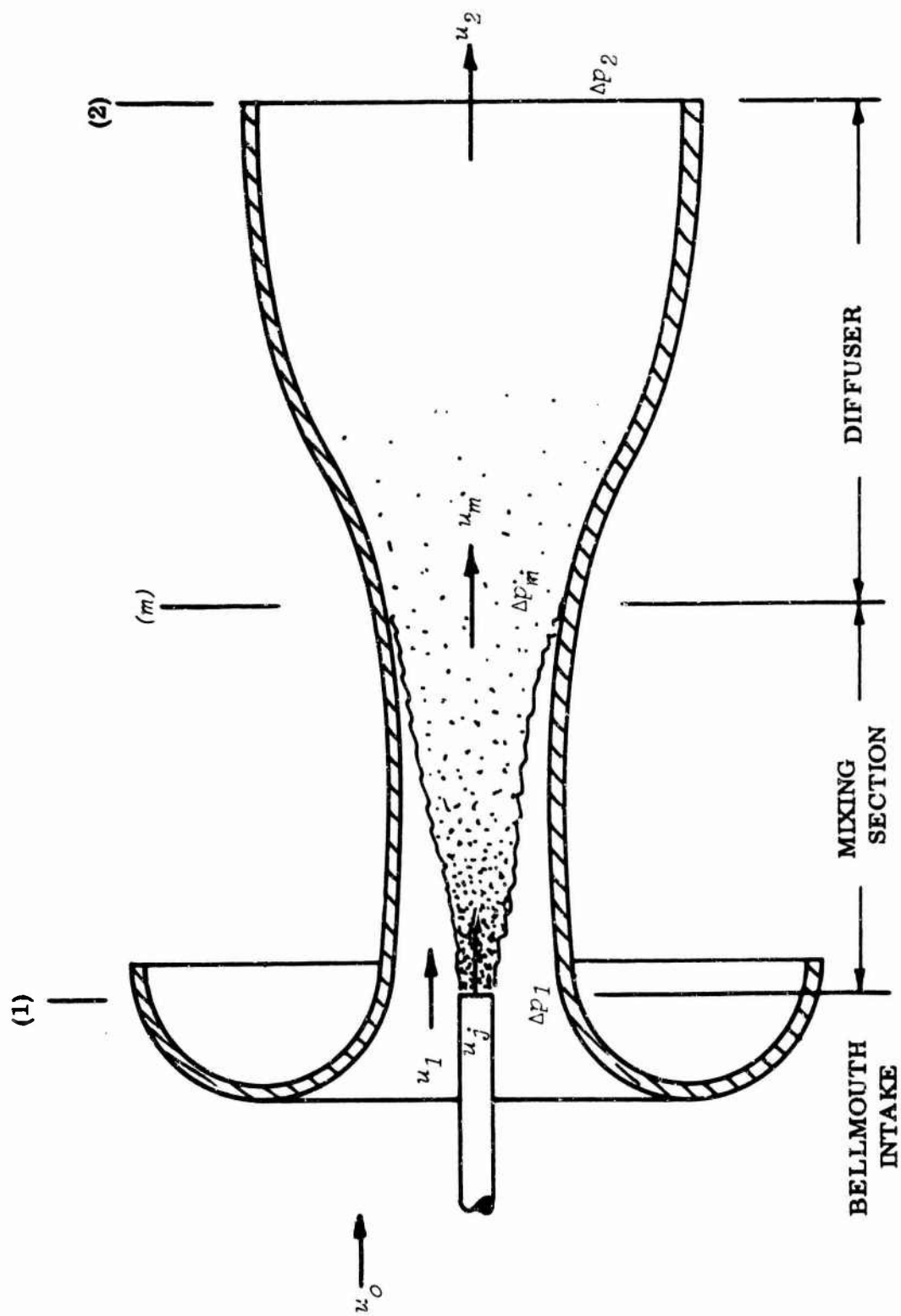
Figure 1.   Geometry of a Typical Eductor.

In its most commonly used application, an eductor augments the mass flow of a jet in order to increase its thrust. In this application it functions as a "transformer," in exactly the same way as a pressure jet helicopter rotor, for example, transforms the high energy, low mass flow gas energy from a turbine exhaust to a high mass flow, low energy flow through the rotor.

The eductor stands alone among other gas energy transformers in that it requires no moving parts to "transform" high pressure, low mass flow gas energy to a low pressure, high mass flow. This advantage is potentially of great importance. Unfortunately, as shown in Figure 2, the "transformer efficiency" of existing eductors is very low indeed, and it more than offsets their savings in weight and mechanical complexity. But, if by properly conducted research the ability to reliably predict eductor performance can be achieved, it may be possible to discover ways of upgrading the overall efficiency to the point where eductors are competitive for many applications.
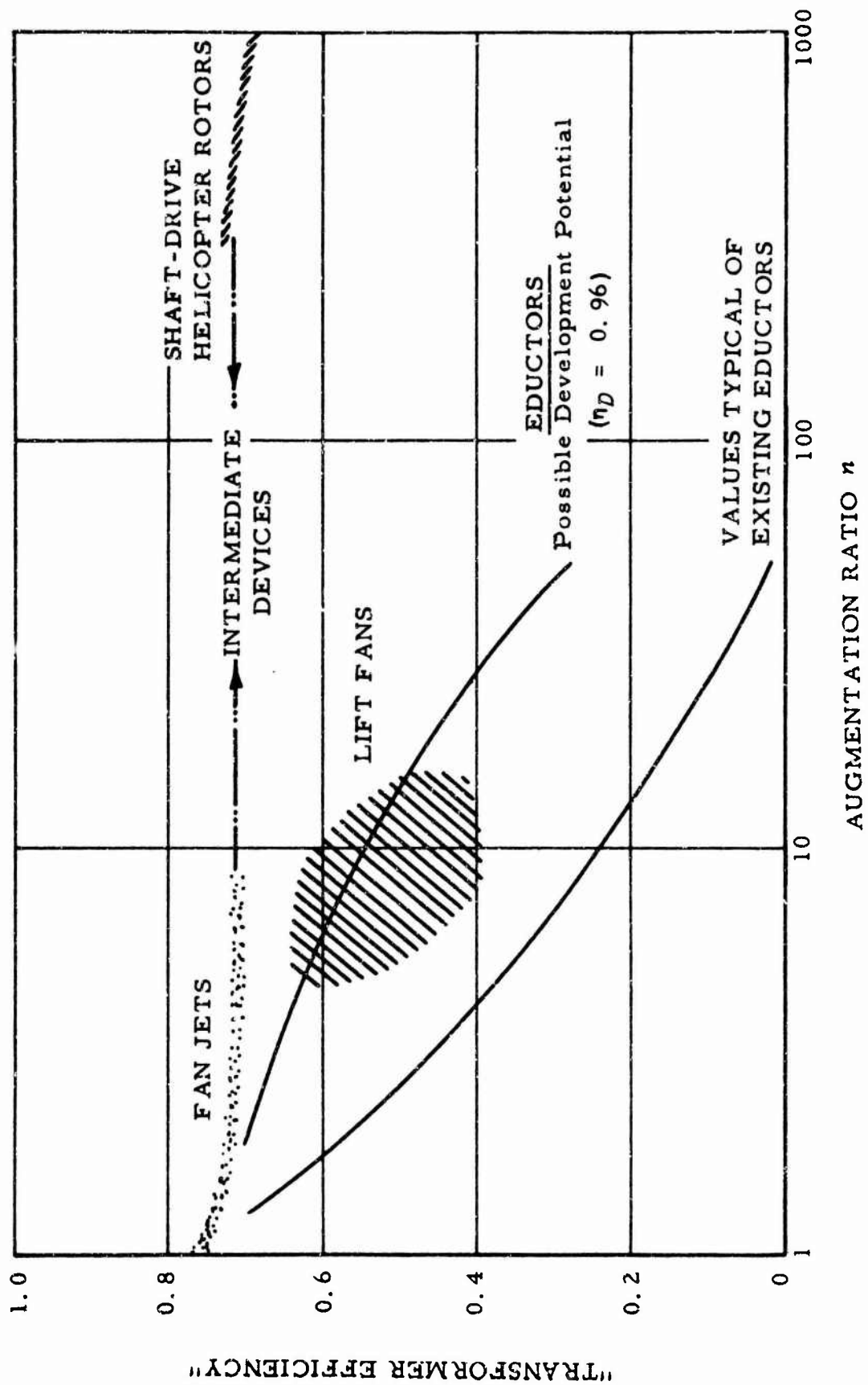
Figure 2. The Efficiency of a Static Eductor in Comparison With Some Alternative Methods of Transforming Gas Energy into Static Thrust.

4

Chapter 1

A BRIEF REVIEW OF THE LITERATURE

The eductor principle has been employed perhaps longer than can be traced, and has certainly occupied the attention of many modern engineers and inventors. Timothy Hackworth and George Stevenson employed eductors to obtain a forced draft, giving more efficient combustion in early railway locomotives, circa 1830. This led naturally to steam-powered water jet pumps for the purposes of re-charging boilers under pressure and to the fairly extensive employment of the eductor principle through the field of mechanical engineering.

Naturally enough, these early developments were based on "cut and try" techniques. Efficiencies were very low. Even today, "Marks Handbook," a universally recognized reference for the mechanical engineer, says "... the external work is usually about two percent of the heat given up by the steam."

Early attempts at analysis were based upon the energy equation. Flugel (Reference 1) summarizes much of this early work, in addition to making a considerable number of original and valuable contributions. In particular he identified the fact that there is an "optimum" mixing pressure, and drew attention to the fact that the mixing section cannot be accurately designed by means of one-dimensional flow theory. To quote Reference 1:

"The greatest drawback of the energy equation is that the assumption of complete intermingling of driving fluid and delivered fluid at constant pressure p_1 is utterly incorrect, resulting from the fact that the narrowest section of the mixing nozzle must be designed from the 'theoretically' narrowest section. In consequence, the calculation method does not give the correct information about the most important section of a jet pump and no data whatsoever regarding the necessary length ratios.

"Practice proves that, under normal operating conditions, the intermingling is practically always accompanied by a pressure rise*, so that at the end of the mixing nozzle usually a substantial or even a major part of the pressure rise will already have been achieved. This fact gives consideration to the subsequent method largely evolved from the impulse theorem according to which, first of all, a length for the mixing nozzle is assumed necessary to assure adequate mixing. The assumption of constant pressure p_1 during mixing can be

---

* That is, when the mixing takes place in a constant area duct.

5

dropped again later. The mixing advances in the narrowest section of the mixing nozzle under a pressure rise until a practically perfect intermingling has been achieved at the end of the narrowest section. This part of the pressure rise is readily computed according to impulse theorem. It is clear and closely according to practice that with the comparative slowness of the mixing process the length L of the narrowest section obviously must be fairly great in order to assure adequate mixing (which, in turn, is the premise for achieving proper energy conversion in the adjoining diffuser); it is therefore recommended that $L = 10\,d$. It may be stated that very favorable results have already been achieved with jet pumps computed on this basis, which are also in good agreement with the preliminary calculation, as will be reported elsewhere."

Flugel's work is apparently not too well known, despite the fact that it is a very exhaustive study, and illuminates a number of problem areas which have troubled subsequent investigators.

The first American workers to develop a theoretical treatment of eductors were McClintock and Hood (Reference 3). Starting from essentially the same assumptions as the theory of the present report, they obtained an equation for thrust augmentation ratio which is

$$J_2/J_0 = (1 + n)^2/(A_2/A_j) \tag{1}$$

for one-dimensional flow, with equal primary and secondary densities. This is merely another way of writing Newton's second law, of course, since

$$J_2/J_0 = \frac{\text{total momentum flux out of eductor}}{\text{momentum flux of primary jet}} = u_2 \dot{m}_j (1 + n)/ u_j \dot{m}_j$$

and $\quad u_n = \dot{m}_n/\rho A_n$.

Thus, in the McClintock and Hood analysis, a solution must be found by obtaining a relationship between the entrainment ratio (n) and the geometrical properties of the eductor. This was done by introducing an empirical constant which was determined from eductor tests. Additionally, the augmentation equation was multiplied by an empirical "thrust coefficient," nominally intended to allow for deviations from one-dimensional flow. The disadvantage of introducing some empiricisms into a theory is obvious. It is as well to note that McClintock

6

and Hood were concerned primarily with the use of eductors to promote piston engine cooling.

Shortly after the advent of the jet engine, several theoretical and experimental studies of very low entrainment ratio "ejectors" were made (References 4 and 5). This stemmed from the need to cool the inside of jet engine nacelles. Obviously the jet engine exhaust provided a convenient means of doing so. The results of these investigations are of little value in the broader context of high entrainment ratio eductors intended to give augmentation, however.

In 1949, von Karman (Reference 6) treated the case of a loss-free eductor with a parallel wall. For area ratios $A/A_j > 15$ and one-dimensional flow, his results are given by the approximate equations

$$u_2/u_j = (A_j/A)^{\frac{1}{2}} - A_j/A \tag{2}$$

$$J_2/J_O = (1 + A/A_j)\left((A_j/A)^{\frac{1}{2}} - A_j/A\right)^2 . \tag{3}$$

Von Karman pointed out that this implied $J_2/J_O < 2.0$, always, so long as the flow was one-dimensional. This of course applies only to constant diameter eductors, higher values being obtainable when a diffuser follows the mixing section.

He also pointed out that non-uniform inlet flow could result in greater augmentation, an observation already implied by the work of McClintock and Hood. This important observation does not seem to have been pursued by subsequent workers.

Von Karman's analysis applies only to rectilinear flow, because Bernoulli's equation is used to relate local speed to local static pressure. It is not easy to see how a non-uniform rectilinear flow could be developed without total pressure loss. This may be the reason for the apparent neglect of his suggestion. Nevertheless, a more thorough analysis of this aspect appears well worthwhile.

It is of interest to note that augmentation ratios greater than the theoretical value of 2.0 were achieved experimentally by Payne (Reference 11) in 1954, using constant diameter ducts.

A number of the larger aerospace companies have conducted experimental studies since the publication of these and other early theoretical studies. Generally

speaking, they made no effort to extend, or even consolidate, the theory, but concentrated on experimental measurements. As might be expected, the results obtained with the relatively large and sophisticated test rigs were no better than the results obtained in small-scale laboratory tests by other experimenters. From hindsight it is easy to identify where deviations from optimum design occurred in these large-scale programs. In the absence of adequate theoretical work, however, it was obviously difficult for the investigators to avoid these deviations at the time they were conducting their programs.

In 1955, Szczeniowski (Reference 12) published a one-dimensional flow analysis of the eductor. He considered a quite general case of varying mixing chamber geometry, using the solutions for constant pressure and constant area mixing as particular solutions of the general case. He discussed the mathematical problem of determining the optimum static pressure distribution along the mixing chamber without reaching any firm conclusions. No absolute optimum exists, but some pressure distributions are better than others.

Szczeniowski's analysis did not include the effects of internal duct losses, which subsequent research has shown to be of dominating importance.

An important program of research was carried out by Helmbold (References 9 and 13) during 1953 and 1954, in which he studied various aspects of the eductor cycle. Of particular interest was his design of a constant static pressure mixing section, which gave 31 percent greater overall efficiency than an equivalent cylindrical mixing chamber. This is in good agreement with Helmbold's theoretical predictions. It would appear that the design and incorporation of a constant static pressure mixing section in the XV-4A research aircraft eductor would have provided worthwhile gains in the system.

Recently, Hill (Reference 56) effected a major consolidation of the theoretical aspects of the mixing chamber phenomena. This work may be represented as a major step toward the goal of a consistently reliable predictive ability.

Wells (Reference 15) advanced Helmbold's constant mixing pressure chamber work a step further by modifying it to maintain a favorable static pressure gradient as far as possible, and hence to reduce skin friction by increasing the length of the laminar boundary layer. He also applied boundary layer control, in the form of blowing from a slot, at the diffuser throat. Although exact comparison with Helmbold's experiments is difficult, there seems little doubt that these innovations resulted in a further improvement in efficiency.

Although this brief review of the literature is by no means exhaustive, it seems clear that a great deal of research work remains to be done before either adequate predictive ability is achieved or maximum theoretical efficiency can be approached in new designs. It seems equally clear that hardware applications of the eductor principle have not profited to the extent made possible by existing research work. Further significant improvements can be made, provided experiment and theory are allowed to develop side by side in the laboratory.

SIMPLE PERFORMANCE RELATIONSHIPS FOR A PROPULSOR
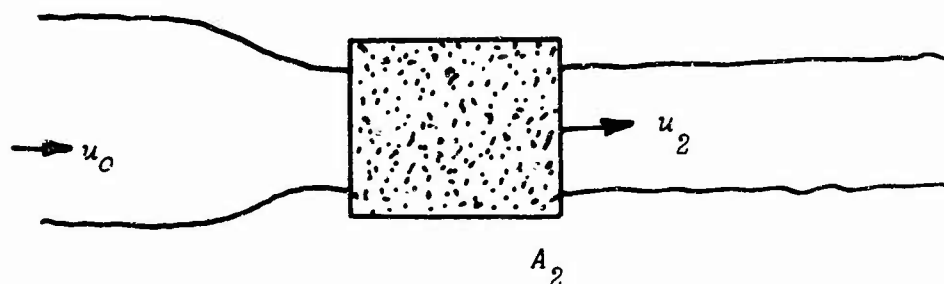
Figure 3.   A Generalized Propulsor.

IDEAL PROPULSIVE EFFICIENCY DEPENDS ONLY ON THE JET VELOCITY

Consider the generalized propulsor in Figure 3, which accelerates ambient fluid from a free-stream velocity u_0 to a final velocity of u_2. The temperature of the downstream jet is not necessarily ambient, so that the efflux density $\rho_2 \neq \rho_0$.

The exit mass flow is ($\rho_2 A_2 u_2$), so that its kinetic energy power is

$$\tfrac{1}{2}(\rho_2 A_2 u_2)\, u_2^2 . \tag{4}$$

Since the fluid originally had some kinetic energy before entering the propulsor, the amount of energy added by the propulsor is

$$\Delta P_j = \tfrac{1}{2}(\rho_2 A_2 u_2)\, (u_2^2 - u_o^2) . \tag{5}$$

10

The developed thrust (T) is equal to the rate of change of momentum. Thus, in unaccelerated motion,

$$T = (\rho_2 A_2 u_2) \ (u_2 - u_o) \ . \tag{6}$$

The ideal efficiency is defined as the ratio of useful propulsive power to the power lost in the jet. That is,

$$\eta_i = T u_o / \Delta P_j = 2 u_o (u_2 - u_o) \ / \ (u_2^2 - u_o^2)$$

$$= \ 2/ \ 1 + (u_2/u_o) \ . \tag{7}$$

Thus, the ideal efficiency is a function only of the velocity ratio u_2/u_o, and has a maximum of unity when $u_2 = u_o$, the zero thrust condition. The temperature of the propulsor efflux, which would cause a change in density of the fluid, has no influence upon the efficiency.

THE RELATIONSHIP BETWEEN THRUST AND TOTAL HEAD INCREASE IN
THE WORKING FLUID

From Figure 3, the total head of the working fluid is increased by

$$\Delta H = \tfrac{1}{2} \rho_2 u_2^2 - \tfrac{1}{2} \rho_o u_o^2$$

as it passes through the propulsor. Using this relationship to define u_2 in terms of u_o and ΔH , the thrust equation becomes

$$T/\rho_o u_o^2 A_2 = \left(1 + \Delta H / \tfrac{1}{2} \rho_o u_o^2 \right) \ (1 - u_o/u_2) \ . \tag{8}$$

Writing $\Delta \hat{H} = \Delta H / \tfrac{1}{2} \rho u_o^2$ also gives

11

$$\Delta \hat{H} = \rho_2/\rho_0 \ (u_2/u_0)^2 - 1 \ ;$$

therefore,

$$T/\rho_0 u_0^2 A_2 = (1 + \Delta \hat{H}) - (\rho_2/\rho_0)^{\frac{1}{2}} (1 + \Delta \hat{H})^{\frac{1}{2}} \ . \tag{9}$$

For the <u>static case</u> ($u_0 = 0$), this reduces to

$$T = 2\Delta H \ A_2 \quad . \tag{10}$$

That is to say, changes in density of the working fluid do not influence the result, but only the total head rise. For <u>a propeller</u>, where $A_2 = \frac{1}{2}\pi R^2$ under static conditions ,

$$T = \Delta H. \ \pi R^2 \ , \tag{11}$$

a result which is already familiar. The ramjet, on the other hand, is a device which cannot increase total head, but must obtain thrust by reducing the density of the efflux by addition of heat in the case of an air ramjet, and by introducing gas bubbles into a water ramjet. In the ideal (loss free) case, where $\Delta H = 0$, the thrust is then given by

$$T/\rho u_0^2 A_2 = 1 - (\rho_2/\rho_0)^{\frac{1}{2}} \ . \tag{12}$$

The eductor normally operates under static ($u_0 = 0$) conditions, so that attention can be focused on its ability to raise the total head of the entrained fluid. The temperature of the primary jet is therefore unimportant.

When the <u>eductor</u> is moving through a fluid, however, a hot primary jet could result in an advantageous increase in efficiency, since it would result in $\rho_2 < \rho_0$.

12

Chapter 3

VISCOUS MIXING

Viscosity is a measure of a fluid's capacity to carry a shear stress. When the stress is low, most fluids react in a "Newtonian" manner, where shear stress varies linearly with strain, the relationship being

$$\tau = \mu \ \partial u / \partial y , \tag{13}$$

or (stress) = (coefficient of viscosity) x (velocity gradient).

When the velocity gradient exceeds a certain critical value usually defined in terms of a "critical Reynolds number," the fluid no longer supports shear stress in a laminar manner. Instead, the smooth flow breaks up into eddies and vortices, giving what is loosely referred to as turbulent flow. It seems likely that the size of these apparently random eddies decreases with increasing Reynolds number, but the whole picture is still very poorly understood.

The concept of an "effective viscosity coefficient" is still useful when the flow is turbulent. Its value is much greater than the laminar value (μ) for the same fluid, and currently there are only empirical expressions for the effective turbulent flow viscosity, which differ widely in their macroscopic detail. The earliest of these was Prandtl's "mixing length" hypothesis,

$$\tau = \rho \ell^2 |\partial u / \partial y| (\partial u / \partial y) , \tag{14}$$

ℓ being the "mixing length" and ρ the fluid mass density. In the free turbulent shear flow characteristic of a jet or wake, it is usual to assume

$$\ell = cx^m , \tag{15}$$

where c is an empirical constant that is obtained from experimental data, and the exponent (m) is evaluated from the appropriate requirements (usually "similarity" requirements) of the particular problem. (Taylor's "vorticity transport model," of more recent date, also leads to Equation 14.)

13

Equation (14) can be criticized on a number of grounds, and later workers have developed alternative formulations; notably the following:

The "Virtual Kinetic Viscosity ε "

$$\tau = \rho\varepsilon \ \partial u/\partial y \quad (\varepsilon = \text{const.}) \ . \tag{16}$$

The "Constant Shear Coefficient" Model of Prandtl

$$\tau = \rho\varepsilon \ \partial u/\partial y$$

$$\varepsilon = kb(u_{max} - u_{min}) , \tag{17}$$

where k = an empirical constant obtained from experiment, and b is the width of the mixing zone.

Von Karman's "Similarity" Hypothesis gives

$$\tau = \rho k^2 (\partial u/\partial y)^3 |\partial u/\partial y|/(\partial^2 u/\partial y^2)^2 , \tag{18}$$

and finally, the "intermittency model" of Townsend, in which Equation (16) is multiplied by an intermittency factor

$$\gamma(y) = (1/(2\pi)^{\frac{1}{2}}) \int_{y/a-s}^{\infty} e^{-\frac{1}{2}u^2} \ du , \tag{19}$$

(a) and (s) being empirical constants.

Despite this wide range of hypotheses (and there are several more), all give about the same velocity distribution when used to solve viscous mixing problems.

SOME PRACTICAL ASPECTS OF VISCOSITY

Because of viscosity, a true velocity discontinuity can never exist between two streams of fluid. As soon as an air jet emerges from a nozzle, for example, it

14

starts to carry along with it some of the previously stationary atmospheric air, and in the process of accelerating this "entrained" air, gives up some of its own momentum. For this reason,the velocity profile of a jet changes rapidly as it travels downstream from its nozzle, and accelerates progressively more and more of the free air around it, until it soon loses all resemblance to a discrete jet.

Also, since the free air in the immediate vicinity is accelerating to move with the jet, the pressure distribution over any solid bodies near the jet will be modified by the secondary airflow, the results of which may be beneficial or adverse, depending on the nature of the problem.

The best known example of this effect is the "mixing drag" experienced by a jet engine in an aircraft. Since the free air is accelerated by the jet, an area of suction is generated over the rear portions of the nacelle. The forces caused by this suction are inclined backwards because of the shape of the nacelle and their horizontal component constitutes a drag which reduces the total thrust of the engine-nacelle combination. In this case the mixing drag forces are usually quite small, amounting to perhaps 1 percent or 2 percent of the engine thrust. However, it is easy to see that in the case of a long two-dimensional jet whose periphery might be ten times the periphery of the equivalent circular jet, the jet drag could amount to 10 - 20 percent of the total jet momentum flux under the same geometrical and flow conditions. Clearly, this would have a large effect upon the determination of optimum jet thickness, and a significant effect upon the calculated performance of an aircraft which used a jet flap for propulsion, or on the performance of an annular jet GEM.

Kuchemann (Reference 83) has observed that the static pressure in the region of a nacelle nozzle exit is given by the empirical equation

$$C_p = -0.01 \left[(u_j/u_o) - 1 \right] , \tag{20}$$

where u_o is the free stream velocity and u_j is the jet velocity.

This result is based upon experimental observations made with a finite free-stream velocity u_o, and cannot, of course, be applied to the static case of $u_o = 0$.

In Reference 51, Payne was able to derive this result theoretically for the two-dimensional case, using the familiar analysis for potential flow constrained by an obtuse angle, as shown in Figure 4.

15

The analogy with an inviscid jet issuing from a body is obvious from Figure 4(a). When entrainment occurs, some of the free-stream air enters the jet, so that the angle through which it is turned at the trailing edge is a little less, by the amount δ as noted below.

(a) Inviscid Flow.   (b) With Jet Entrainment.
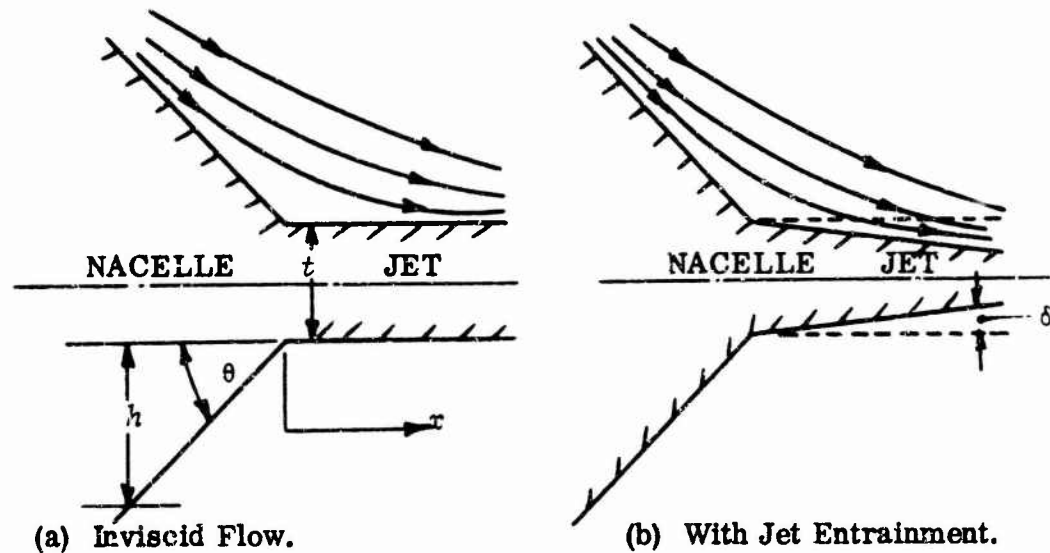
Figure 4.   A Potential Flow Model of Jet Entrainment.

It is easy to show that

$$\delta = \left(\partial n / \partial (x/t) \right) u_j, \tag{21}$$

where $n = \dfrac{\text{entrained air mass flow}}{\text{jet mass flow}}$.

From this, it follows that the pressure decrement over the rear of the body is

$$C_p = -K\left((u_j/u_0) - 1 \right), \tag{22}$$

where $K = .08/\pi\left(1 + (\theta/\pi) \right)^2$ if $\partial n/\partial (x/t) = .08$.

For $\theta =$ 0° 20° 40° 60°

      $K =$ $.0254$ $.0206$ $.0170$ $.0143$.

16

Kuchemann's experimental observation of $K = .01$ was for axisymmetric flow, whereas the above values are for two-dimensional flow, which is bound to give somewhat higher suction. Thus, the theoretical result can be considered reasonable, without including boundary layer effects. Also, since it is based on the Rouse et al (Reference 37) measurement of $\partial n/\partial (x/t)=.08$, which strictly applies only at $\theta = 90^{O}$, the theoretical result probably has errors attributable to the change of the mixing derivative with wall angle.

A more dramatic example of the potentially large effect due to mixing occurs when a jet issues from a bluff body, as illustrated in Figure 5.
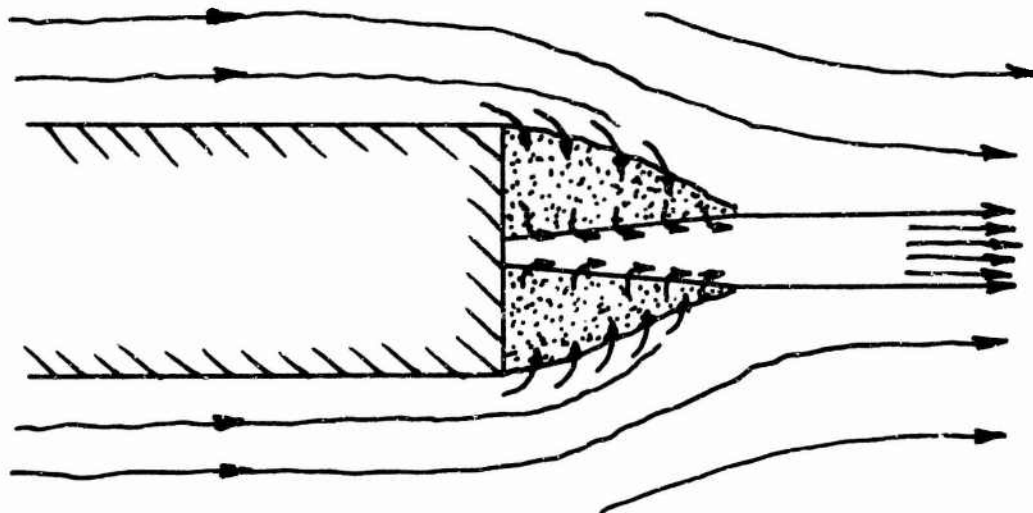
Figure 5. Jet Issuing From the Stern of a Bluff Body.

In Reference 30, Payre and Anthony show, both theoretically and experimentally, that viscous mixing effects in this case are so large that the drag coefficient of the body is increased by several hundred percent when the jet is operating. Viewed alternatively, half the jet thrust is lost.

Another effect of mixing, and in some ways the most important, is the effect which it has on the jet. Until the advent of jet flaps and ground effect machines, aerodynamics was primarily concerned with the reaction force obtained from a jet, or its momentum flux, neither of which was significantly influenced by mixing. In fact, one of the fundamental theorems of mixing is that momentum is conserved if the process takes place at constant pressure. Total pressure is not conserved, however, so that when we are concerned with jet characteristics some way downstream of its nozzle, the conditions bear little relationship to the same problem in inviscid flow.

This observation leads to a further aspect of viscous mixing: the apparent "skin friction" loss involved in fluid shear.

Skin friction results in a drag force which is defined as

$$D_{SF} = C_f \cdot \tfrac{1}{2}\rho u_O^2 \, S_{WET} ,$$ (23)

a typical value for C_f being $.005$, for a smooth solid surface in air, although it varies with Reynolds number, of course.

We can obtain an equivalent value for C_f when air flows into contact with an air surface (Figure 6) rather than a solid surface. At constant static pressure, the total momentum flux will be constant. That is,

$$\int_O^\infty \rho u_1^2 \, dy \; + \; \int_{-\infty}^O \rho u_O^2 \, dy \; = \; \int_{-\infty}^{+\infty} \rho u^2 dy$$ (24)
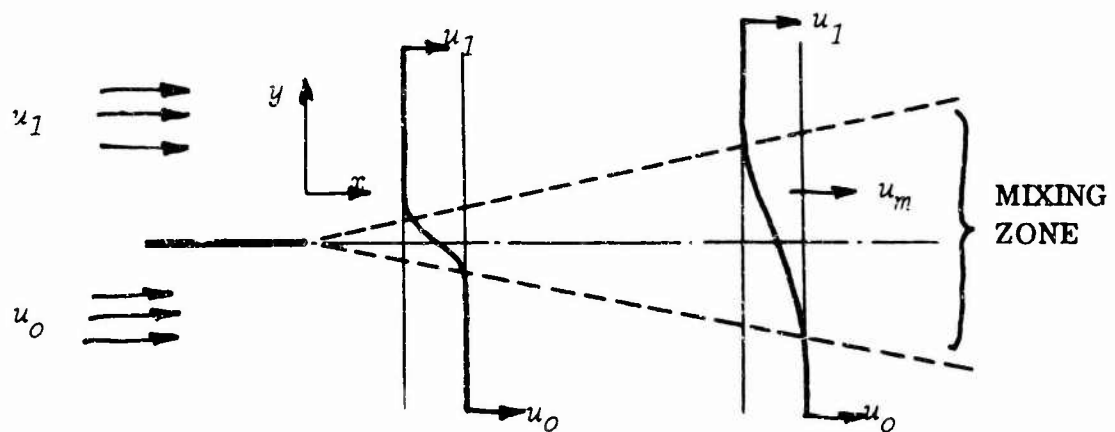
Figure 6. Velocity Shear at the Edge of a Jet.

18

The faster stream of air has given up energy in order to achieve this result, however.

For convenience, and because it greatly simplifies the equations, a one-dimensional analysis is used to determine the value of C_f . If the faster stream of air is regarded as a two-dimensional jet of thickness t , and if we define a ratio

$$n = \frac{\text{entrained air mass flow}}{\text{initial jet mass flow}} , \tag{25}$$

then the air mass in the mixing zone is

$$(n + 1) \, \dot{m}_o \ .$$

For conservation of momentum

$$\dot{m}_o u_o + n \dot{m}_o u_1 = \dot{m}_o \, (n+1) \, u_m \ ,$$
$$u_m = (u_o + n u_1)/(n + 1) \ . \tag{26}$$

The loss of momentum in the original jet air mass flow is

$$D_{SF} = \dot{m}_o u_o - \dot{m}_o u_m \ ;$$

therefore,

$$C_f = 2 \ (t/x) \ \left(n/(n+1) \right) \left(1 - (u_1/u_o) \right) \ . \tag{27}$$

For a two-dimensional jet, in the zone of flow establishment (Reference 37 for example),

$$n = \partial n/\partial (x/t) \ . \ x/t \ ;$$

therefore,

$$C_f = 2 \left(\partial n/\partial (x/t) \right) \ . \ \left(1 - (u_1/u_o) \right) / \left(1 + (x/t) \left(\partial n/\partial (x/t) \right) \right) \ . \tag{28}$$

19

Rouse et al (Reference 37) measurements, modified (Reference 51) for velocity, give

$$\partial n / \partial (x/t) = .08 \left[1 - (u_1/u_o) \right] ;$$

therefore,

$$C_f \approx 0.16 \qquad \text{based on relative velocity} \quad ,$$

or approximately thirty times as great as the value of .005 obtained for air flowing over a smooth, solid boundary.

This result is significant and one which is often not sufficiently appreciated by engineers, perhaps.

TRANSFER OF POWER BY VISCOUS MIXING
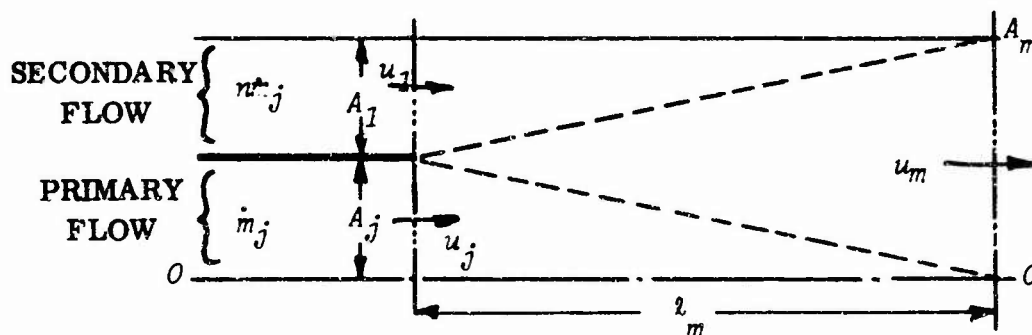
Figure 7.   Basic Geometry for Calculating Power
Transfer Between Two Streams.

To study power transfer from a primary to a secondary flow, the imaginary line O - O is drawn along a jet streamline, as shown in Figure 7. Thus, no flow crosses this line. From Equation (26), for constant static pressure Δp_1,

$$u_m/u_j = \left(1 + n \ (u_1/u_j) \right) / (n+1) = \left(1 + n^2 \ (A_j/A_1) \right) / (n+1)) \qquad . \tag{29}$$

If ΔH is the total pressure rise which occurs in the secondary flow, the power added to it is

$$n\dot{m}_j \, \Delta H / \rho \quad . \tag{30}$$

For constant static pressure,

$$\Delta H_1 = \left(\tfrac{1}{2}\rho u_j^2 / (n+1)^2 \right)\left(1 - (u_1/u_j) \right) \left\{ 1 + (u_1/u_j) \{ 1 + 2n \} \right\} \quad . \tag{31}$$

Thus, the secondary flow power increase is

$$\Delta P_1 = \left(\tfrac{1}{2}n\dot{m}_j u_j^2 / (n+1)^2 \right)\left(1 - (u_1/u_j) \right) \left(1 + (u_1/u_j) \{ 1 + 2n \} \right) \quad . \tag{32}$$

The total pressure <u>drop</u> in the primary is

$$\Delta H_j = \tfrac{1}{2}\rho u_j^2 \left(1 - (u_m/u_j)^2 \right)$$

$$= \left(\tfrac{1}{2}\rho u_j^2 / (n+1)^2 \right) n \left(1 - (u_1/u_j) \right)\left(1 + (u_1/u_j) \{ 1 + 2n \} \right) \quad . \tag{33}$$

The power lost by the primary fluid is therefore

$$\Delta P_j = \left(\tfrac{1}{2}\dot{m}_j u_j^2 / (n+1)^2 \right) n \left(1 - (u_1/u_j) \right) \left(n\{ 1 + (u_1/u_j) \} + 2 \right) \quad . \tag{34}$$

Thus, the efficiency of power transfer is obtained by dividing Equation (34) into Equation (32). That is,

$$\eta = \left(1 + (u_1/u_j)\{ 1 + 2n \} \right) / \left(2 + n \{ 1 + (u_1/u_j) \} \right) \quad . \tag{35}$$

21

The entrainment ratio n is defined by the mixing length ℓ_m. For the two-dimensional case, from Reference 37, in the zone of flow establishment,

$$n = (.08\ell_m/t_j)(1-(u_1/u_j)) \quad . \tag{36}$$

Equations (35) and (36) permit the efficiency of power transference to be plotted as a function of u_1/u_j and ℓ_m/t_j. The secondary air-mass flow is $n\dot{m}_j$, of course, and the total secondary flow power is given by Equation (32). More conveniently, writing

$$\dot{m}_j = \rho A_j u_j = \rho b t u_j \quad ,$$

$$P_j/\ell_m b\rho u_j^3 = (.04\{1-(u_1/u_j)\}^2/(n+1)^2)\left(1+(u_1/u_j)(1+2n)\right) , \tag{37}$$

where b is the width of the mixing zone normal to the plane of the paper.

The ratio ℓ_m/t_j is a fixed quantity. From Reference 37, an average value is

$$\ell_m/t_j = 5.2 \times 2 = 10.4 \quad .$$

Thus, all the important variables are a function of u_1/u_j only.

The specific mass flow is obtained from the relationship

$$n\dot{m}_j/\ell_m b\rho u_j = .08\left(1-(u_1/u_j)\right) \quad . \tag{38}$$

Efficiency is plotted in Figure 8 and the specific power loading in Figure 9. Even at low values of the velocity ratio u_1/u_j, the efficiency of the transfer process is quite reasonable. It is evident that an explanation of the very low efficiencies currently measured for eductors must be sought elsewhere.
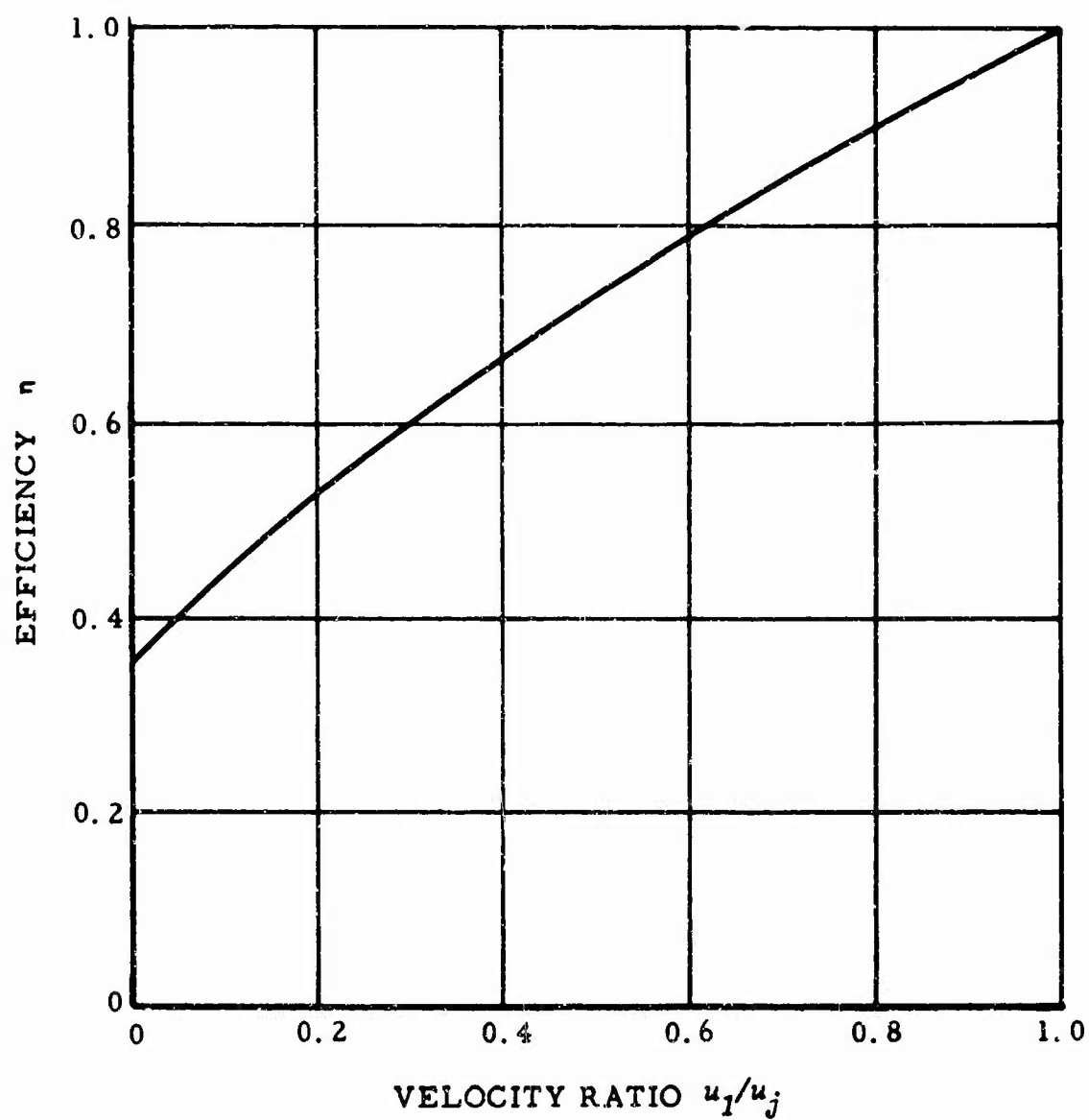
Figure 8. Efficiency of Power Transference
Through Mixing (Equation 35).

23
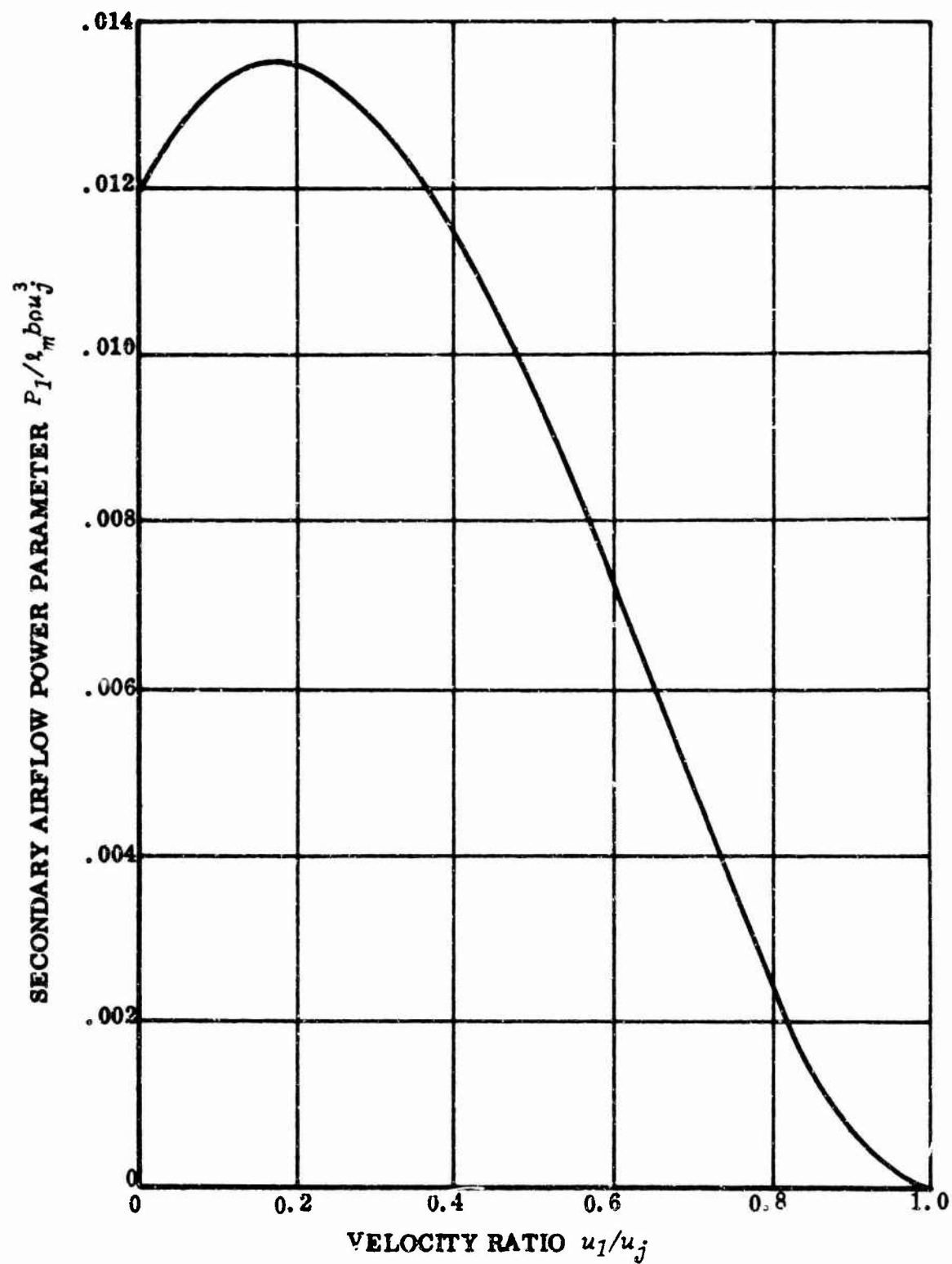
Figure 9. Variation of Secondary Airflow Power Parameter with the Velocity Ratio u_1/u_j .

24

THE CHARACTERISTICS OF JET FLOW

EXPERIMENTAL OBSERVATIONS

Before discussing the effects of mixing on eductor performance, it would be well to review a few of the known facts about the phenomenon of jet flow.

As an initial generalization, jet flow may be divided roughly into four separate categories, the Reynolds number (Re) of a jet determining the category which best describes its behavior.

Reynolds number is defined as

$$Re = ut/\nu \qquad\qquad (39)$$

where u = the jet velocity.

ν = the kinematic viscosity μ/ρ .

μ = the viscosity of the fluid.

ρ = the density of the fluid.

t = a characteristic length, usually the minimum dimension across the jet nozzle.

At very low velocities, the flow of a jet is laminar and is described by the Navier-Stokes equations, which, for two-dimensional flow, are

$$\partial u/\partial t + u(\partial u/\partial x) + \nu(\partial u/\partial y) = -1/\rho(\partial p/\partial x) + (\mu/\rho)\nabla^2 u$$

$$\qquad\qquad (40)$$

$$\partial v/\partial t + u(\partial v/\partial x) + \nu(\partial v/\partial y) = -1/\rho(\partial p/\partial x) + (\mu/\rho)\nabla^2 v$$

When the Reynolds number is very small ($R_e < 1$), the inertial terms on the left hand side can be neglected, and the simplified equations describe "creeping

flow." In this region, theory gives good agreement with experimental observations. Needless to say, this is not a flow condition which has much practical application.

Below Reynolds numbers in the range 25 - 1000, the flow pattern of a jet is characteristically laminar, and of the type illustrated in Figure 10.

(a) Laminar Jet From an Orifice.   (b) Laminar Jet From a Thin Tube.
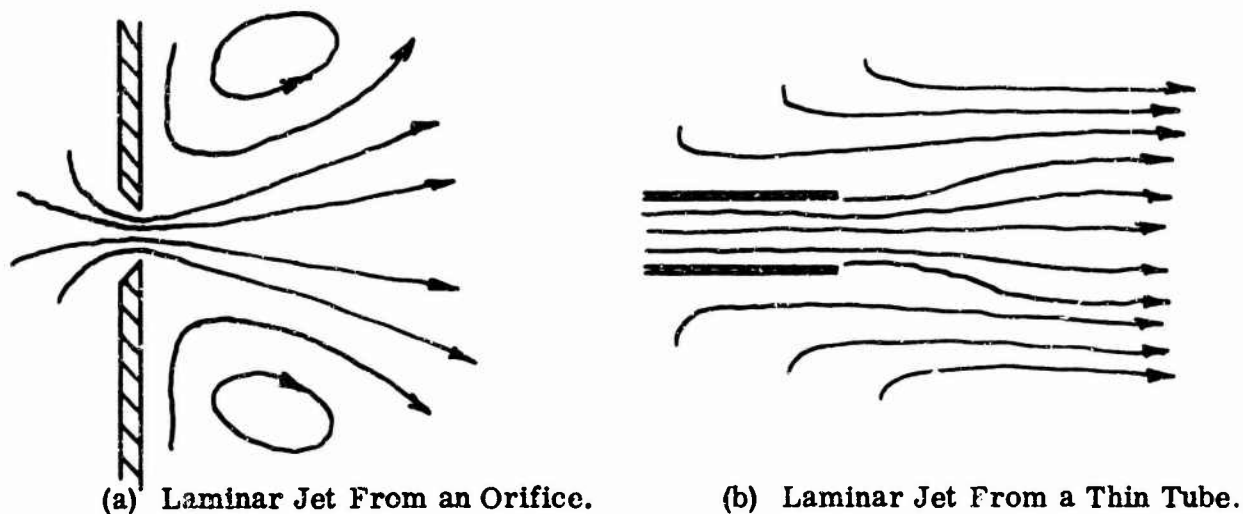
Figure 10. Typical Laminar Flow Jets.

A few solutions exist for idealized laminar jets, but again the Reynolds number is so low that the results could be applied only to small models, since $R_e = 25$ to 1000 implies $0.004 < u\ell < 0.16$ ft^2/sec. at sea level. The usefulness of laminar solutions is extended by three considerations, however. At high Reynolds numbers, when the jet is turbulent, it is surrounded by a laminar "sheath" in the region where the local velocity is less than half the maximum jet velocity. This is presumably because of the low velocity gradients involved, away from the actual shear region. Secondly, it is theoretically possible to assume an effective "eddy-viscosity" coefficient which permits turbulent flow to be represented by the Navier-Stokes equations. The "eddy-viscosity" has a much larger value than the true (laminar flow) viscosity, and is not a linear function of shear velocity gradient, so that its usefulness is limited at the present stage of theoretical development. Thirdly, it has been suggested that although the near field mixing process is basically turbulent, the jet may be laminar for a short distance downstream from its nozzle. The laminar theory may be applied in this area.

Returning to the description of jet characteristics as a function of Reynolds number, it has been established that the creeping flow which occurs at very low values

of R_e becomes laminar as R_e increases. A further increase to the region $100 < R_e < 6000$ causes the jet to become "ragged" and periodic, as illustrated in Figure 11.
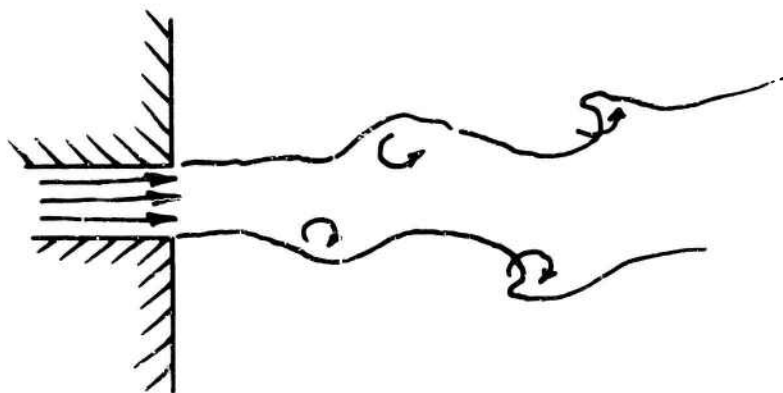
Figure 11. Periodic Jet Structure in the "Transition" Reynolds number Region.

Since the transition Reynolds number region corresponds to the range $0.016 < ut < 0.375$, small models could experience this phenomenon. If the jet nozzle of a peripheral jet GEM model were one-eighth of an inch wide, for example, the jet velocity would have to be about 36.0 ft/sec. to insure that periodic jet flow did not occur. This corresponds to a cushion pressure of $1.0 - 1.5$ lb/ft.^{2}. Thus, lightly loaded GEM models could experience scale effects which would make their performance quite different from that of geometrically similar but larger models.

The "super-critical" Reynolds number region starts at roughly $R_e \approx 6000$, and is the region of interest in most practical applications. For a two-dimensional jet, the flow picture is indicated in Figure 12. It should be noted that there are two distinct flow regimes and that the theoretical analysis is quite different in each regime.

THEORETICAL ANALYSIS OF TURBULENT JET FLOW

At present, the theory of turbulent jet flow, or indeed of any turbulent mixing process, is rather tenuous and unsatisfactory because of the mathematical difficulties introduced by the turbulence. However, it may be useful to briefly re-

27

view some approaches which have been taken to see how experimental data can be correlated and analyzed.

For flows which are nearly parallel to the x axis (v an order of magnitude less than u), the Navier-Stokes equations can be simplified by assuming quasi-static flow ($\partial u / \partial t = 0$) and by neglecting the normal velocity component (v) entirely. This gives the approximate boundary layer equations of Prandtl,

$$u \ (\partial u/\partial x) + v \ (\partial u/\partial y) = -(1/\rho)(dp/dx) + (\mu/\rho) \ (\partial^2 u/\partial x^2)$$

$$\partial u/\partial x + \partial v/\partial y = 0 \ .$$

(41)
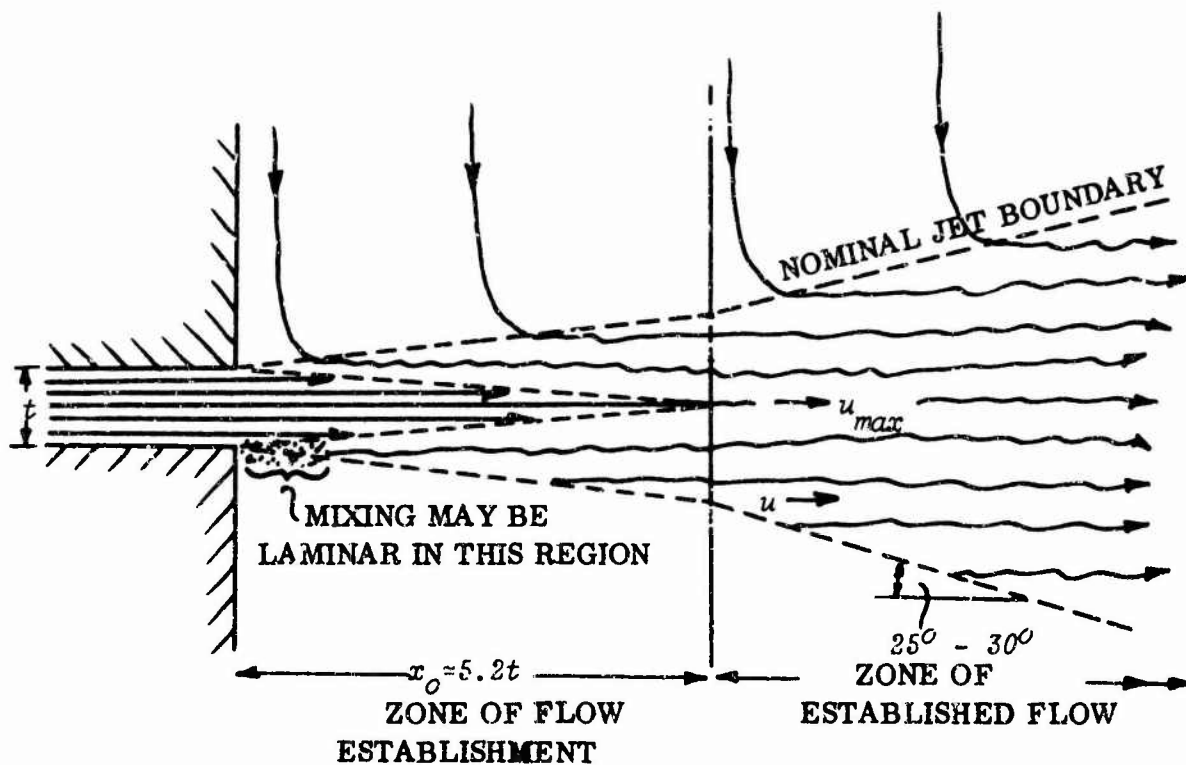
Figure 12. Approximate Flow Picture for a Turbulent Jet.

The static pressure p is a function of the external flow field, and is therefore assumed to be known. In the most usual case, $dp/dx = 0$, and it then follows from Equation (41) that momentum is conserved. That is,

$$\int_{-\infty}^{+\infty} u^2 dy = const.$$

(42)

Equation (41) has been solved for laminar flow by many investigators, for both free and fixed boundary problems. It can only be applied to turbulent problems by using the fictitious scalar "eddy-viscosity" coefficient (ϵ) in place of the Newtonian coefficient (μ/ρ) for laminar flow. Although (μ/ρ) is constant in Newtonian fluids, (ϵ) is not, so that the resulting analysis is considerably in error. Also, the actual value of the eddy-viscosity can only be defined as the value which gives the right answer! Thus, it performs the function of an empirical constant.

Other and quite different approaches have been used, employing either dimensional analysis or momentum theory analysis. In each approach, however, empirical constants appear and must be evaluated by appeal to experiment.

Perhaps the most elegant analysis is based upon momentum considerations. An excellent example is that presented by Holdhusen in the discussion section of Reference 37. Holdhusen points out that there are three basic assumptions needed to derive the momentum equations: hydrostatically distributed pressure, constancy of momentum, and the dynamic similarity of the diffusion process at all positions along the jet. The first assumption is easy to justify, the pressure differences arising as a result of flow in the y direction being less than 1 percent of the jet dynamic pressure. The second assumption, constant momentum flux, follows from the assumption of constant static pressure and Newton's second law. Alternatively, it may be derived from the Prandtl equations, as mentioned earlier. The third assumption is simply an assumption, and although widely used in this and other problems (such as the wall jet problem, for example) it can only be justified by appeal to experiment.

Defining $\quad \eta = y/x$, $\hspace{8cm}$ (43)

the "similarity" hypothesis implies

$$u/u_{max} = f(\eta) \quad .$$ $\hspace{7cm}$ (44)

In the zone of established flow, conservation of momentum gives the equality

$$\rho t u_o^2 = \int_{-\infty}^{+\infty} \rho u_{max}^2 \, f^2(\eta) \, dy \quad ;$$

therefore,

$$(x/t) \int_{-\infty}^{+\infty} f^2(\eta) \, dy = (u_o/u_{max})^2 \quad .$$ $\hspace{4cm}$ (45)

Because of the similarity hypothesis, therefore,

$$u_{max}/u_o = (t/x)^{\frac{1}{2}} / \left(\int_{-\infty}^{+\infty} f^2(\eta)\, d\eta \right)^{\frac{1}{2}} . \tag{46}$$

For the zone of flow establishment, in order to use the similarity hypothesis, we must take the origin $y = 0$ to be on the edge of the diffusion zone. Then for conservation of momentum in this region, where $u_{max} = u_o$,

$$\rho t u_o^2 = 2 \int_o^\infty \rho u_o^2\, f^2(\eta)\, dy + 2 \int_{-y\ c.l.}^o \rho u_o^2\, dy \ ;$$

therefore,

$$(x/t) \int_{-\infty}^{+\infty} f^2(\eta)\, d\eta + 2y_{c.l.}/t = 1.0 \quad . \tag{47}$$

Thus, the width of the potential zone is

$$2y_{c.l.}/t = 1 - (x/t) \int_{-\infty}^{+\infty} f^2(\eta)\, d\eta \ , \tag{48}$$

showing it to be bounded by planes. The value of x at which it vanishes is given by

$$x_o/t = 1 / \int_{-\infty}^{+\infty} f^2(\eta)\, d\eta \quad . \tag{49}$$

Thus, knowing x_o/t, we know the value of the momentum integral. For the average value of

$$x_o/t = 5.2$$

given by Rouse et al (Reference 37),

$$\int_{-\infty}^{+\infty} f^2(\eta)\, d\eta = 1/5.2 \quad .$$

Baines, in the discussion following Reference 37, reported values of x_o/t in the range 5.0 - 7.0 for circular jets, the value varying with Reynolds number.

Thus, the function $f(\eta)$ would seem to be a function of Reynolds number, a result which is not too surprising perhaps, but which gives an indication of the difficulties inherent in analyzing turbulent processes.

By substituting Equation (49) into Equation (46), we have, for the zone of established flow,

$$u_{max}/u_O = (x_O/x)^{\frac{1}{2}} \quad . \tag{50}$$

The jet mass flow is obviously

$$\dot{m}_j/\dot{m}_O = \left(\int_{-\infty}^{+\infty} \rho u_{max} \{ f(\eta) dy \} / \rho t u_O \right) = (u_{max}/u_O) \ (x/t) \int_{-\infty}^{+\infty} f(\eta) d\eta$$

$$= \ (x/t) \ \{ (x_O/t) \}^{\frac{1}{2}} \int_{-\infty}^{+\infty} f(\eta) d\eta \tag{51}$$

in the zone of established flow.

In the zone of establishment,

$$\dot{m}_j/\dot{m}_O = \left(\int_{-\infty}^{+\infty} \rho u_O f(\eta) dy + 2y_{c.l.} \ \rho u_O \right) / \rho t u_O = x/t \int_{-\infty}^{+\infty} f(\eta) d\eta \tag{52}$$
$$+ \ (2y_{c.l.} \ /t),$$

or substituting Equation (48) for $y_{c.l.}$,

$$\dot{m}_j/\dot{m}_O = 1 + (x/t) \ \left(\int_{-\infty}^{+\infty} f(\eta) d\eta - \int_{-\infty}^{+\infty} f^2(\eta) d\eta \right) \quad (x>x_O) \ . \tag{53}$$

Momentum analysis reveals a great deal about the entrainment process. However, experiment is still needed to determine "arbitrary constants." In the approach described earlier using the Prandtl equations, only one "constant", the "eddy-viscosity" (ϵ), was apparently needed. However, the assumption that it was constant also implied assumption of a velocity distribution which would satisfy Prandtl's equations; therefore, really two assumptions were made.

31

The same remarks are true of all other analyses of this type, such as Tollmein's (Reference 35) classical analysis, for example, which uses the Prandtl "mixing length" hypothesis for defining viscosity.

The case of momentum analysis is no worse, since the momentum integral ($\int f^2 (\eta) \, d\eta$) can be determined from measurements of (x_o), and the remaining integrals follow when the velocity distribution f (η) is defined. Many investigators have used the normal error function,

$$u/u_{max} = e^{-y^2/2\sigma^2}$$

(54)

for analysis and for correlation of test data. As pointed out by Reichardt (Reference 40), however, it has the inherent weakness of assuming that the turbulence generated by mixing extends to infinity.

As a matter of fact, there is no need to make any assumption in regard to velocity distribution, since it can be measured quite accurately at various stations, and non-dimensionally plotted as a single curve, permitting the integrals of f (η) to be evaluated graphically. It is even possible that the values of these integrals of f (η) could be used to deduce characteristics of the function itself, and hence reveal something of the mixing process. This is unnecessary from an engineering point of view, however, since only predictive ability is required.

The measurements of Rouse et al (Reference 37) give the following equations for the two-dimensional mixing process when suitably analyzed to give the required "empirical constant," and using the Gaussian velocity distribution.

$$\dot{m}_j/\dot{m}_o = 1 + 0.08 \ x/t \qquad (x < x_o)$$

(55)

$$= 0.62 \ (x/t)^{\frac{1}{2}} \qquad (x > x_o)$$

(56)

If the mass of entrained air is defined as $\dot{m}_1 = n\dot{m}_o$, so that

$$\dot{m}_j/\dot{m}_o = (n + 1) \quad or \quad n = \left((\dot{m}_j/\dot{m}_o) - 1\right) \; ,$$

then $\quad n = .08 \; x/t \qquad\qquad (x < x_o)$ (57)

$$= \left(0.62 \; (x/t)^{\frac{1}{2}} - 1\right) \quad (x > x_o) \; ,$$

and the entrainment per unit (x/t)

$$\partial n/\partial (x/t) = .08 \qquad (x < x_o)$$

$$= 0.31/(x/t)^{\frac{1}{2}} \qquad (x > x_o) \quad .$$ (58)

These results are plotted in Figures 13 and 14. It is interesting to note that the value of $\partial n/\partial \; (x/t)$ is constant for $x/t < 5.2$, which is the region of greatest interest for many practical applications, although not for the eductor problem.
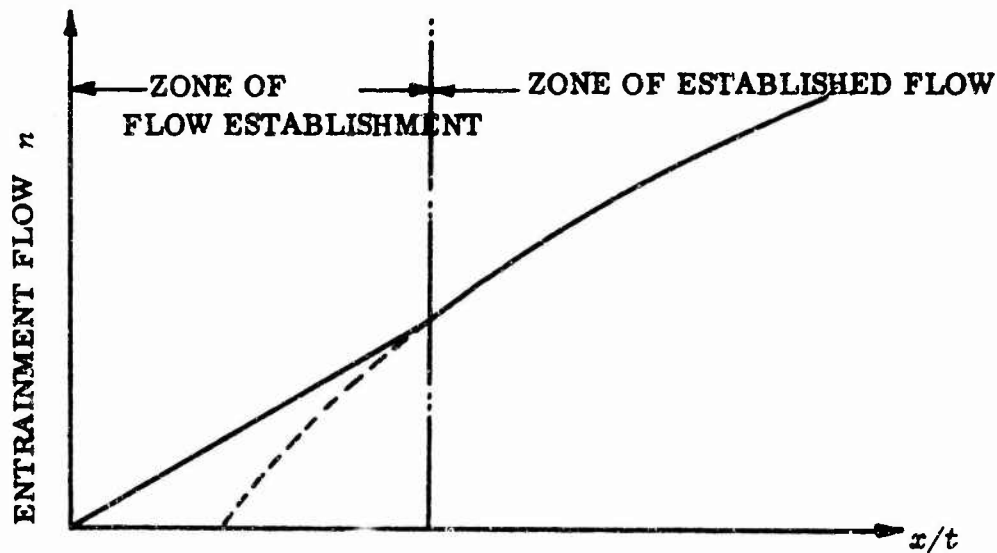
Figure 13. Variation of Entrainment Ratio
n with x/t .

33
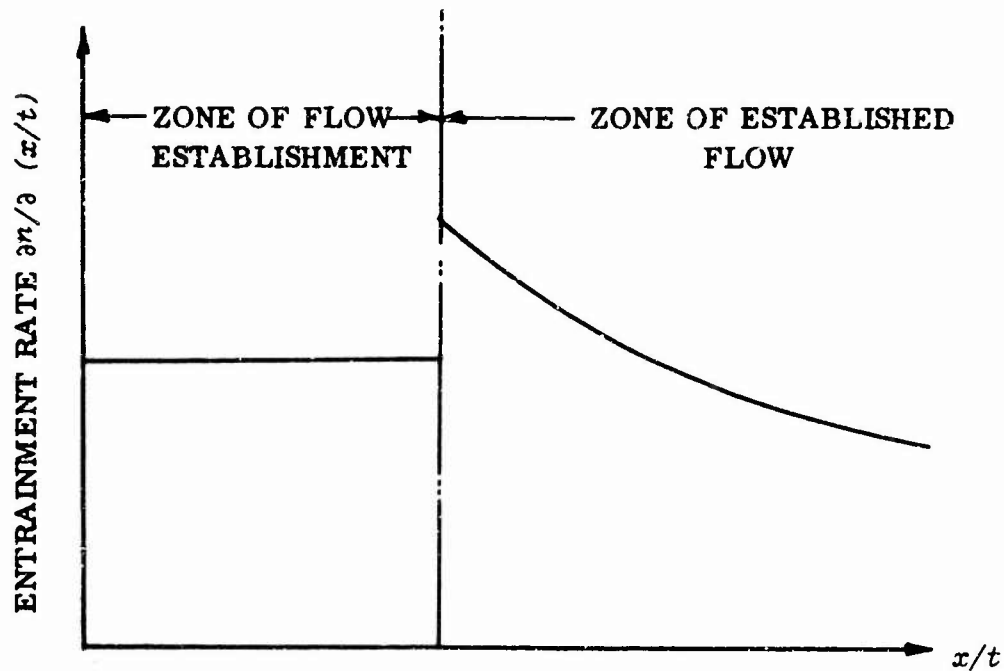
Figure 14. Variation of Entrainment Function Derivative $\partial n/\partial\ (x/t)$ with x/t .

When a jet exhausts parallel to an axial free stream (u_0),following a suggestion made by Kuchemann in Reference 83, it can be assumed that the rate of mixing is proportional to the shear velocity ($u-u_0$). This amounts to multiplying the x-ordinates by the factor

$$u_j/(u_j-u_0) = 1/\left(1 - (u_0/u_j)\right) \tag{59}$$

so that the entrainment functions become, from Equations (57) and (58),

$$n = .08\ (x/t)\ \left(1 - (u_0/u_j)\right) \qquad (x < x_0)$$

$$= 0.62\ \left((x/t)\ (1 - (u_0/u_j))\right)^{\frac{1}{2}} - 1 \qquad (x > x_0) \tag{60}$$

34

$$\partial n / \partial (x/t) = .08 \left(1 - (u_o/u_j) \right) \qquad (x < x_o)$$

$$= \left(0.31/ (x/t)^{\frac{1}{2}} \right)\left(1 - (u_o/u_j) \right) \qquad (x > x_o) . \tag{61}$$

When a jet exhausts <u>normal</u> to a free-stream flow, a transverse flow field, as such, cannot occur across it. Instead, an initially normal airflow (of velocity u_o) will be arrested by the jet, resulting in a local static pressure differential of $\Delta p = \frac{1}{2}\rho u_o^2$, or will be deflected by the jet in a manner which will depend upon the strength and size of the jet and the boundary conditions.

Chapter 5

THE EFFECT OF MIXING STATIC PRESSURE

A basic phenomenon is the effect of mixing which occurs at a static pressure which is not equal to ambient.
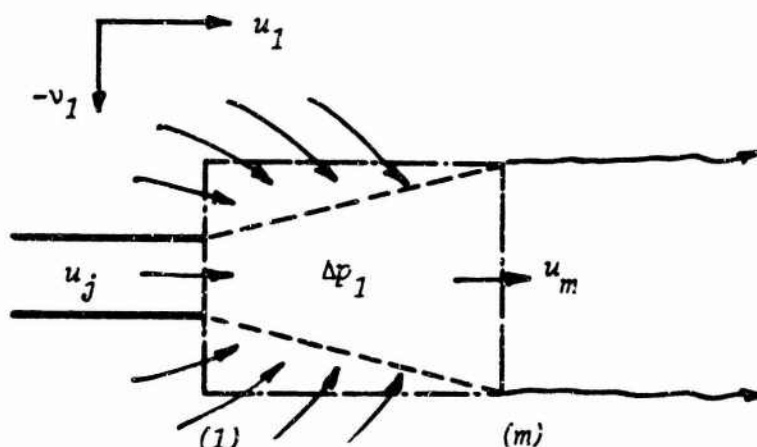
Figure 15.   Localized Mixing in a Jet.

At constant static pressure (Δp_1), two streams of fluid will mix in accordance with the law of conservation of momentum, as discussed previously. Assume now that a jet entrains a secondary flow within a control volume ($1 - m$), as shown in Figure 15.

If the static pressure in the control volume is Δp_1 , if $\dot{m}_j$ is the jet mass flow in at station (1), and if ($1+n$) $\dot{m}_j$ is the mass flow out at (m), then from Equation (29) ,

$$u_m/u_j = (1 + n \; (u_1/u_j))/(n + 1) \; . \tag{62}$$

So long as the mixing pressure continues at Δp_1 , there will be no change of momentum.   Eventually the jet must return to ambient static pressure ($\Delta p = 0$), however, and if this is achieved without loss of total head,

$$\Delta \bar{p}_1 + \tfrac{1}{2}\rho u_m^2 = \tfrac{1}{2}\rho u_2^2 \quad .$$

Thus, the final (u_2) velocity is

$$u_2 = \left(2/\rho \ (\Delta p_1 + \tfrac{1}{2}\rho u_m^2) \right)^{\tfrac{1}{2}} , \tag{63}$$

and the final momentum flux

$$J_2 = (n + 1) \ \dot{m}_j u_2$$

$$= (n + 1) \ \dot{m}_j \left((2/\rho) \ \Delta p_1 + u_m^2 \right)^{\tfrac{1}{2}} . \tag{64}$$

Expressing this as a ratio of the initial jet momentum flux,

$$J_2/J_o = (n + 1) \left(\Delta \bar{p}_1 + (u_m/u_j)^2 \right)^{\tfrac{1}{2}} , \tag{65}$$

where $\Delta \bar{p}_1 = \Delta p_1 / \tfrac{1}{2}\rho u_j^2$.

Substituting Equation (62) for u_m/u_j ,

$$J_2/J_o = \left((n + 1)^2 \ \Delta \bar{p}_1 + (1 + n \ \{u_1/u_j\})^2 \right)^{\tfrac{1}{2}} . \tag{66}$$

This equation offers some interesting special cases. For an ideal <u>static augmentor</u> with no internal losses,

$$\tfrac{1}{2}\rho u_1^2 = - \Delta p_1 \quad ;$$

therefore,

$$u_1/u_j = (-\Delta \bar{p}_1)^{\frac{1}{2}}$$

and

$$J_2/J_o = \left((n + 1)^2 \Delta \bar{p}_1 + \{1 + n (-\Delta \bar{p}_1)^{\frac{1}{2}}\}^2\right)^{\frac{1}{2}} . \tag{67}$$

This function is plotted in Figure 16 for $n = 10.0$. It is evident that there is an optimum value of $\Delta \bar{p}_1$ for maximum increase in momentum flux. Static eductors should obviously be designed to take advantage of this optimum.

For static entrainment in a jet,

$$u_1 = 0 ;$$

therefore,

$$J_2/J_o = (n + 1) (\Delta \bar{p}_1)^{\frac{1}{2}} + 1 . \tag{68}$$

That is, $J_2/J_o > 1.0$ for greater than ambient mixing pressure, the reverse of a static augmentor.

An example of such entrainment occurs on the high-pressure side of a jet flap, which is deflected through a large angle. Close to the nozzle the relative static pressure may be taken as the free-stream dynamic head $\frac{1}{2}\rho u_o^2$ on the high-pressure side of the jet. On the rear side of the jet, the static pressure will be ambient, or somewhat lower. Thus, the mean effective jet static pressure will be between these two extremes, and will, in fact, be the arithmetic mean if the jet is thin in relation to its local radius of curvature. Thus, approximately

$$\Delta p_1 = \Delta p_j = \frac{1}{2}(\frac{1}{2}\rho u_o^2) ;$$

therefore,

$$\Delta \bar{p}_1 = \frac{1}{2}(u_o/u_j)^2$$

and

$$J_2/J_o = \left(\frac{1}{2} (n + 1)^2 (u_o/u_j)^2 + 1\right)^{\frac{1}{2}} . \tag{69}$$

This equation does not account for the momentum lost by the air which is entrained by the jet, a drag force which is $n\dot{m}_j u_o$. When this is included,
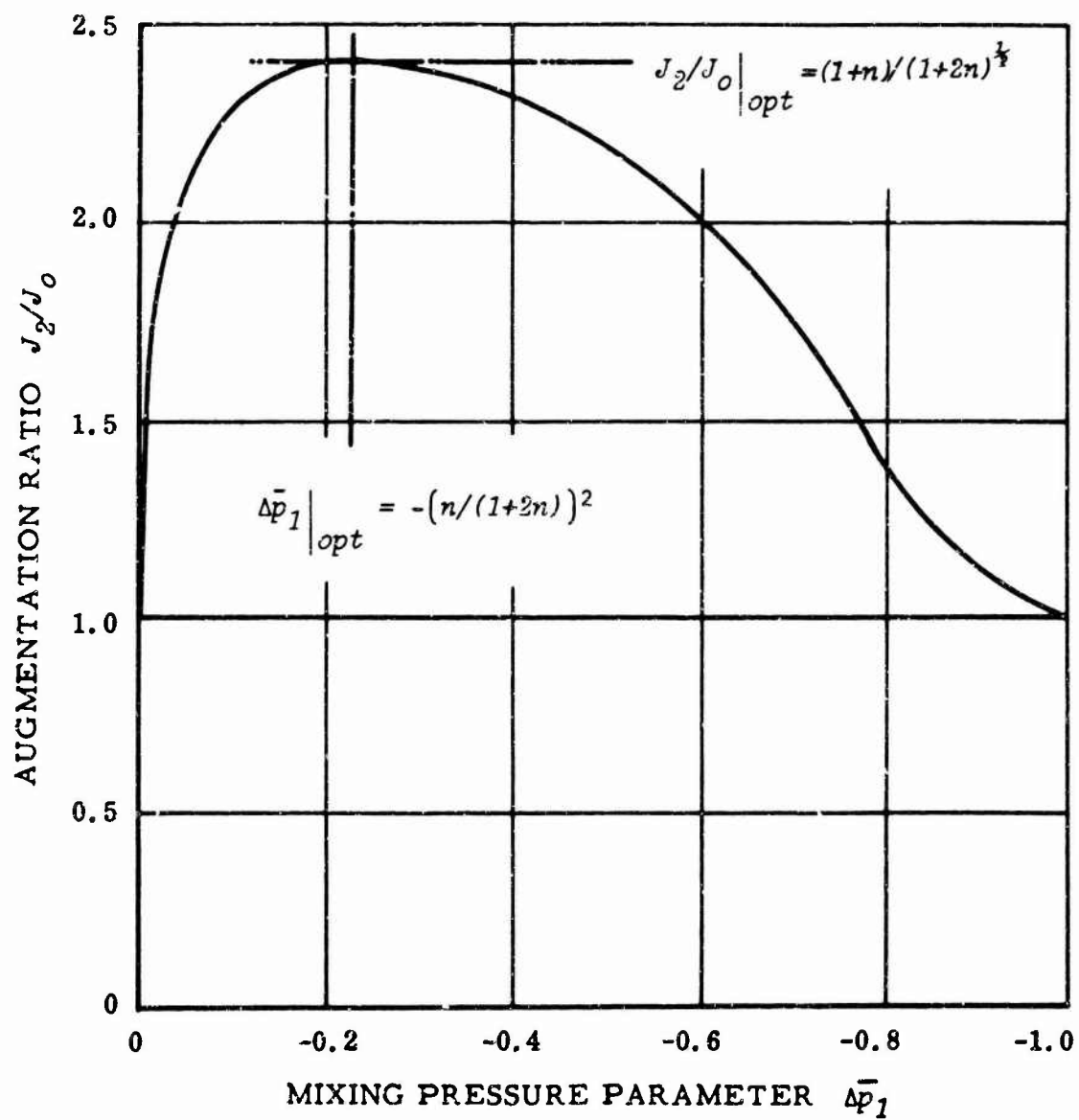
Figure 16. Variation of Ideal Static Augmentation With
Mixing Pressure for $n = 10$.

$$J_2/J_O \Big|_{NET} = \left(\tfrac{1}{2}(n+1)^2(u_O/u_j)^2 + 1\right)^{\tfrac{1}{2}} - n\,(u_O/u_j) \quad . \tag{70}$$

Note that as $u_O/u_j \to 0$,

$$J_2/J_O \Big|_{NET} \to 1 - n(u_O/u_j) \quad . \tag{71}$$

As $\quad n \to 0$

$$J_2/J_O \Big|_{NET} \to \left(\tfrac{1}{2}(u_O/u_j)^2 + 1\right)^{\tfrac{1}{2}} \quad , \tag{72}$$

which describes the effect of the pressure energy in the jet.

In general, the ratio J_2/J_O will be less than unity. Thus, this mixing loss is the reason for the so-called "thrust loss anomaly" of the jet flap.

While it is not the primary purpose of this report to discuss jet dra̲g̲   ̲eful to note that the variation of (n) with u_O/u_j can obviously be accou̲ṉ̲_̲ ̲_̲ed using results of the type given in the foregoing chapter on jet characteristics.

Free-air entrainment is by no means the only cause of "jet drag." Apart from "apparent" force changes due to the change of local static pressure near the jet nozzle, diffusion losses occur on the pressure side of a nozzle which has a pressure differential across it. Also, in some configurations, the jet can increase the size of the wake. During recent experiments, for example, a jet-flapped wing generated a wake three times as deep as the wing wake with the jet inoperative.

Another interesting form for Equation (66) is appropriate to a jet issuing parallel to a free-stream flow. If the free-stream velocity is u_O , then for zero losses

$$\tfrac{1}{2}\rho u_O^2 = \Delta p_1 + \tfrac{1}{2}\rho u_1^2 \quad ;$$

therefore,

$$(u_1/u_j)^2 = (u_O/u_j)^2 - \Delta \bar{p}_1$$

and $\quad J_2/J_O = \left((n+1)^2\,\Delta\bar{p}_1 + (1 + n\,\{(u_O/u_j)^2 - \Delta\bar{p}_1\}^{\tfrac{1}{2}})^2\right)^{\tfrac{1}{2}} - n(u_O/u_j).$ (73)

40

The thrust ratio is always less than unity if the mixing pressure is greater than ambient, but augmentation can occur if $\Delta \bar{p}_1 < 0$. As indicated in Figure 17, the maximum attainable augmentation diminishes with increasing forward speed.

When $\Delta \bar{p}_1 = 0$, $J_2/J_o = 1.0$ always.

Since the static pressure behind a wing or nacelle is usually greater than ambient, Equation (73) describes a "jet drag" which is the same as that discussed in the beginning of this report. Instead of using a potential flow analysis, a different approach has been used to obtain the same result.
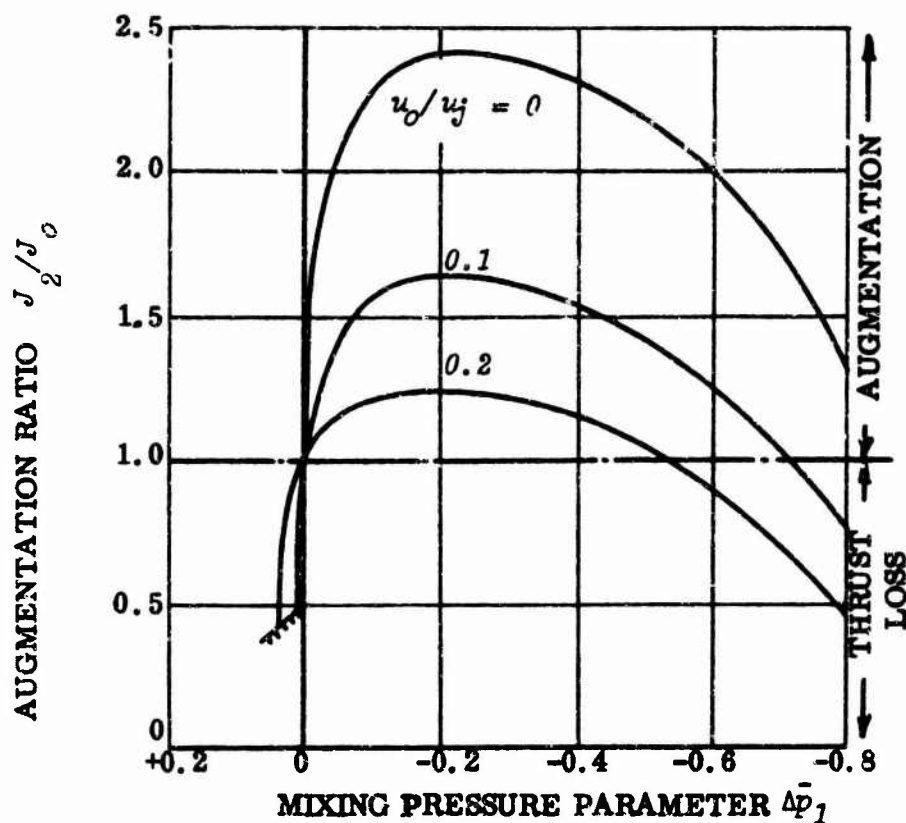
Figure 17. Effect of Forward Speed on Augmentation for $n = 10$.

Chapter 6

GENERAL ONE-DIMENSIONAL FLOW THEORY OF AN EDUCTOR

THE BASIC EQUATIONS

As already discussed, the ability of an eductor to increase the primary jet thrust is predicated upon the mixing pressure's(p_1) being less than ambient, so that diffusion must take place in order to bring the static pressure of the fully mixed jet up to the exit pressure. There is an optimum value for the mixing pressure (p_1) which gives maximum augmentation, and this leads to the concept of an "optimum augmentor." This is the augmentor which, for a given diffuser efficiency η_D, gives the absolute maximum augmentation possible. The ability to generate equations for this optimum reduces the computational load by an order of magnitude for a static eductor. When the upstream and diffuser exit pressures are not ambient, the saving is even greater, of course.

Let J = momentum flux

$\dot{m}$ = a mass flow

P = a total pressure

p = a static pressure

n = a ratio of entrained to primary mass flow

The suffixes j, 1, 2, and m refer to the respective positions in Figure 1. The suffix a refers to ambient conditions, as when the primary exhausts to ambient.

The diffuser efficiency is defined as

$$\eta_D = \left((p_2 + \tfrac{1}{2}\rho u_2^2) - p_1 \right)/\tfrac{1}{2}\rho u_m^2 \quad , \tag{74}$$

so that it experiences a dynamic loss $(1-\eta_D)\ \tfrac{1}{2}\rho u_m^2$, and

$$\tfrac{1}{2}\rho u_2^2 = p_1 - p_2 + \eta_D\ \tfrac{1}{2}\rho u_m^2 \quad . \tag{75}$$

42

Substituting Equation (62) for u_m,

$$\tfrac{1}{2}\rho u_2^2 = p_1 - p_2 + \eta_D \, \tfrac{1}{2}\rho u_j^2 \left\{1 + n \, (u_1/u_j)\right\}^2 / \, (n + 1)^2 \quad . \tag{76}$$

To non-dimensionalize, for convenience, divide by $\tfrac{1}{2}\rho u_j^2$, so that

$$\bar{p}_n = p_n / \tfrac{1}{2}\rho u_j^2$$

and Equation (76) becomes

$$(u_2/u_j)^2 = \bar{p}_1 - \bar{p}_2 + \eta_D \left\{1 + n \, (u_1/u_j)\right\}^2 / \, (n + 1)^2 \quad . \tag{77}$$

From Figure 1,

$$\bar{P}_c = \bar{p}_1 + (u_1/u_j)^2 \quad ;$$

therefore,

$$u_1/u_j = (\bar{P} \; - \bar{p}_1)^{\frac{1}{2}} \quad .$$

Substituting into Equation (77) ,

$$u_2/u_j = \left\{(\bar{p}_1 - \bar{p}_2) + \{\eta_D/(n+1)^2\}\{1 + n \, (\bar{P}_c - \bar{p}_1)^{\frac{1}{2}}\}^2\right\}^{\frac{1}{2}} \quad . \tag{78}$$

The augmentation ratio is

$$J_2/J_a = (n+1)\dot{m}_j u_2 / \dot{m}_{ja} u_{ja} = (\dot{m}_j / \dot{m}_{ja})^2 (u_2/u_j) \, (n + 1). \tag{79}$$

Substituting Equation (78) for u_2/u_j ,

$$J_2/J_a = (\dot{m}_j / \dot{m}_{ja})^2 \left\{(\bar{p}_1 - \bar{p}_2) \, (n + 1)^2 + \eta_D \{1 + n \, (\bar{P}_c - \bar{p}_1)^{\frac{1}{2}}\}^2\right\}^{\frac{1}{2}} . \tag{80}$$

Since $(m_j/m_{ja})^2 = (u_j/u_{ja})^2 = \tfrac{1}{2}\rho u_j^2/(P_j - p_c)$

$$= 1/\Delta \bar{P}_j \quad ,$$

(81)

if $\quad \Delta P_j = P_j - p_a \quad ,$

$$J_2/J_a = (1/\Delta \bar{P}_j)\left((\bar{p}_1 - \bar{p}_2)(n+1)^2 + \eta_D \{1 + n(\bar{P}_c - \bar{p}_1)^{\frac{1}{2}}\}^2 \right)^{\frac{1}{2}} \quad . \qquad (82)$$

Equation (82) is a complete (one-dimensional flow) statement of augmentor performance, although the independent variables $\bar{p}_1$ and n are rather inconvenient in this form.

OPTIMUM MIXING PRESSURE

The optimum mixing pressure parameter is that value of $\bar{p}_1$ which gives the maximum value of J_2/J_a with $\bar{P}_c$ and $\bar{p}_2$ being fixed. Differentiating Equation (82) with respect to $\bar{p}_1$ and equating to zero, the optimum value of P_1 is found to be

$$P_1\Big|_{opt} = \bar{P}_c - n^2 \eta_D^2/((n+1)^2 - n^2\eta_D)^2 \quad . \qquad (83)$$

Substituting for $P_1\Big|_{opt}$ into Equation (82) ,

$$J_2/J_a\Big|_{opt} = \left((n+1)/\Delta\bar{P}_j\right)\left(\eta_D + (\bar{P}_c - \bar{p}_2)\{(n+1)^2 - n^2\eta_D\}\right)^{\frac{1}{2}}/\left((n+1) - n^2\eta_D\right)^{\frac{1}{2}}$$

(84)

$$J_2/J_a\Big|_{opt}^2 = J_2/J_a\Big|_{opt}^2 + \left((n+1)/\Delta\bar{P}_j\right)^2 \bar{P}_c - \left((n+1)/\Delta\bar{P}_j\right)^2 \ddot{p}_2 \quad .$$
$$P_c = p_2 = 0$$

44

This is an interesting result. The effects of upstream and diffuser exit pressure appear as simple Southwell coefficients. It is obvious that an increase of inlet total head will increase J_2/J_a, while an increase in back-pressure will decrease it, as should be expected. Also, for ambient inlet total head, the thrust falls to zero when

$$\Delta \bar{p}_2 = \eta_D / \left((n + 1)^2 - n^2 \eta_D \right) \quad . \tag{85}$$

It is important to note from Equation (83) that the back pressure p_2 does not influence the optimum value of p_1. This means that an optimum injector is merely an optimum eductor with a larger diffuser.

THE OPTIMUM STATIC EDUCTOR

The preceding section shows that the optimum eductor is directly related, by appropriate Southwell coefficients, to the optimum static eductor, for which

$$J_2/J_a \Big|_{opt} = \left((n + 1) \ (\eta_D)^{\frac{1}{2}} \right) / \left(\Delta \bar{P}_j \ \{(n + 1)^2 - n^2 \eta_D \}^{\frac{1}{2}} \right) \quad . \tag{86}$$

In the limit $n \to \infty$,

$$J_2/J_a \Big|_{opt} \to \left(\eta_D / (1 - \eta_D) \right)^{\frac{1}{2}} \quad , \tag{87}$$

and as $n \to 0$,

$$J_2/J_a \Big|_{opt} \to (\eta_D)^{\frac{1}{2}} \quad . \tag{88}$$

Equation (86) is plotted in Figure 18, where the dominating effect of diffuser efficiency is clearly seen. Use of boundary layer control or similar techniques to give very high diffuser efficiencies makes possible augmentations as high as 3 or 4, or possibly even more.

Calculation of geometrical variables which give optimum augmentation follows:
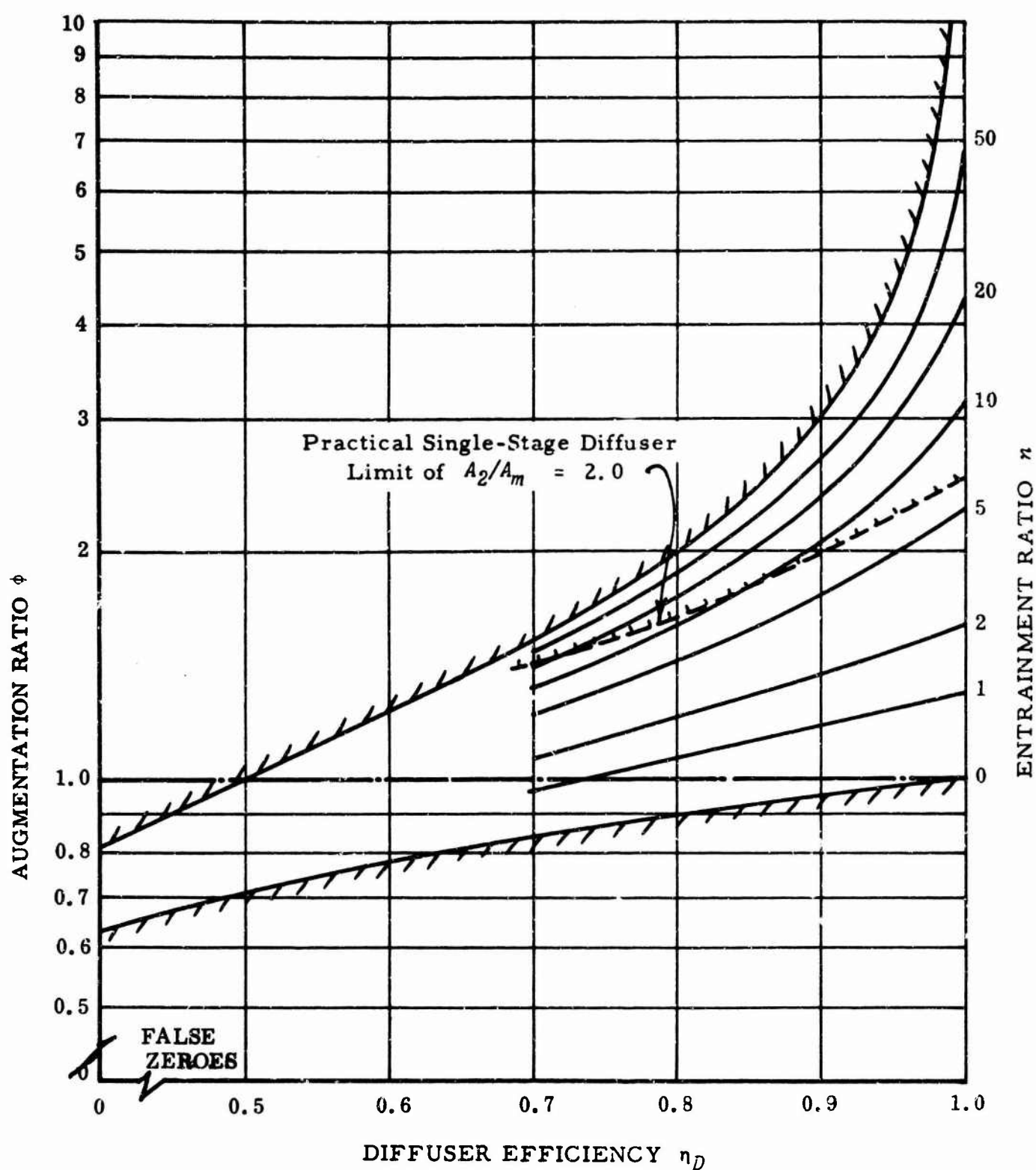
Figure 18. Variation of Optimum Static Thrust Augmentation With
Entrainment Ratio *n* and Diffuser Efficiency η_D.

Since

$$\Delta p_1 \Big|_{opt} = -n^2 \eta_D^2 / \left((n+1)^2 - n^2 \eta_D \right)^2 = \Delta p_1 / (\Delta P_j - \Delta p_1) \quad , \tag{89}$$

$$\Delta p_1 / \Delta P_j \Big|_{opt} = \bar{\Delta p}_1 \Big|_{opt} / (1 + \bar{\Delta p}_1 \Big|_{opt}) \tag{90}$$

$$= -n^2 \eta_D^2 / \left(\{ (n+1)^2 - n^2 \eta_D \}^2 - n^2 \eta_D^2 \right) \quad . \tag{91}$$

This relationship is plotted in Figure 19. The value of $\bar{\Delta P}_j$ in Equation (86) can now be calculated, since

$$\bar{\Delta P}_j = \Delta P_j / (\Delta P_j - \Delta p_1) = 1 / \left(1 - (\Delta p_1 / \Delta P_j) \right) \quad . \tag{92}$$

If we substitute this in Equation (86),

$$J_2 / J_a \Big|_{opt} = \left((n+1)^2 - n^2 \eta_D \right)^{3/2} \left((n+1) (\eta_D)^{\frac{1}{2}} \right) /$$
$$\left(\{ (n+1)^2 - n^2 \eta_D \}^2 - n^2 \eta_D^2 \right)^{\frac{1}{2}}, \tag{93}$$

which is, of course, the equation actually used to compute Figure 18.

Now,

$$n (A_j / A_1) = (-\bar{\Delta p}_1)^{\frac{1}{2}} = \left(\{ -\Delta p_1 / \Delta P_j \} / \{ 1 - (\Delta p_1 / \Delta P_j) \} \right)^{\frac{1}{2}} \quad . \tag{94}$$

The area ratio of the mixing tube is obtained from the equation for continuity of mass flow,

$$A_m / A_1 = \left((n+1)^2 A_j / A_1 \right) / \left(1 + n^2 (A_j / A_1) \right) \quad . \tag{95}$$

The diffuser area ratio A_2 / A_m is found from the relationship of Equation (75), substituting $u_m = u_2 (A_2 / A_m)$ so that

47
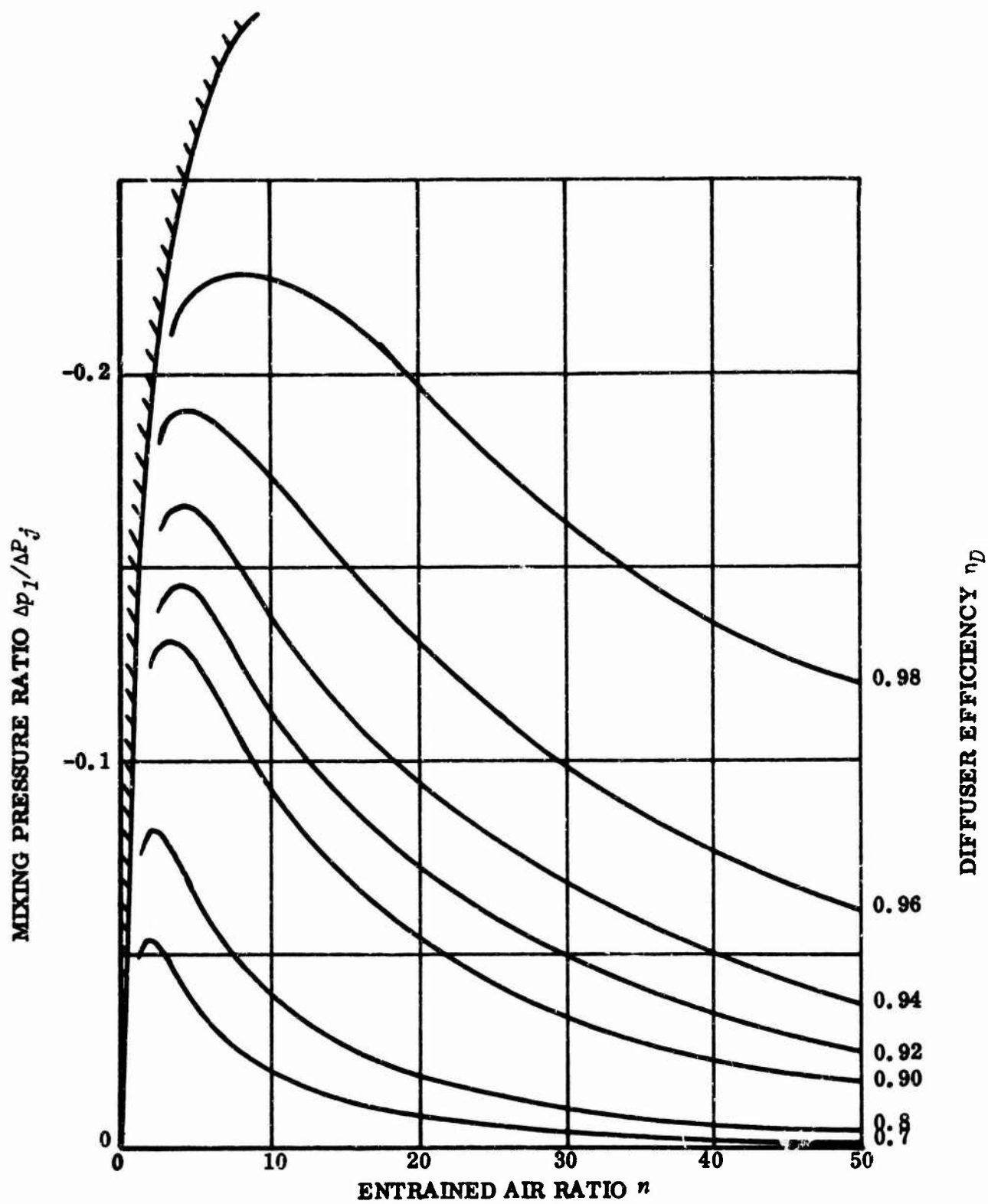
Figure 19.   Optimum Mixing Pressure
for a Static Eductor.

$$\Delta p_1 + \eta_D \tfrac{1}{2}\rho u_2^2 (A_2/A_m)^2 = \tfrac{1}{2}\rho u_2^2$$

$$\eta_D \ (A_2/A_m)^2 = 1 - \Delta \bar{p}_1 \ (u_o/u_2)^2 \qquad . \tag{96}$$

The velocity ratio can be obtained from Equation (78). More conveniently, from Equations (79) and (81), and (92),

$$u_j/u_2 = \left((\dot{m}_j/\dot{m}_{ju})^2 \ (n+1)/(J_2/J_a) \right) = \left(\{1-(\Delta p_1/\Delta P_j)\} \ (n+1)/J_2/J_a \right) \ ;$$

therefore,

$$A_2/A_m = (n+1) \ / \left(\eta_D \{(n+1)^2 - n^2 \eta_D\} \right)^{\frac{1}{2}} \qquad . \tag{97}$$

The optimum area ratio values are plotted in Figures 20 through 22, and the optimum equations are summarized in Table I.

EFFICIENCY OF THE OPTIMUM STATIC EDUCTOR

The total eductor efficiency may be calculated from the relationship

$$\eta = \left((J_2/J_a)^2 \ (\dot{m}_{ja}/\dot{m}_j) \right) \ / \ (n+1)$$

$$= (J_2/J_a)^2 \ / \ (n+1) \ \left(1 - (\Delta p_1/\Delta P_j)\right)^{\frac{1}{2}} \qquad . \tag{98}$$

For the case of $\eta_D = 1.0$, $\eta \rightarrow (8/9)(3/4)^{\frac{1}{2}} = 0.77$ as $n \rightarrow \infty$. For any value of η_D as $n \rightarrow o$, $\eta \rightarrow \eta_D$.

Equation (98) is plotted in Figure 23 for optimum static eductors.
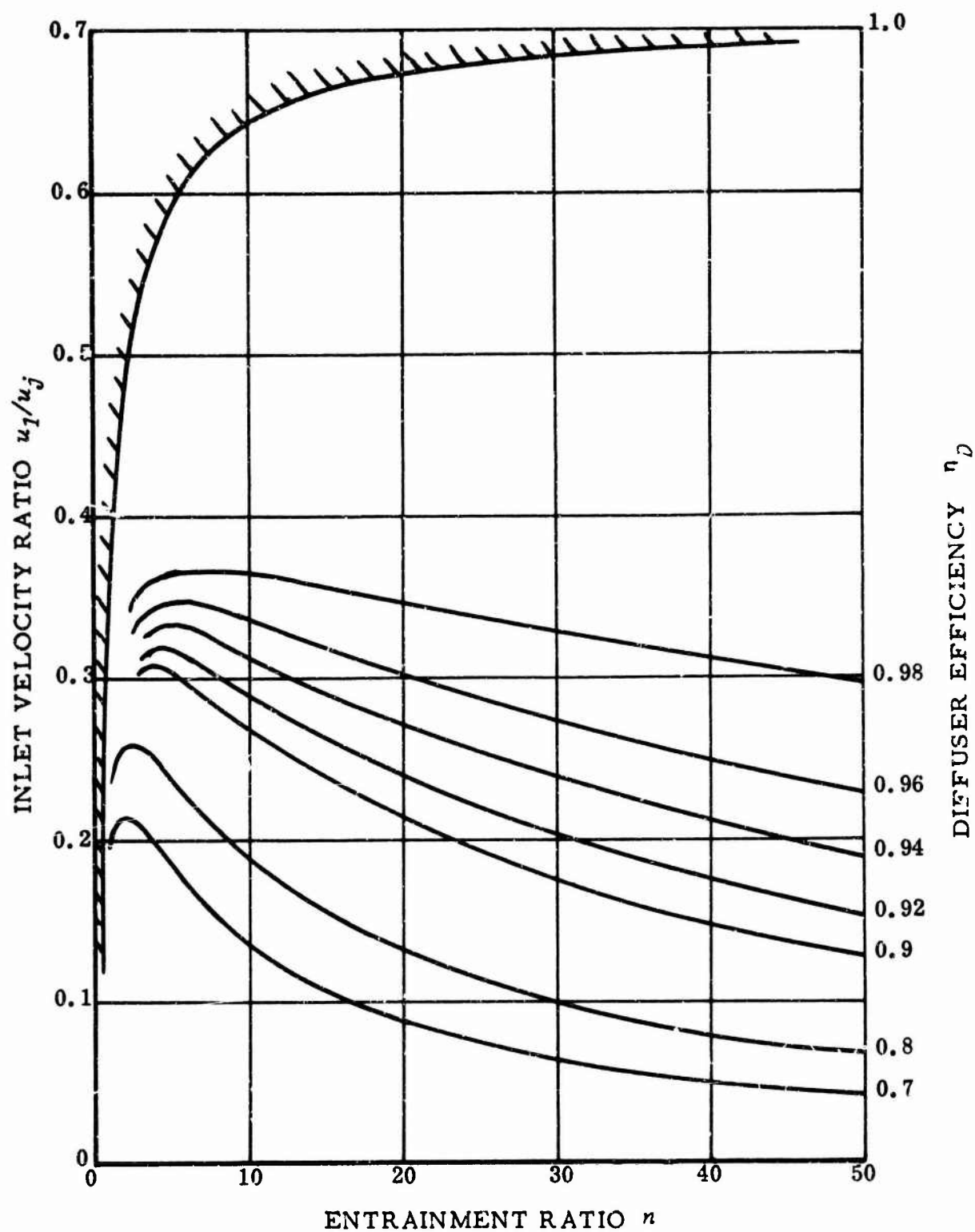
Figure 20. Variation of Optimum Inlet Velocity Ratio With Entrainment Ratio. (Note that $u_1/u_j = (n) A_j/A_1$).

50
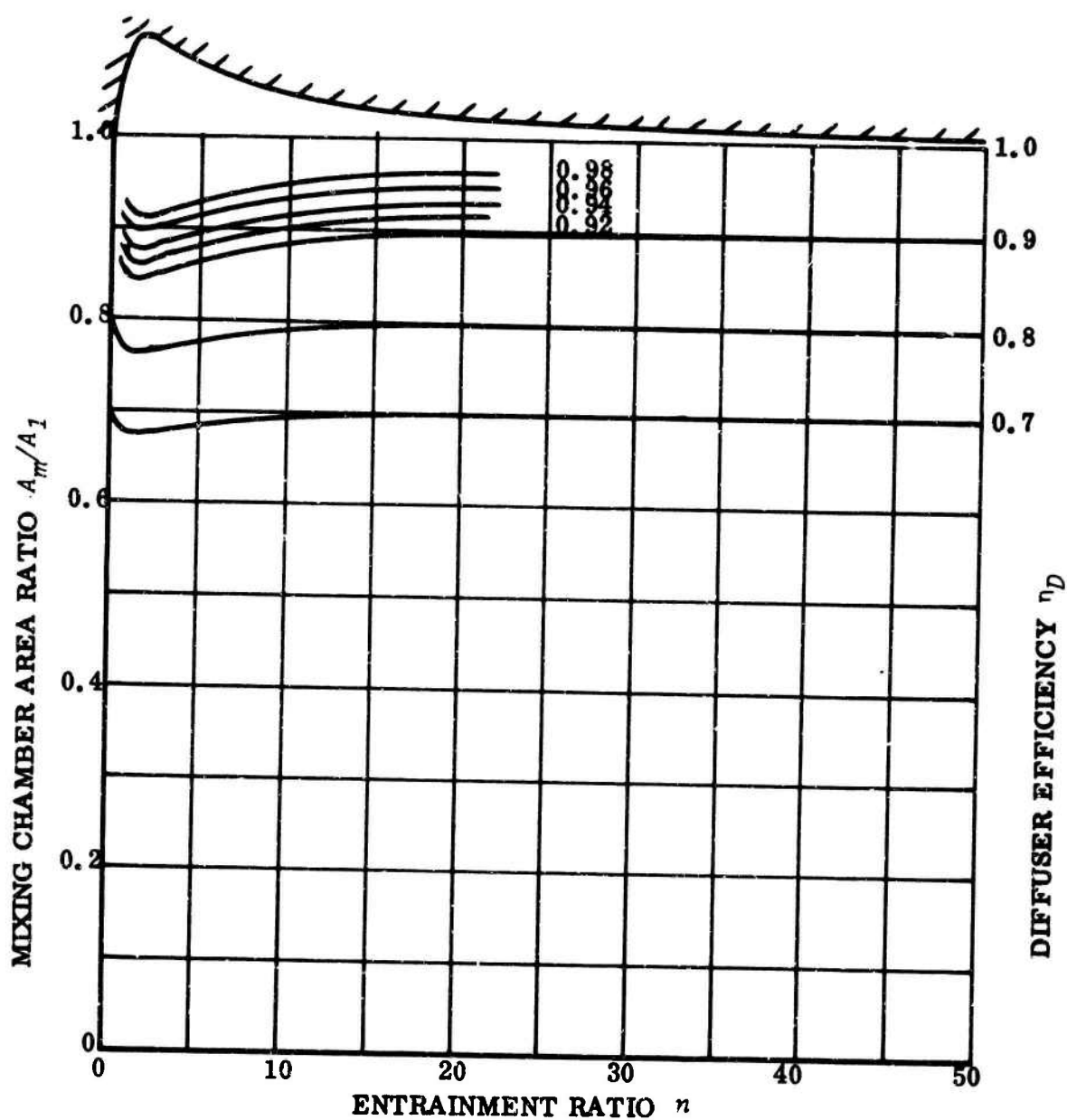
Figure 21. Optimum Mixing Duct Area at Completion of Mixing.
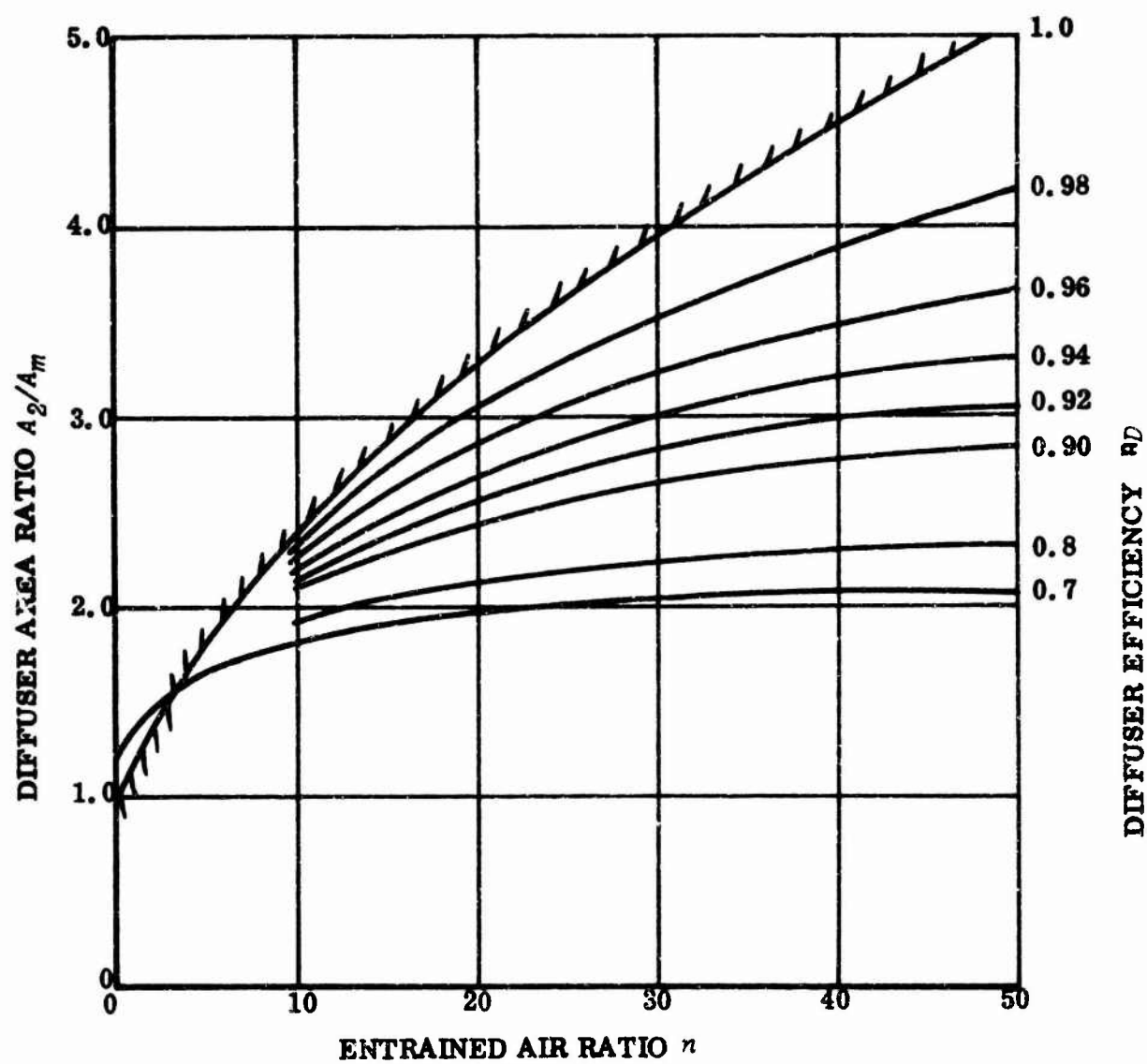
Figure 22.   Optimum Diffuser Ratio for a
Static Eductor.

Table I
OPTIMUM STATIC EDUCTOR PARAMETERS AS A FUNCTION OF ENTRAINMENT RATIO n

Parameter	Equation	Limit $n \to 0$	Limit $n \to \infty$
Total momentum Actual jet momentum	$J_2/J_o\big|_{opt} = \left((n+1)(\eta_D)^{\frac{1}{2}}\right) / \left((n+1)^2 - n^2\eta_D\right)^{\frac{1}{2}}$	$(\eta_D)^{\frac{1}{2}}$	$\left(\eta_D/(1-\eta_D)\right)^{\frac{1}{2}}$
Total momentum Jet momentum to ambient	$J_2/J_a\big|_{opt} = (1/\bar{\Delta P}_j)\, J_2/J_o\big|_{opt}$	$(\eta_D)^{\frac{1}{2}}$	$\left(\eta_D/(1-\eta_D)\right)^{\frac{1}{2}}$
Jet total pressure parameter	$\bar{\Delta P}_j = 1/\, 1-(\Delta p_1/\Delta P_j)$	---	-----------
Mixing pressure	$\Delta p_1/\Delta P_j\big|_{opt} = -n^2\eta_D^2 / \left(\{(n+1)^2 - n^2\eta_D\}^2 - n^2\eta_D^2\right)$	0	$0\ (\eta_D \neq 1)$ $1/3\ (\eta_D = 1)$
Intake area ratio	$A_1/A_j\big|_{opt} = (1/\eta_D)\{\{(n+1)^2 - n^2\eta_D\}^2 + 2n^2\eta_D^2\}^{\frac{1}{2}} = (1/n)\left((-\Delta p_1/\Delta P_j)/\, 1-\Delta p_1/\Delta P_j\,\right)^{\frac{1}{2}}$	$1/\eta_D$	0
Mixing tube area ratio	$A_m/A_1\big|_{opt} = (1+n)^2 (A_j/A_1)/\left(1+n^2 A_j/A_1\right)\eta_D$	η_D	
Diffuser area ratio	$A_2/A_m\big|_{opt} = (n+1)/\left(\eta_D\{(n+1)^2 - n^2\eta_D\}\right)^{\frac{1}{2}}$	$1/(\eta_D)^{\frac{1}{2}}$	$1/\left(\eta_D(1-\eta_D)\right)^{\frac{1}{2}}$

53
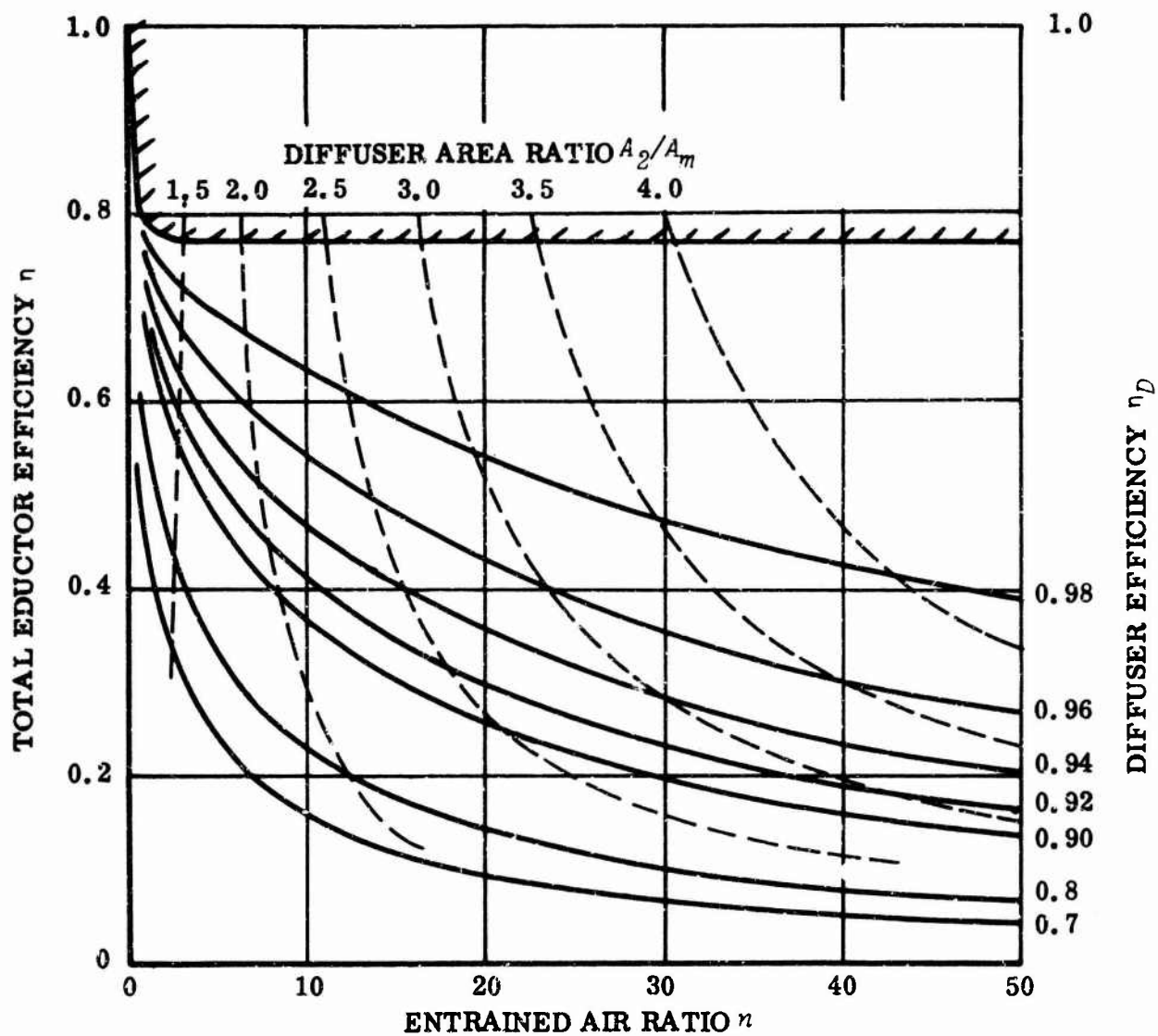
Figure 23.   Total Efficiency of Optimum
             Static Eductors.

DIFFUSER EFFICIENCY

Thus far, the fact that a conventional single-stage diffuser can accommodate only a velocity ratio $u_2/u_m > \frac{1}{2}$ has been ignored, as well as the fact that diffuser technology is still a crude and inefficient business. There are several ways of improving both efficiency and diffusion ratio; the most obvious is boundary layer control utilizing the mixing section suction. To adequately discuss this and other approaches is beyond the scope of this report, however.

HEATING THE PRIMARY AIR TO GIVE INCREASED PERFORMANCE

The density (ρ) of a gas is given by the equation

$$\rho = p/RT \quad . \tag{99}$$

The momentum flux through the primary nozzle is

$$\dot{m}_j u_j = \dot{m}_j \left((2/\rho)(\Delta P_j - \Delta p_1) \right)^{\frac{1}{2}} \quad . \tag{100}$$

Thus, if the primary air is heated, a primary momentum flux increase results in the ratio

$$\dot{m}_j u_{jT}/\dot{m}_j u_j = (T/T_o)^{\frac{1}{2}} \quad , \tag{101}$$

if the mass flow is held constant by using variable area primary nozzles. This increase can give an important "boost" capability to certain types of eductors.

When the nozzle area is not variable, the mass flow varies inversely as $(T/T_o)^{\frac{1}{2}}$, so that the primary momentum flux (and therefore the total thrust) is independent of temperature. This has been well confirmed in a number of experimental programs. Indeed, so extensively have the effects of temperature been investigated, one wonders whether the experimenters appreciated the significance of Equation (99)!

PHYSICAL LOCATION OF FORCES ON AN EDUCTOR

The additional momentum flux of an eductor is transmitted to its wall in the form of static pressure. For the optimum case, calculations can be made for the relative magnitude of the primary entry lip, diffuser and mixing chamber contributions.

Primary Jet

Assuming constant nozzle total head ,

$$F_o = A_j \Delta p_1 + \rho A_j u_j^2$$

but $\quad \rho u_j^2 = 2(\Delta P_j - \Delta p_1) \; ;$

therefore,

$$F_o = 2A_j \Delta P_j \left(1 - \tfrac{1}{2} \{\Delta p_1 / \Delta P_j\}\right) , \qquad (102)$$

where $\quad 2A_j \Delta P_j \quad$ is the value obtained in exhausting to ambient static pressure, of course.

Mixing Chamber

$$F_m = -(A_1 - A_m) \Delta p_1$$

$$= -A_1 \Delta p_1 \left(1 - A_m / A_1\right) . \qquad (103)$$

Diffuser

$$-F_D = - (\rho u_2^2 + p_2) A_2 + (\rho u_m^2 + p_1) A_m \quad .$$

For $\quad p_2 = p_a \quad ,$

56

$$-F_D = -\rho A_2 u_2^2 + (\rho u_m^2 + \Delta p_1) \; A_m \quad .$$

For continuity,

$$u_m A_m = u_2 A_2 \quad ;$$

therefore,

$$- F_D = \left((A_2/A_m) - 1 \right) J_2 + A_m \Delta p_1 \qquad . \tag{104}$$

Note that the diffuser thrust is always negative.

Summation of Forces

It is logical to divide the component forces by $2A_j \Delta P_j$, the primary thrust to ambient.

Then $\quad F_j/J_a = \left(1 - \tfrac{1}{2}(\Delta p_1/\Delta P_j) \right)$,

$$F_m/J_a = -\tfrac{1}{2} \, (A_1/A_j)(\Delta p_1/\Delta P_j)\{1-(A_m/A_1)\} \quad ,$$

$$F_D/J_a = -(J_2/J_a)\{(A_2/A_m)-1\}-\tfrac{1}{2}(A_m/A_j) \, (\Delta p_1/\Delta P_j) \qquad . \tag{105}$$

Table II summarizes design calculations for three eductors optimized around conventional conical diffusers, and summarizes the location of the forces which contribute to the augmentation. It is notable that the bellmouth inlet carries all the net thrust increase, and also most of the "negative thrust" generated in the diffuser. The importance of careful bellmouth design therefore is clear.

Table II

SUMMARY OF THREE "OPTIMUM EDUCTOR" DESIGN CALCULATIONS

Entrained air ratio n	5.000	10.000	15.000
Augmentation J_2/J_a	2.000	2.300	2.600
Diffuser efficiency η_D	0.960	0.945	0.940
Diffuser area ratio A_2/A_m	1.800	2.200	2.470
Diffuser diameter ratio d_2/d_m	1.340	1.490	1.570
Diffuser length ratio ℓ_D/d_m	6.530	9.220	10.920
Primary jet area ratio A_1/A_j	14.370	31.400	51.000
t_j/D_1 (jet ring diameter $=D_1$)	0.017	0.008	0.005
ℓ_m/t_j	143.000	461.000	935.000
ℓ_m/D_1	2.500	3.680	4.500
Mixing zone area ratio A_2/A_1	0.920	0.920	0.920
Mixing zone diameter ratio d_m/d_1	0.960	0.960	0.960
Bell mouth diameter ratio $d_B/d_1 =$	2.000	2.000	2.000
Mixing pressure $\Delta p_1/\Delta P_j$	-0.190	-0.150	-0.110

Breakdown of Location of Thrust Increase

Thrust increase $\left((J_2/J_a)-1\right)$	1.000	1.300	1.600
Primary jet nozzle	+0.092	+0.053	+0.036
Mixing chamber wall	+0.113	+0.129	+0.138
Diffuser wall	-0.363	-0.548	-0.719
Bellmouth lip	+1.158	+1.358	+1.545

PERFORMANCE OF A STATIC EDUCTOR OF ARBITRARY GEOMETRY

In the previous chapter, the "optimum eductor" was analyzed and defined as an eductor whose geometry is optimized for maximum performance. In this section the equations are rearranged to permit the performance of a specific augmentor to be calculated for static conditions.

There does not appear to be an explicit solution for an arbitrary eductor geometry, and a solution must be obtained by iteration, or by plotting two functions against the entrainment ratio n, in order to determine their intersection.

In an "optimum eductor", both the intake and exit areas are defined by the entrainment ratio (n). If the intake area (A_1) is already defined, there is still an optimum mixing pressure and, consequently, an optimum diffuser area ratio. The equations defining this optimum are defined later in this section.

<u>Performance Equations</u>

Since $A_m u_m = A_2 u_2$,

$$\Delta p_1 + \eta_D \tfrac{1}{2}\rho u_2^2 \ (A_2/A_m)^2 = \tfrac{1}{2}\rho u_2^2 \ ,$$

or $\quad \Delta \bar{p}_1 = -(u_2/u_j)^2 \ \left(\eta_D(A_2/A_m)^2 - 1 \right)$. (106)

Now $\quad J_2/J_o = (n + 1) \ (u_2/u_j)$, (107)

$$\Delta \bar{p}_1 = -(J_2/J_o)^2 \ \left(\eta_D(A_2/A_m)^2 - 1 \right)/(1 + n)^2 \ .$$ (108)

But $\quad (J_2/J_o)^2 = \Delta \bar{p}_1 \ (1 + n)^2 + \eta_D \left(1 + n \ (-\Delta \bar{p}_1)^{\frac{1}{2}} \right)$. (109)

Substituting Equation (108) for $\Delta \bar{p}_1$,

$$(J_2/J_o)^2 \ \left(1 + \{ \eta_D(A_2/A_m)^2 - 1 \} \ \{ 1 - (n^2 \eta_D/(1+n)^2) \} \right)$$ (110)

$$-2 \ (J_2/J_o) \ \left(n\eta_D/(1+n) \right) \ \left(\eta_D(A_2/A_m)^2 - 1 \right)^{\frac{1}{2}} - \eta_D = 0 \ ;$$

therefore,

$$J_2/J_o = (A_m/A_2) \left(1 + (n/n+1) \ \{ \eta_D - (A_m/A_2)^2 \}^{\frac{1}{2}} \right)/\left(1 - \{ n^2/(n+1)^2 \} \right)$$ (111)
$$\{ \eta_D - (A_m/A_2)^2 \} \right) \ .$$

Now

$$n = A_1/A_j \ (-\Delta \bar{p}_1)^{\frac{1}{2}}$$

59

$$= \left((A_1/A_j)(J_2/J_o) \ \{ \eta_D \ (A_2/A_m)^2 - 1 \}^{\frac{1}{2}} \right)/(n + 1) \tag{112}$$

from Equation (108). Therefore,

$$J_2/J_o = \left((A_m/A_2) \ (A_j/A_1) \ \{ n(n+1) \} \right)/\left(\eta_D - (A_m/A_2)^2 \right)^{\frac{1}{2}} \quad . \tag{113}$$

By evaluating Equations (111) and (113) for a range of n values, the point of coincidence may be determined, and hence both J_2/J_o and n. J_2/J_a is obtained by the relations

$$\Delta \bar{p}_1 = n^2 (A_j/A_1)^2$$

$$\Delta \bar{P}_j = 1 + \Delta \bar{p}_1$$

$$J_2/J_a = \ (J_2/J_o) \ (1/\Delta \bar{P}_j) \ = (J_2/J_o) \ / \ \{ 1 + n^2(A_j/A_1)^2 \} \quad . \tag{114}$$

Optimum Diffuser Area Ratio

From Equation (83) of the previous chapter,

$$\Delta \bar{p}_1 \Big|_{opt} = \cdot - n^2 \eta_D^2 \ / \ \left((n+1)^2 - n^2 \eta_D \right)^2 \tag{115}$$

and $\quad J_2/J_a = \left((n+1)^2 - n^2 \eta_D \right)^{3/2} \ (n+1) \ (\eta_D)^{\frac{1}{2}} \ / \ \left((n+1)^2 - n^2 \eta_D \right)^2 - n^2 \eta_D^2 \quad . \tag{116}$

From Equation (114),

$$n \Big|_{opt} = (A_1/A_j)(-\Delta \bar{p}_1 \Big|_{opt})^{\frac{1}{2}}$$

$$= (A_1/A_j) n \eta_D \ / \left((n+1)^2 - n^2 \eta_D \right) \ . \tag{117}$$

Therefore,

$$(1 - \eta_D) \, n^2 + \; 2n \; + \; 1 - (A_1/A_j) \eta_D \; = 0 \quad . \tag{118}$$

Therefore,

$$n = \; -1 + \left(\eta_D \, (1 - \eta_D) \, (A_1/A_j) + \eta_D \right)^{\frac{1}{2}} / \, (1 - \eta_D), \tag{119}$$

from which J_2/J_a can be determined from the calculations already available.

From Equation (108),

$$\left. A_2/A_m \right|_{opt} = \left(1/(\eta_D)^{\frac{1}{2}} \right) \left(1 + \; n^2 \eta_D / \{ (n+1)^2 - n^2 \eta_D \} \; \right)^{\frac{1}{2}} \tag{120}$$

$$= \left(\{ 1 + (A_j/A_1) \; n \Big|_{opt}^{2} \} / \; \eta_D \right)^{\frac{1}{2}} \quad . \tag{121}$$

Chapter 7

COMPARISONS BETWEEN THEORY AND EXPERIMENT
FOR STATIC EDUCTORS

THE LOCKHEED EXPERIMENTS

Reference 16 reports a comprehensive test program on two-dimensional eductors, similar to that used in the Lockheed XV-4A aircraft. Because of the large size of the models used, the measurements can be anticipated to be more than adequately accurate.

The total pressure loss through the duct was not measured separately, so that it is difficult to know what value to assign to the loss factor η_D. However, since both the diffuser semi-angle and the expansion ratio are conservative, it is reasonable to expect η_D to lie in the range 0.90 - 0.95.

The arbitrary geometry theory of the previous chapter has been worked out for the geometry of the Lockheed eductors, using η_D = 0.90 and 0.95.

As shown in Figure 24, the agreement obtained is good. From the positions of the experimental points relative to the theoretical curves, the actual loss factor η_D can be deduced. This is plotted in Figure 25. This variation seems reasonable.

The measured entrained air ratio (n) is seen in Figure 26 to be somewhat higher than the theoretical value, a result which may be attributable to the non-uniform flow distribution which occurs in practice.

In general, the agreement between theory and experiment appears good, and gives confidence that "optimum eductors" can be built with much better efficiencies. On the Lockheed eductors, for example, a simple redesign of the diffuser to give optimum mixing pressure should give the roughly 50 percent increase in augmentation noted in Figure 27. Improvement in diffuser efficiency would give a further increase, and should not be hard to achieve on this particular configuration.

A SURVEY OF EXPERIMENTAL RESULTS GIVEN IN THE LITERATURE

Table III lists the "best results" obtained by various investigators. That is to say, when an investigator experimentally measured the variation of J_2/J_a with some parameter, such as diffuser area ratio, for example, Table III lists the conditions under which he obtained the maximum value of J_2/J_a. It is usual to plot results such as these against a geometric area ratio, rather than the entrainment ratio (n),
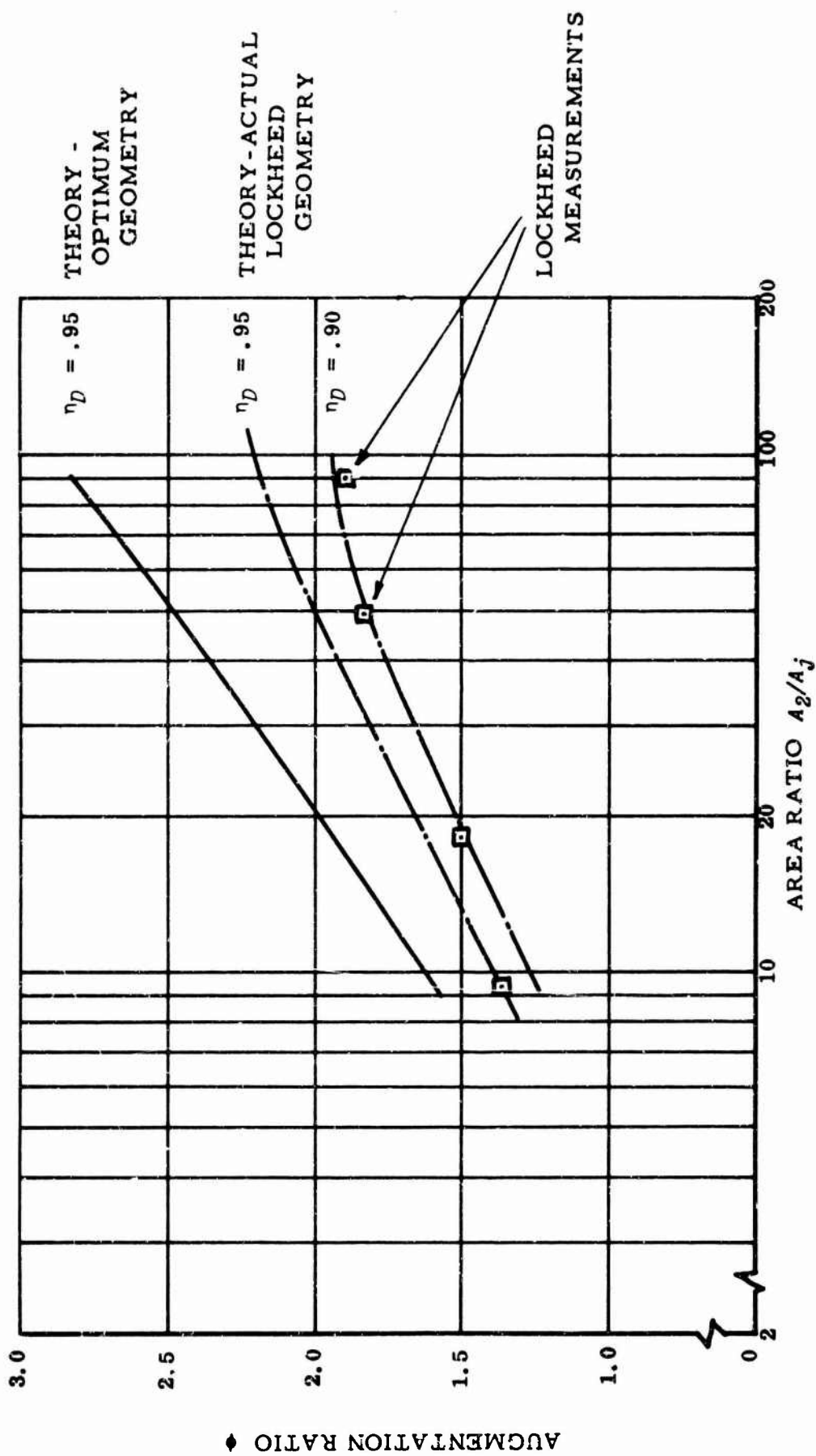
Figure 24. Performance of the Lockheed Eductors Compared With Theory.

THEORY - OPTIMUM GEOMETRY

$n_D = .95$

THEORY - ACTUAL LOCKHEED GEOMETRY

$n_D = .95$

LOCKHEED MEASUREMENTS

$n_D = .90$

AREA RATIO A_2/A_j

AUGMENTATION RATIO

63
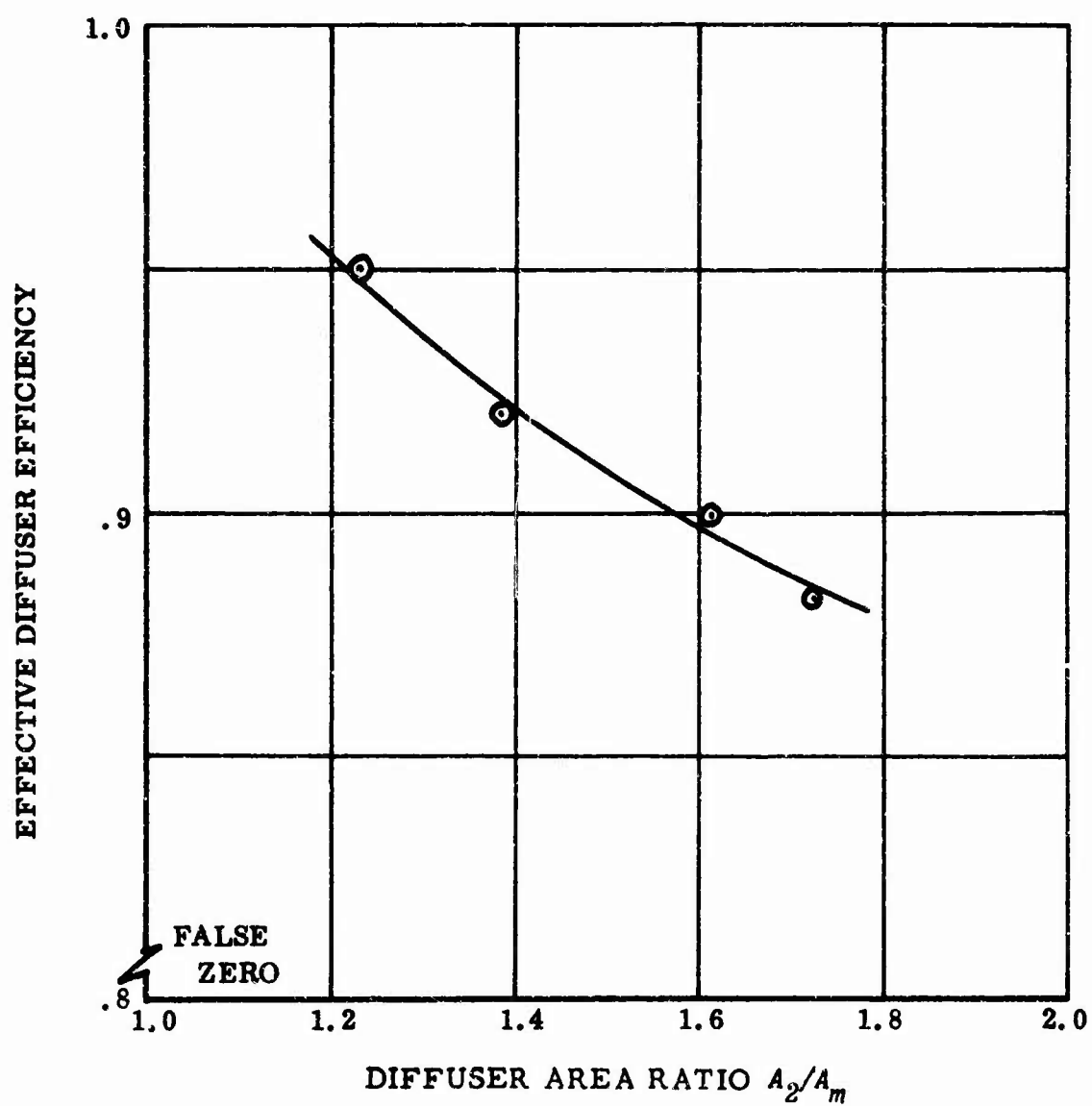
Figure 25.   Inferred Variation of Effective Diffuser Efficiency
With Area Ratio for the Lockheed Eductors.
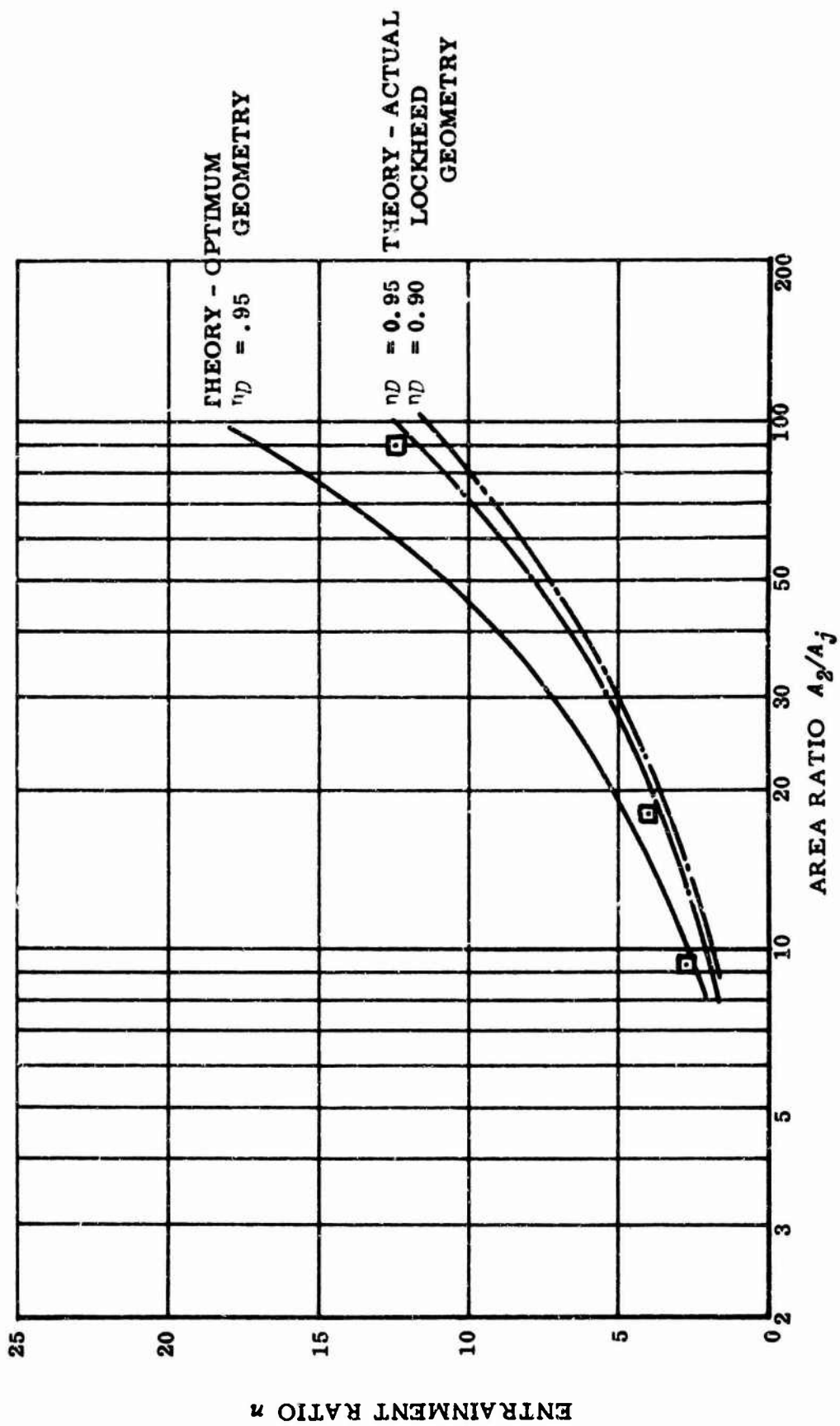
Figure 26. Predicted and Measured Mass Flow Ratio n for the Lockheed Eductors.

65

because (n) is rarely determined during test.

For parallel tube eductors, Figure 28 shows that the state of the art corresponds roughly to

$$J_2/J_a = 0.614 + 0.636 \ log_{10} \ (A/A_j) \ , \tag{122}$$

where A is the eductor tube cross-sectional area $(A_1 + A_2) = A_2$.

The highest augmentation was reported by Payne in Reference 11. It was achieved in a program directed by N. K. Walker, who was chiefly responsible for the excellence of the results.

It is of interest to note that the multi-staged eductors reported by Morrison in Reference 2 appear to show no advantage over the single stage when the eductor tubes are parallel-walled.

When the duct is not parallel, the appropriate area ratio for correlation is A_2/A_j . As shown in Figure 29, the "apparent state of the art" is now somewhat better for smaller entrainment ratios, being given by

$$J_2/J_a = 0.995 + 0.565 \ log_{10} \ (A_2/A_j) \ . \tag{123}$$

The Payne data points still give the highest augmentation and tend to depress the apparent state-of-the-art line below its true position at the higher area ratios, because they were obtained with constant area tubes. It is most probable that eductors fitted with diffusers would have achieved better results in this region of high area ratio.

In Figure 30 the data points are compared with the "optimum eductor" theory of this report. They correspond to equivalent diffuser efficiencies in the range 0.8 $< n_D < 0.9$. Since much of the inefficiency of the tested eductors must be charged to non-optimum mixing pressure, that is, incorrect area ratios, their actual internal losses will be less than Figure 30 implies. Probably, the Lockheed eductor losses inferred in Figure 25 are more generally representative.

The area ratio A_1/A_j is sometimes used as a means of correlating augmentation ratio. As shown in Figure 31, this does not reduce the scatter. Since it is a less fundamental parameter than A_2/A_j , its use is not recommended.

66
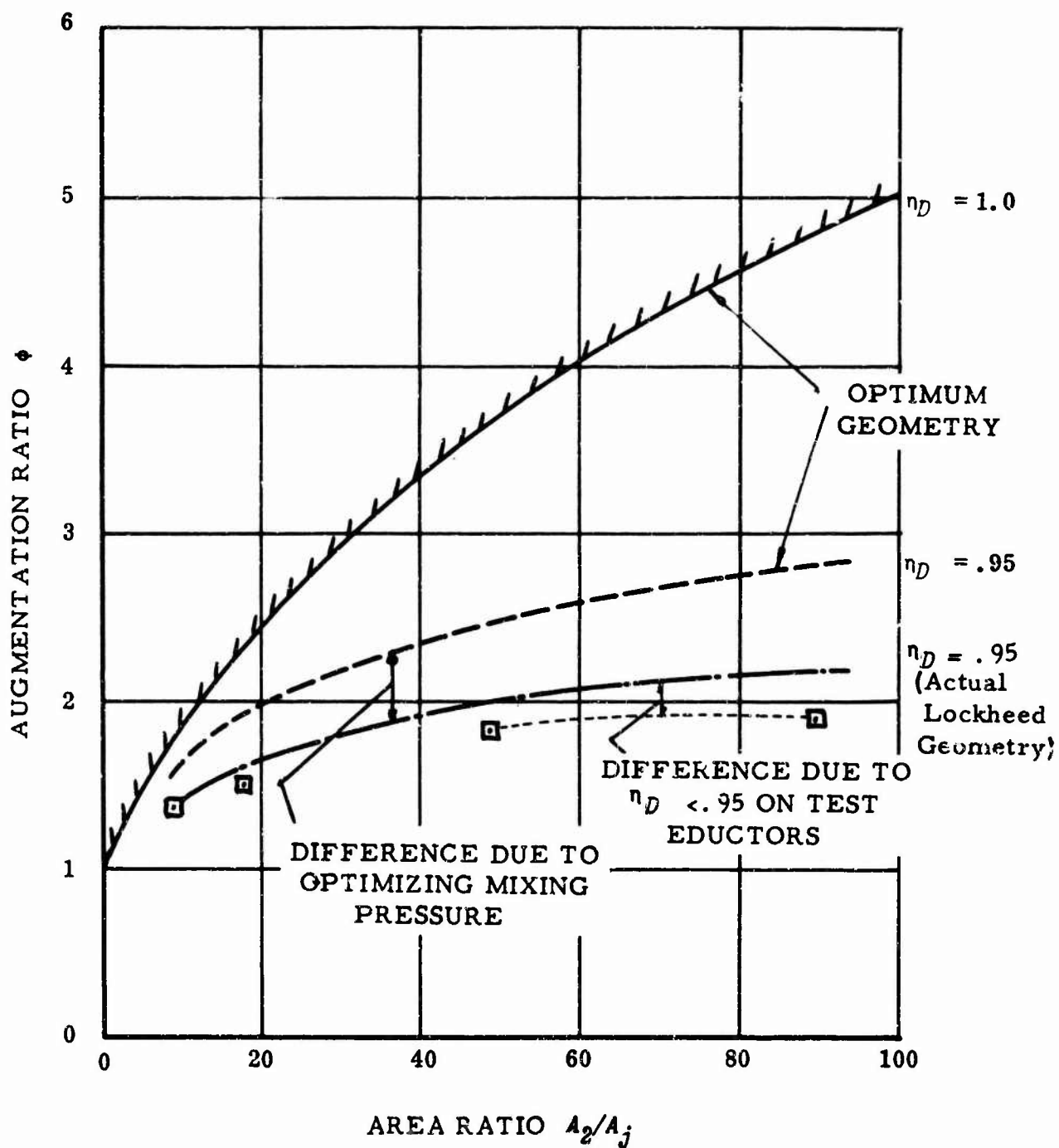
Figure 27. Performance of the Lockheed (Reference 1) Eductor Geometry as a Function of Diffuser Exit/Primary Nozzle Area Ratio.
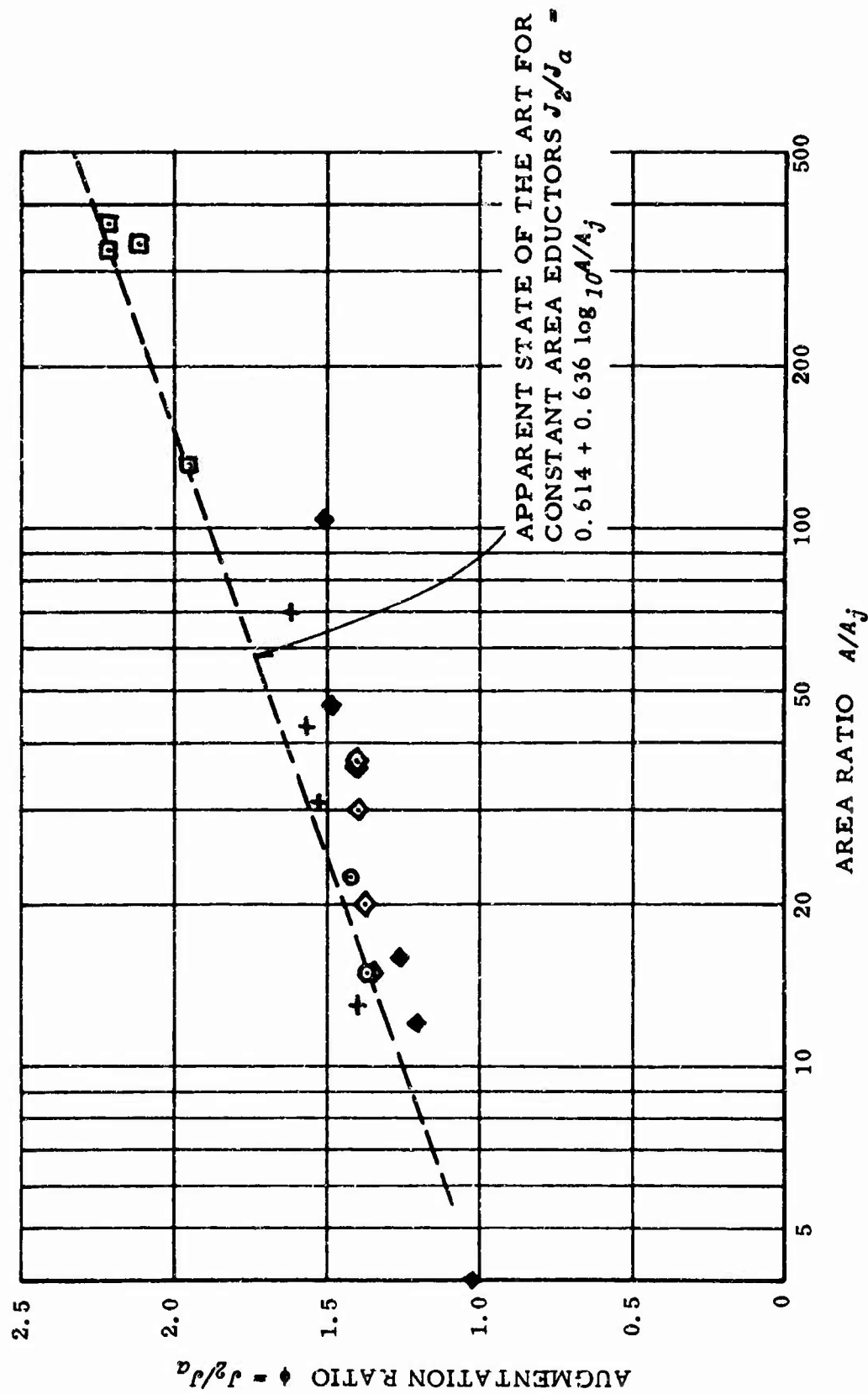
Figure 28. Best Augmentation Ratios Obtained by Various Investigators with Constant Area Eductors.
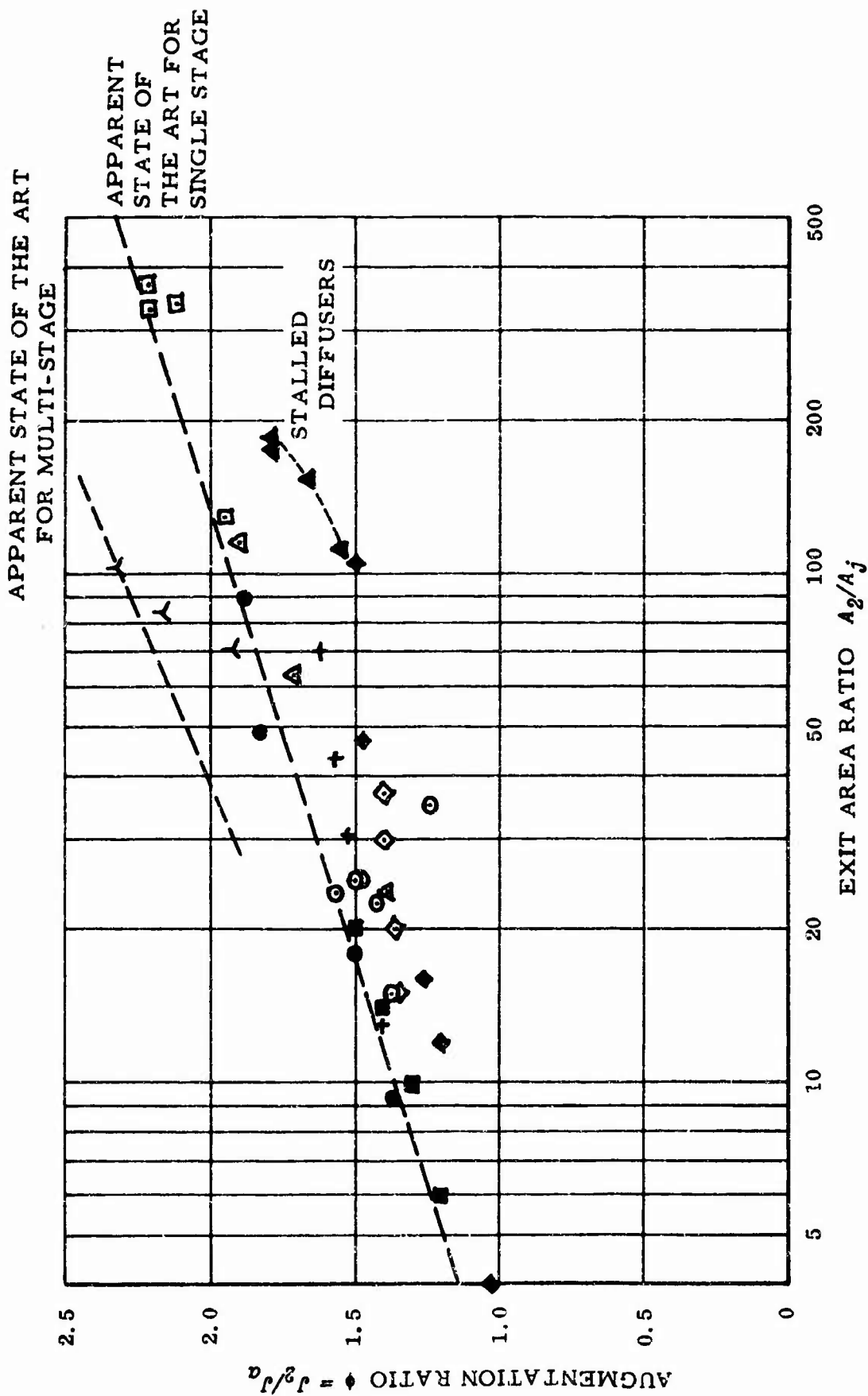
Figure 29. Best Augmentation Ratios Obtained by Various Investigators, as a Function of Exit Area Ratio.
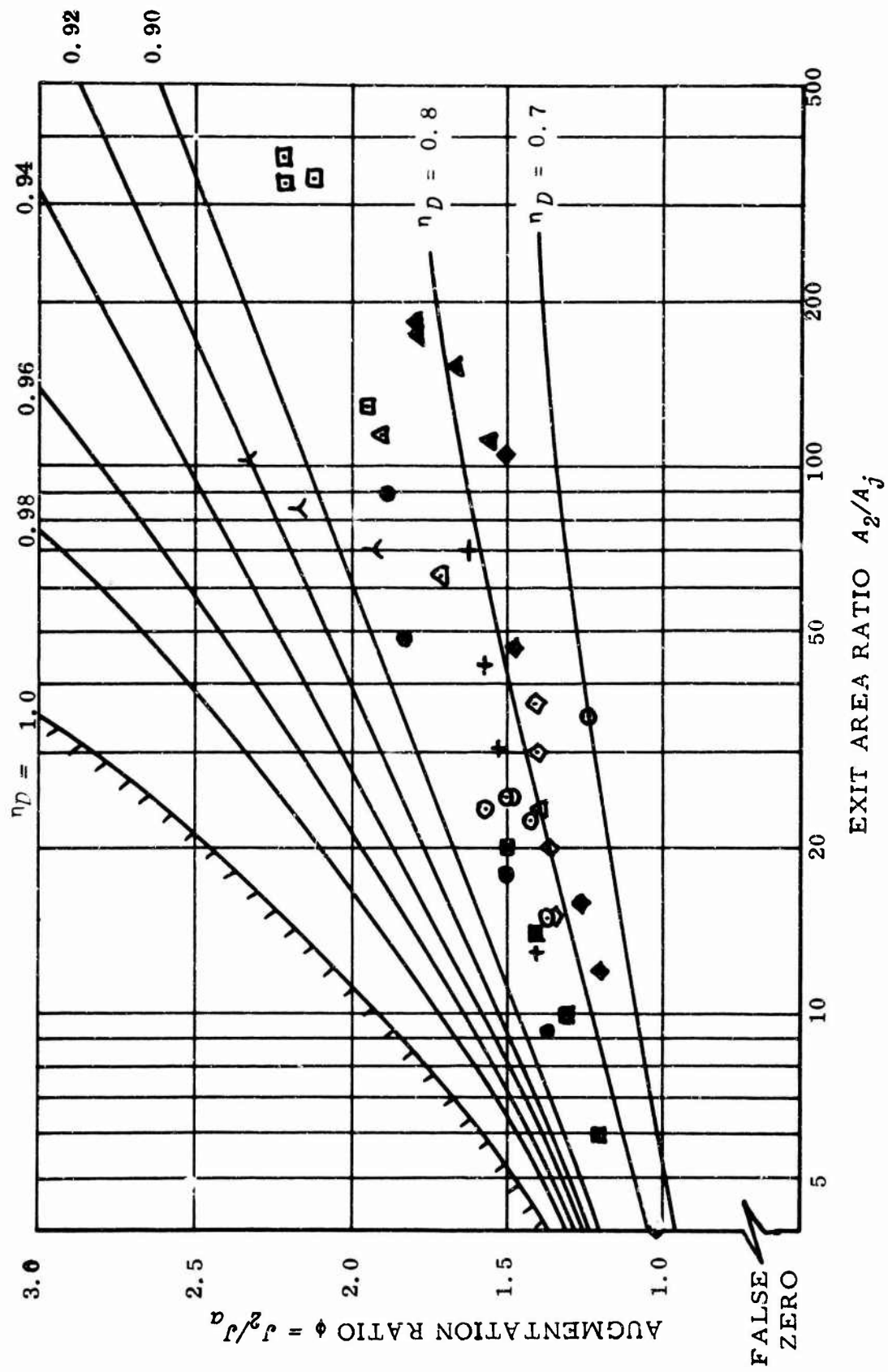
Figure 30. Comparison of Experimental Results with the "Optimum Augmentor" Theory of this Report.

70
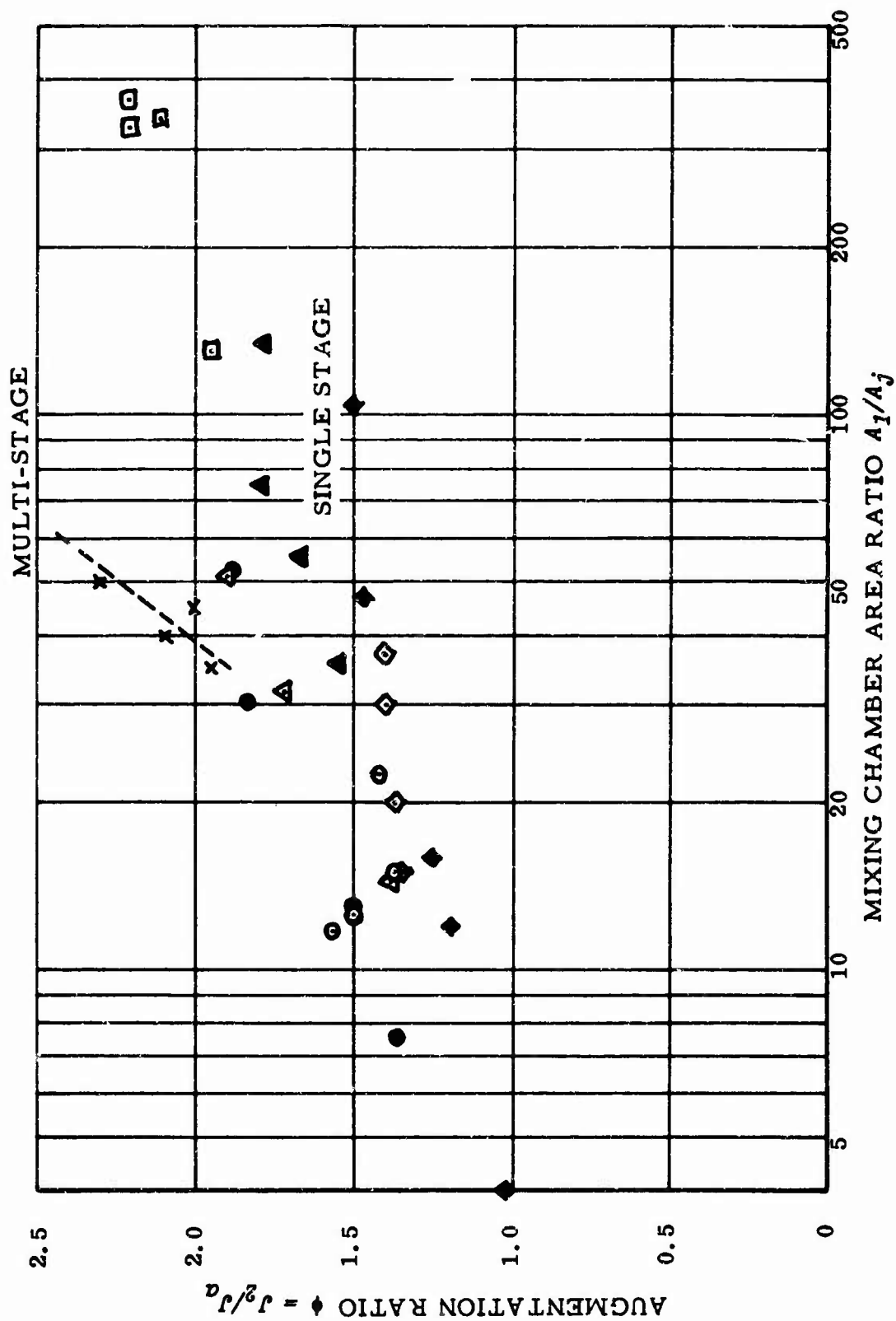
Figure 31. Best Augmentation Ratios Obtained by Various Investigators, as a Function of Mixing Chamber Area Ratio.

71

Table III
BEST AUGMENTATION RATIO MEASURED BY VARIOUS INVESTIGATORS

SINGLE STAGE STATIC EDUCTORS

SYMBOL	AUTHOR	A_2/A_1	A_1/A_j	A_2/A_j	J_2/J_a	REMARKS
◈	R. Morrison (Reference 2)	1.0	15.0	15.0	1.35	(Data Abstracted from Reference 17)
		1.0	20.0	20.0	1.37	
		1.0	30.0	30.0	1.40	
		1.0	37.0	37.0	1.40	
▣	Peter R. Payne (Reference 11)	1.0	130.5	130.5	1.95	Axisymmetric.
		1.0	340.0	340.0	2.11	
		1.0	330.0	330.0	2.21	No Diffuser.
		1.0	370.0	370.0	2.21	
●	G. L. Rabeneck P. K. Shunpert and J. F. Sutton (Reference 16)	1.73	52.0	90.0	1.89	2-D Models.
		1.61	30.3	48.8	1.83	
		1.38	13.0	18.0	1.50	
		1.23	7.55	9.3	1.36	
■	Jean Bertin (Reference 17)	----	----	6.0	1.20	Presumably Axisymmetric.
		----	----	10.0	1.30	
		----	----	14.0	1.40	
		----	----	20.0	1.50	
◉	M. F. Gates and J. W. Fairbanks (Reference 18)	2.0	12.5	25.0	1.50	2-D Model Test. 0° Diffuser Angle.
		1.0	15.0	15.0	1.37	0° Diffuser Angle.
		----	----	25.0	1.49	30° Diffuser Angle.
		---	----	35.0	1.245	60° Diffuser Angle.
		1.0	22.5	22.5	1.42	Axisymmetric.
		2.0	11.8	23.6	1.56	Axisymmetric.
▲	K. Cossairt (Reference 19) (TCREC 62-66)	3.11	35.5	111.0	1.55	Axisymmetric. Stalled Diffuser Flow.
		2.73	55.5	153.0	1.66	Stalled Diffuser
		2.36	74.4	177.0	1.79	Flow.
		1.36	135.5	189.0	1.78	
△	Peter R. Payne and Alastair Anthony (Reference 27)	1.65	14.4	23.8	1.39	Axisymmetric. Stalled Diffuser Flow.
		2.02	31.4	63.5	1.71	Stalled Diffuser
		2.27	51.0	115.8	1.90	Flow.

72

	Chia-An Wan (Reference 29)	1.0	4.0	4.0	1.03	Axisymmetric.
◆		1.0	12.0	12.0	1.20	
		1.0	16.0	16.0	1.26	
		1.0	36.0	36.0	1.40	
		1.0	47.0	47.0	1.48	
		1.0	105.0	105.0	1.50	

MULTI-STAGE EDUCTORS

SYMBOL	AUTHOR	No. of Stages	A_1/A_j	J_2/J_a	REMARKS
+	Reaves Morrison (Reference 2)	3	13.0	1.40	Data Taken From
		3	31.0	1.52	Reference 17.
		3	43.0	1.56	Constant Section
		3	70.0	1.62	Duct.
✕	Jean Bertin (Reference 17)	?	35.0	1.95	Possibly Three
		?	40.0	2.10	Stages.
		?	45.0	2.00	
		?	50.0	2.30	
			A_2/A_j	J_2/J_a	
⅄	Paul Guienne (Reference 17)	?	71.0	1.92	Possibly Three
		?	84.0	2.16	Stages.
		?	102.0	2.32	

Chapter 8

SOME SPECIAL SOLUTIONS

PERFORMANCE OF AN EDUCTOR IN AN AXIAL STREAM

Earlier in this report it was observed that the augmentation ratio can be expected to be less when an eductor is moving axially or is immersed in an axial stream. This phenomenon is due to two effects. First, the secondary airflow entering the eductor corresponds to a momentum drag of $n\dot{m}_j u_o$, and this can be wholly cancelled only by additional thrust if there are no losses in the eductor. Since loss must occur, and the energy content of the secondary fluid is relatively large, the eductor experiences a rapid fall-off in thrust with increasing speed.

The second reason is more fundamental. Relative to vehicle axes, the jet has a kinetic energy of $\frac{1}{2}\dot{m}_j u_j^2$. A certain ratio (ψ) of this can be transferred to the secondary flow. That is,

$$\frac{1}{2}n\dot{m}_j \ (u_2^2 - u_o^2) = \psi \ \frac{1}{2}\dot{m}_j u_j^2 \ ;$$

therefore,

$$(u_2/u_j)^2 = \psi/n \ + \ (u_o/u_j)^2 \quad . \tag{124}$$

But the thrust gain is given by

$$\Phi = \ n \ \left((u_2/u_j) \ - \ (u_o/u_j) \right)$$

$$= n\left(\{ (\psi /n) \ + \ (u_o/u_j)^2 \}^{\frac{1}{2}} - u_o/u_j \ \right) \ , \tag{125}$$

which tends to $\left(n\psi^{\frac{1}{2}} - n \ (u_o/u_j) \right)$ as $(u_o/u_j) \to 0$.

Consequently, as the axial speed increases, the same energy exchange between the primary and secondary flows is progressively of less value in producing a thrust increase.

Expressing the previously given general eductor theory in a form more suitable for studying this effect, the augmentation ratio is

$$J_2/J_a = \left((n+1)\dot{m}_j u_2 - n\dot{m}_j u_o \right) / \dot{m}_{ja} u_{ja} \tag{126}$$

$$= (\dot{m}_j/\dot{m}_{ja})^2 \ (u_2/u_j) \ (n+1) - (\dot{m}_j/\dot{m}_{ja})^2 \ (u_o/u_j) \ n \tag{127}$$

$$= \left(1/\Delta\bar{P}_j\right) \left(\Delta\bar{p}_1 \ (n+1)^2 + \eta_D \ (\ 1+n \ \{(u_o/u_j)^2 - \Delta\bar{p}_1 \ )^2 \}^{\frac{1}{2}} - n \, u_o/u_j \right) \tag{128}$$
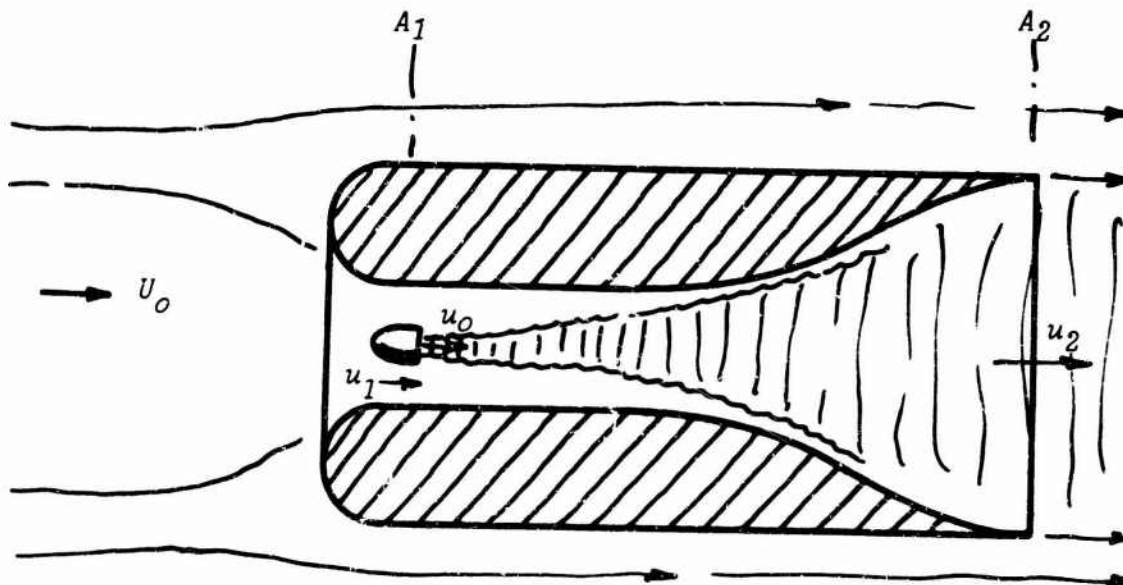
Figure 32.   Augmentor in an Axial Stream.

Taking the optimum value of $\Delta \bar{p}_1$ given by Equation (83) .

$$\left. J_2/J_o \right|_{opt} = \left((n+1)/\Delta\bar{P}_j\right)\left(\{\eta_D/\{(n+1)^2-n^2\eta_D\}+(v_o/u_j)^2\}^{\frac{1}{2}}\right. \tag{129}$$
$$\left. -\{n/(n+1)\}(u_o/u_j)\right) .$$

From Equations (91) and (92), therefore,

$$(n+1)/\Delta\bar{P}_j = \left(\{(n+1)^2-n^2\eta_D\}^2 (n+1)\right) / \left(\{(n+1)^2-n^2\eta_D\}^2-n^2\eta_D^2\right) . \tag{130}$$

Thus, Equations (129) and (130) give an explicit variation of $J_2/J_a|_{opt}$ with the velocity ratio u_o/u_j . To determine variation with u_o , u_j must be calculated.

Now $\Delta P_j = \Delta p_1 + \frac{1}{2}\rho u_j^2$;

therefore,

$$\frac{1}{2}\rho u_j^2 = \Delta P_j \left(1- \Delta p_1/\Delta P_j \right) \tag{131}$$

$$= \Delta P_j/\Delta\bar{P}_j \qquad \text{from Equation (132).} \quad \text{Therefore,}$$

$$(u_o/u_j)^2 = (\Delta P_o/\Delta\bar{P}_j)\, \Delta\bar{P}_j , \tag{132}$$

$$(u_o/u_j)^2 = \left(\{(n+1)^2-n^2\eta_D\}^2-n^2\eta_D^2\right)/\left((n+1)^2-n^2\eta_D\right)^2 . \tag{133}$$

Thus, Equations (129), (130), and (133) completely determine the augmentation ratio as a function of $\Delta P_o/\Delta P_j$. They are used to produce the curves of augmentation ratio, as a function of n and $\Delta P_o/\Delta P_j$ in Figures 33 – 36, taking a typical loss coefficient of η_D = 0.95.

It is evident that a significant degree of augmentation is obtained only when the total pressure ratio $\Delta P_o/\Delta P_j$ is quite low. However, there may be applications where this requirement is met. An example might be the application of an eductor to water jet propulsion of a ship, where the eductor intake is immersed in the ship boundary layer so that its effective intake velocity is much lower than u_o .
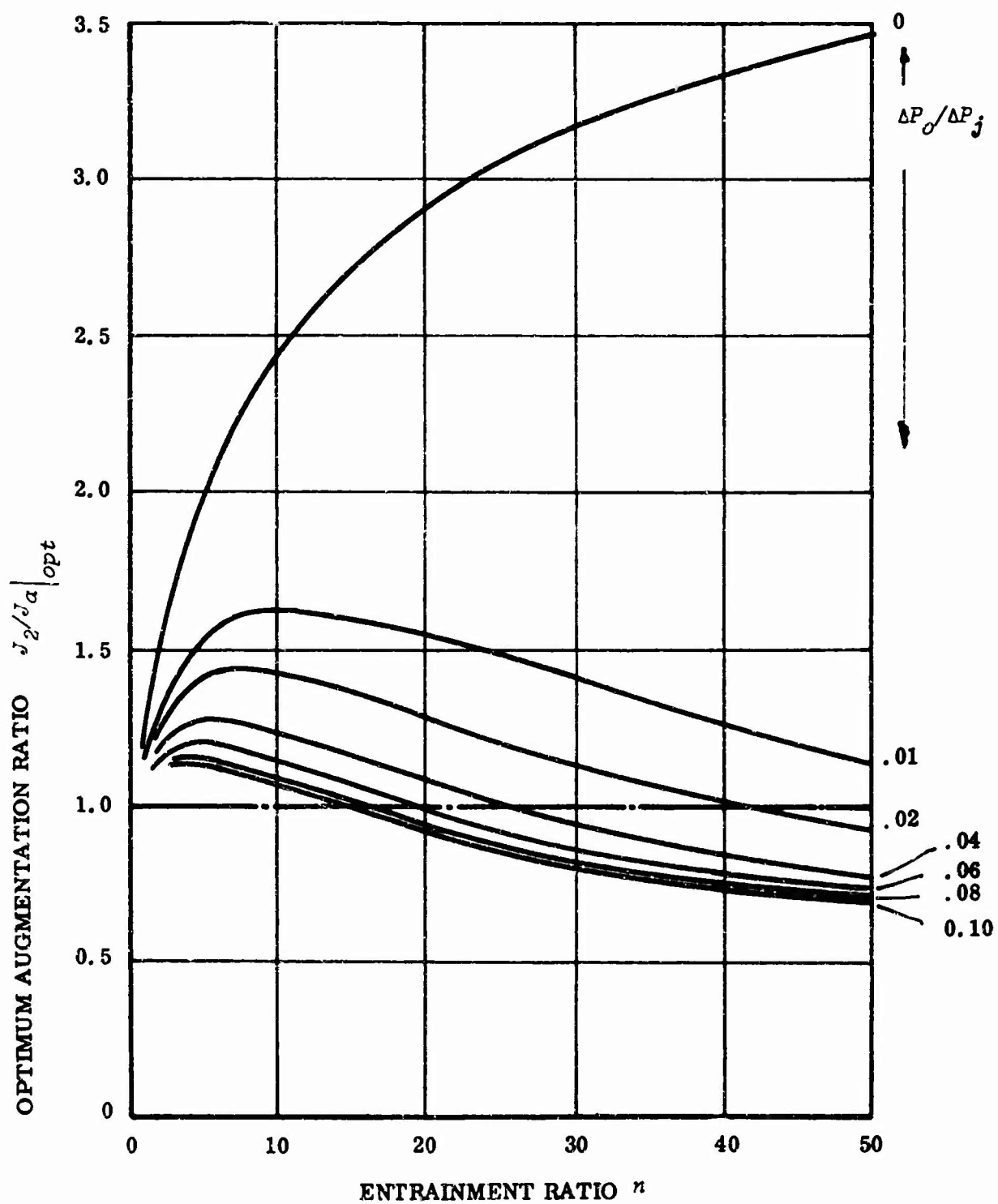
Figure 33.   Variation of Augmentation Ratio with Entrainment
Ratio n and Total Pressure Ratio $\Delta P_o/\Delta P_j$
(η_D = 0.95).

77
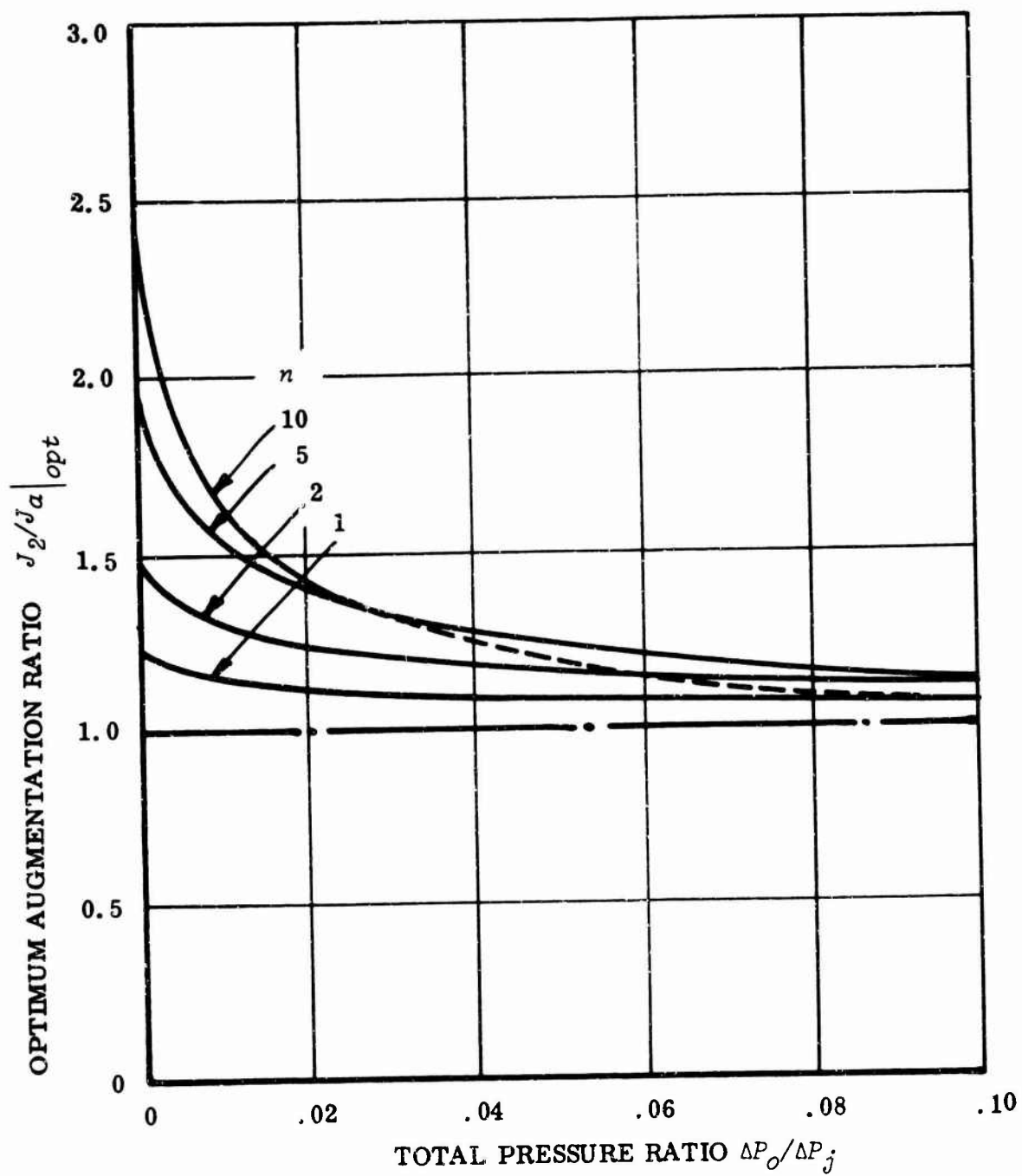
Figure 34. Cross-Plot of Figure 33 for Low Entrainment Ratios.
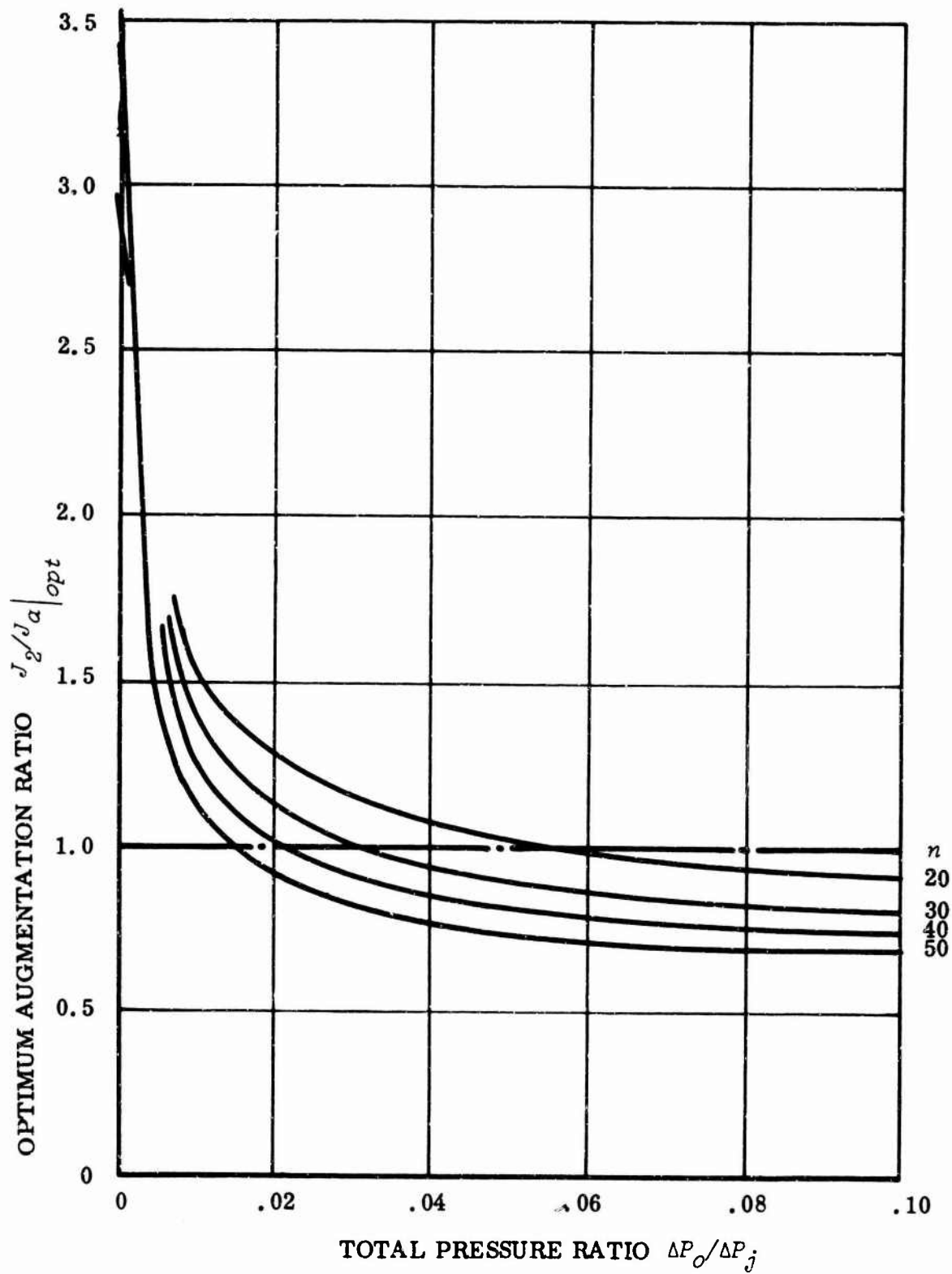
Figure 35.   Cross-Plot of Figure 33 for High
Entrainment Ratios.
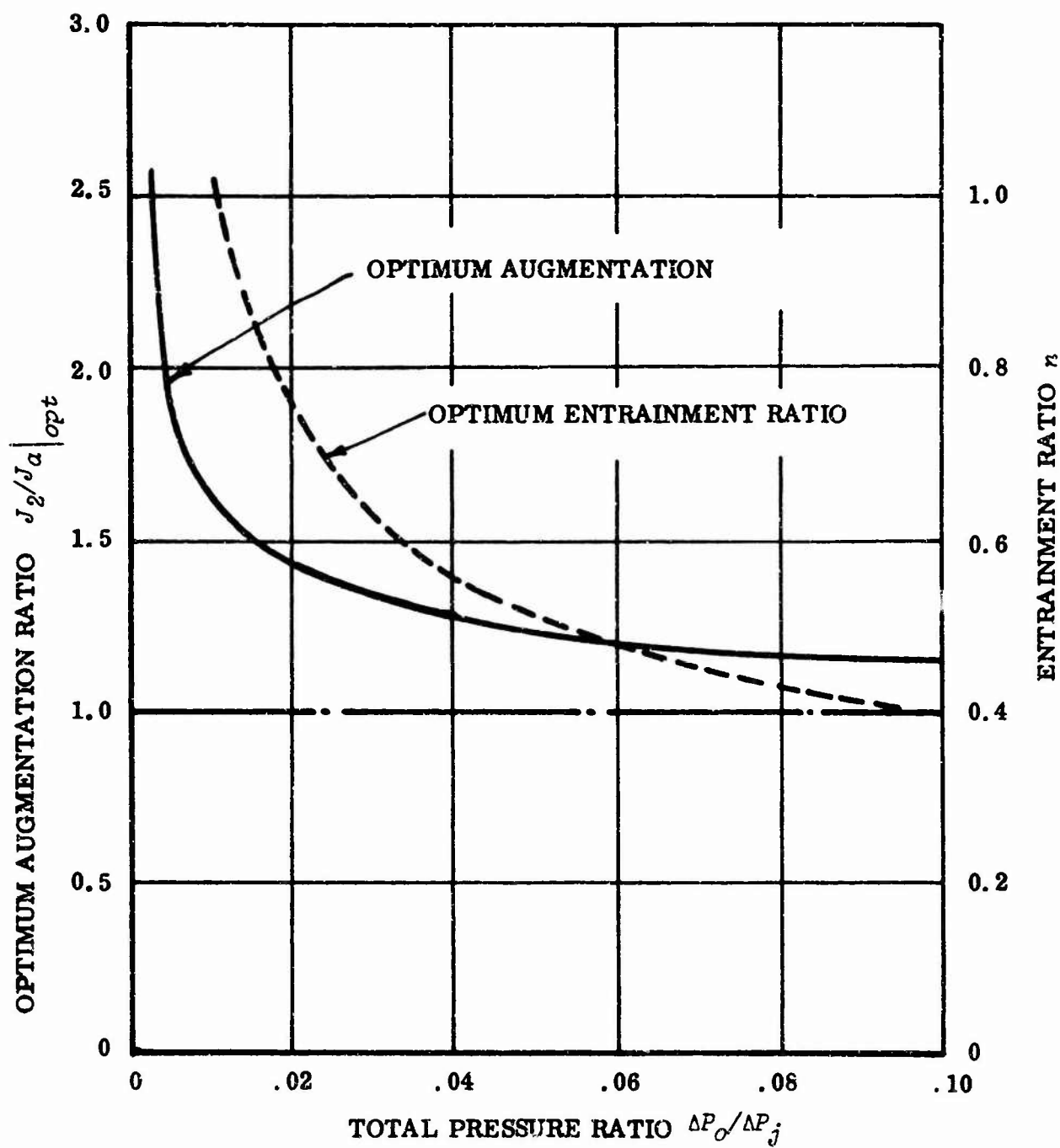
Figure 36.   Best Possible Augmentation Ratio, as a
Function of the Pressure Ratio $\Delta P_o / \Delta P_j$
(η_D = 0.95).

THE TOTAL HEAD RISE ATTAINABLE THROUGH AN EDUCTOR

In the application of eductor technology to many problems, the total head rise through the eductor may be of greater interest than its thrust or force augmentation. The Martin recirculation GEM lift system (Reference 19) is a particularly good example. The theory of earlier chapters of this report is accordingly reworked in this section to include an analysis of total pressure.

Since
$$\Delta p_2 + \tfrac{1}{2}\rho u_2^2 = \Delta p_1 + \eta_D \tfrac{1}{2}\rho u_j^2 \left(1+n(u_1/u_j)\right)^2/(n+1)^2 \; , \tag{134}$$

the total pressure rise through the eductor is

$$\Delta H = \Delta P_2 - \Delta P_1 = \eta_D \tfrac{1}{2}\rho u_j^2\left(\{1+n(u_1/u_j)\}^2/(n+1)^2\right) - \tfrac{1}{2}\rho u_1^2 \tag{135}$$

$$\Delta H/\tfrac{1}{2}\rho \, u_j^2$$

$$= \left(\eta_D/(n+1)^2\right) + \left(2n\eta_D/(n+1)^2\right)(u_1/u_j) + \left(n^2\eta_D/(n+1)^2 - 1\right)(u_1/u_j)^2 \; . \tag{136}$$

Differentiating with respect to (u_1/u_j) and equating to zero to find the value of (u_1/u_j) for maximum total head rise,

$$2n\eta_D/(n+1)^2 = 2(u_1/u_j)\left(1 - \{n^2\eta_D/(n+1)^2\}\right)$$

$$\left.u_1/u_j\right|_{opt} = n\eta_D/\left((n+1)^2 - n^2\eta_D\right) \; . \tag{137}$$

Substituting Equation (137) in Equation (136),

$$\left.\Delta H/\tfrac{1}{2}\rho \, u_j^2\right|_{opt} = \eta_D/\left((n+1)^2 - n^2\eta_D\right) \tag{138}$$

81

or
$$\left. \Delta H / \tfrac{1}{2}\rho\, u_0^2 \right|_{opt} = (1/n)(u_1/u_j) \Big|_{opt} \quad . \tag{139}$$

Note that since

$$\Delta \bar{p}_1 = \Delta p_1 / \tfrac{1}{2}\rho\, u_0^2 = \Delta P_c - \tfrac{1}{2}\rho\, u_1^2 / \tfrac{1}{2}\rho\, u_0^2 = \Delta \bar{P}_c - (u_1/u_j)^2 \quad ,$$

$$\Delta \bar{p}_1 \Big|_{opt} = \Delta \bar{P}_c - n^2 \eta_D^2 / \{ (n+1)^2 - n^2 \eta_D \}^2 \quad . \tag{140}$$

This is the same optimum mixing pressure as that obtained earlier for maximum thrust augmentation. Thus, optimization for maximum total head rise gives the same geometry as optimization for maximum thrust augmentation.

RECIRCULATING EDUCTORS

In this section, the "optimum eductor" concept is extended to include the effect of recirculation. Examples of recirculating eductors are jet-driven gas or water tunnels, and the Martin recirculating GEM system (Reference 19).

When the diffuser exit static pressure is equal to ambient, Equation (84) becomes

$$J_2/J_a \Big|_{opt}^2 = J_2/J_a \Big|_{P_c=0}^2 + (n+1)^2 (\Delta P_c / \Delta P_j)\, 1/\Delta P_j \quad , \tag{141}$$

the second term being the effect of the increase above ambient of the inlet total head.

Now, since

$$J_2/J_a = (1/\Delta \bar{P}_j)(J_2/J_0) = \left((n+1)/\Delta \bar{P}_j \right)(u_2/u_j) \tag{142}$$

$$u_2 = \Delta \bar{P}_j\, (J_2/J_a)\, u_j/(n+1) \quad , \tag{143}$$
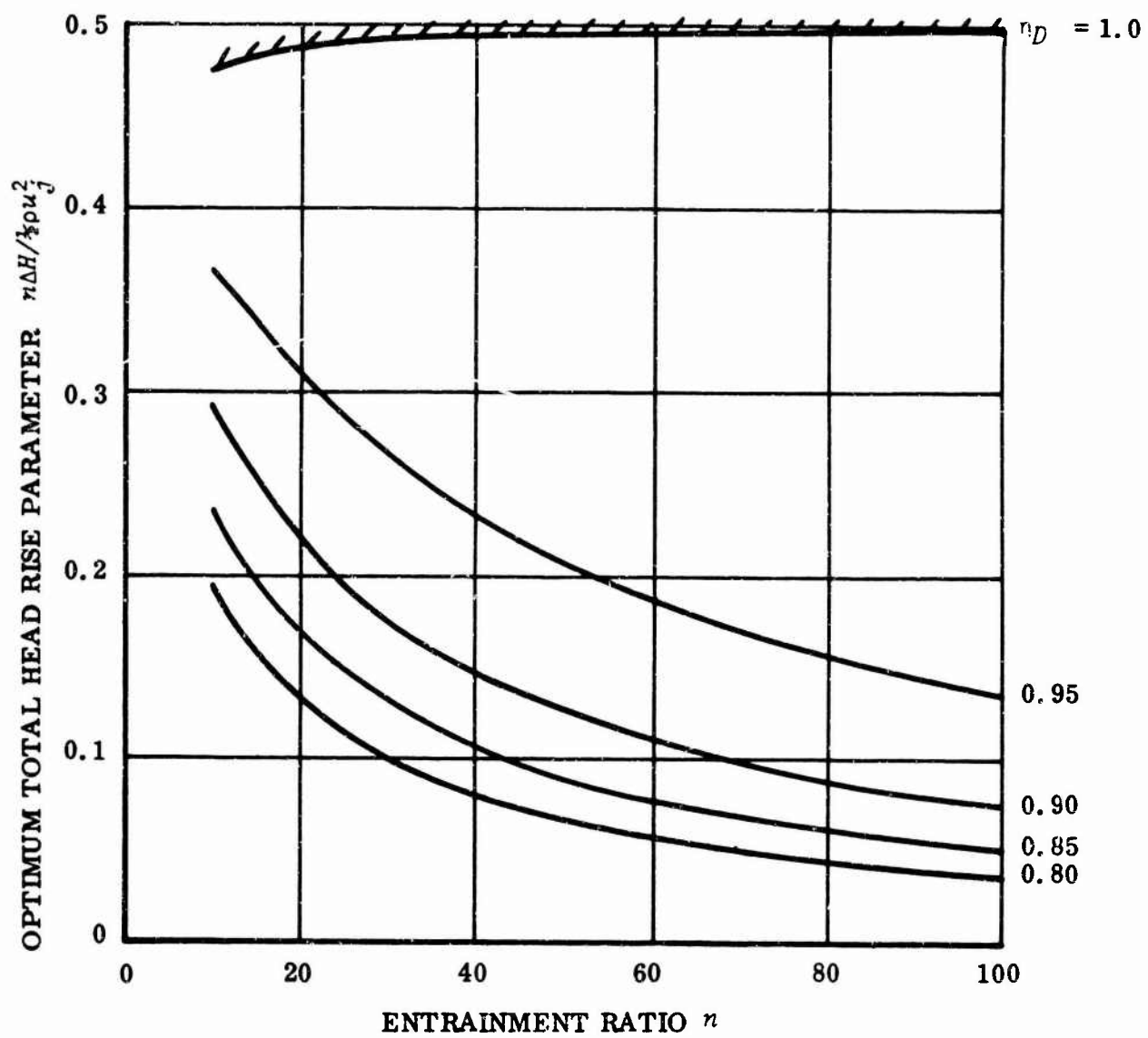
Figure 37.   Variation of Optimum Mixing Velocity Ratio
for Large Entrainment Ratios.

$$\Delta P_2 / \Delta P_j = \tfrac{1}{2} \rho \, u_2^2 / \Delta P_j = \Delta \bar{P}_j \, (J_2 / J_a)^2 \; i / (1+n)^2$$

$$\Delta P_c / \Delta P_j = \xi \Delta P_2 / \Delta P_j = \left(\xi \Delta \bar{P}_j / (n+1)^2 \right) (J_2 / J_a)^2 \quad . \tag{144}$$

Substituting in Equation (141),

$$(J_2 / J_a)^2 = (J_2 / J_a)^2_{\;P_c=0} + \xi (J_2 / J_a)^2 \quad ; \tag{145}$$

therefore,

$$\left. J_2 / J_a \right|_{opt} = \left(1 / (1-\xi)^{\tfrac{1}{2}} \right) (J_2 / J_a)_{\substack{opt \\ P_c=0}} \tag{146}$$

ξ being the total head recovery factor.

Thus, optimum static eductor curves can be used directly to find the optimum augmentation possible with recirculation.

For ξ = 20%   40%   60%   80%   90%
      $1/(1-\xi)^{\tfrac{1}{2}}$ = 1.117   1.29   1.58   2.235   3.16 .

In other words, the thrust increase due to recirculation is not particularly under optimum conditions, until the total head loss falls below 20 percent. Such a low head loss is difficult to achieve.

SOME EDUCTOR COMPONENT DESIGN CONSIDERATIONS

The quality of the eductor design has so far been considered only in terms of "effective diffuser efficiency" (η_D), which accounts for all the total pressure losses attributable to the duct or shroud. It is clear that the value of (η_D) actually achieved will depend largely upon the skill with which the duct is shaped. The purpose of this chapter is to review briefly the major design variables which influence overall performance.

It should be recognized that, in addition to mixing losses, there are four main sources of energy loss:

1. Intake loss.
2. Loss attributable to the secondary air flowing past the primary nozzles.
3. Wall skin-friction loss in the mixing chamber.
4. Diffuser loss.

The reference velocity for the first three of these can conveniently be u_1 . Thus, if $(1 - \eta_n)$ $\frac{1}{2}\rho u_1^2$ is the loss involved,

$$\left[(1-\eta_1) + (1-\eta_2) + (1-\eta_3) \right] \tfrac{1}{2}\rho u_1^2 = (1-\eta_{DE}) \tfrac{1}{2}\rho u_m^2 \quad ;$$

therefore,

$$(1-\eta_{DE}) = (u_1/u_m)^2 \sum (1-\eta_n) . \tag{147}$$

From Equation (76) ,

$$u_j/u_m = (n+1)/(1+n u_1/u_j) \quad ;$$

therefore,

$$u_1/u_m = (u_j/u_m) (u_1/u_j) = (n+1)/\left((u_j/u_1)+n \right) . \tag{148}$$

This is plotted in Figure 38 for a typical optimum eductor. Note that, particularly at the smaller entrainment ratios, a change in an upstream component efficiency η_n causes a significantly smaller change in the effective diffuser efficiency η_D . In part, then, this constitutes some justification for the
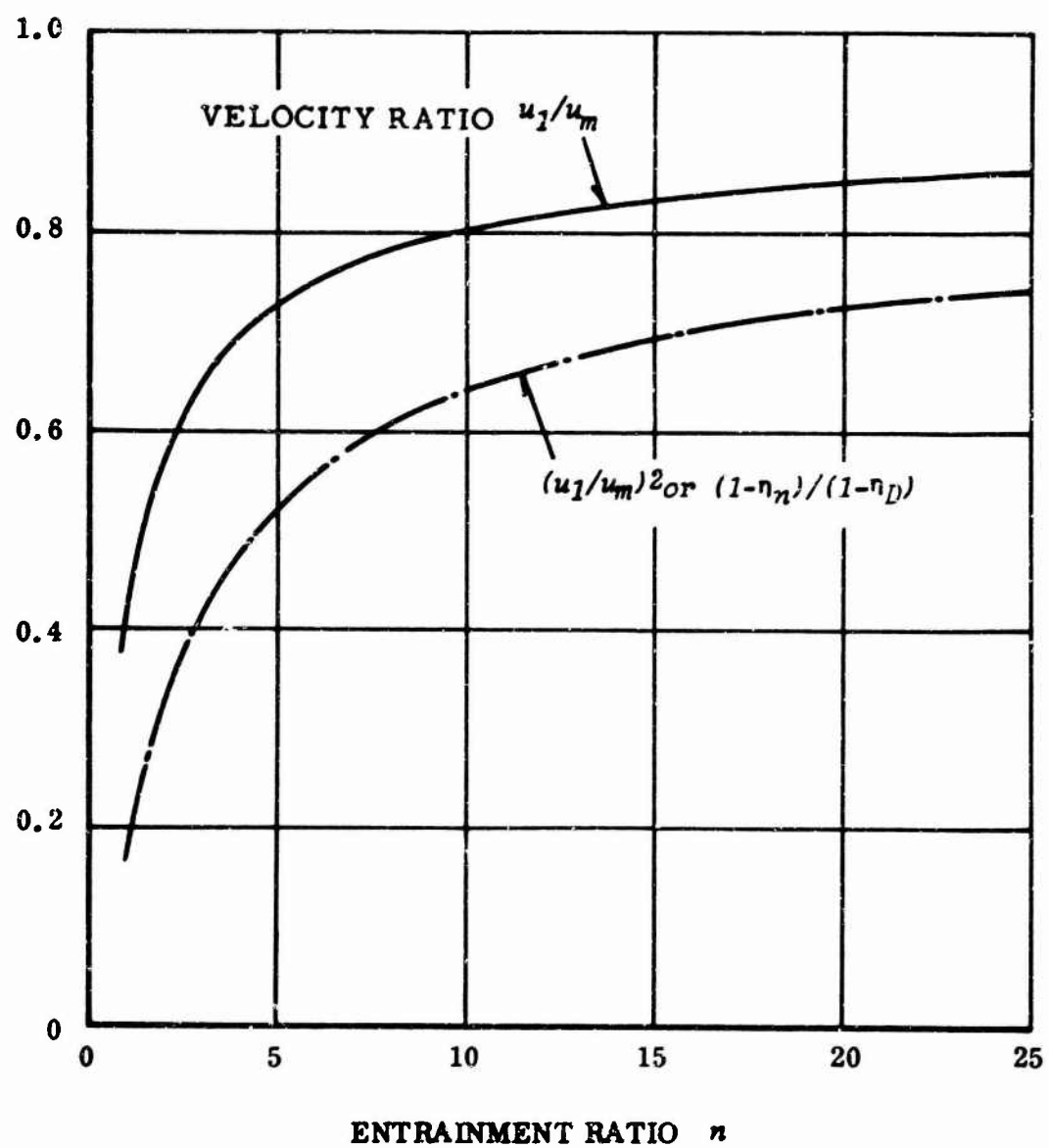
Figure 38. Typical Variation of the Velocity Ratio (u_1/u_m) with Entrainment Ratio for a Diffuser Efficiency $\eta_D = 0.9$.

simplification introduced by referring all losses to the diffuser throat position.

THE INTAKE LOSS

In Reference 16, Rabeneck et al considered an eductor whose bellmouth intake lip was made up of a circular arc. After testing various lip sizes, they concluded:

"An entrance radius approximately equal to the ejector mixing section width appears to be optimum. A radius of 0.40 times the mixing section width, however, results in only a 2.5 percent reduction in augmentation factor.

"Ejector performance is sensitive to ejector entrance total pressure losses in the secondary stream."

Other experimenters have also pointed out that their results appear sensitive to both the size and the shape of the inlet, although without suggesting any underlying reason. The following arguments are presented as an explanation for at least some of the observed anomalies.

When a fluid flows around a curved surface, the centrifugal force field generated in the flow results in the wall static pressure's being lower than it would be in rectilinear flow under the same conditions. Among other references, this subject is discussed in detail by Payne and Anthony in Reference 84.

If this curved surface is tangential to a straight surface, the fluid near the wall must experience a rapid increase in static pressure when it passes the point of tangency. This amounts to a "rapid diffusion" from a velocity u_1 to a lower velocity u_2, which Payne and Anthony have shown to result in a total pressure loss,

$$\Delta H / \tfrac{1}{2} \rho \, u_1^2 = \left(1 - (u_2 / u_1) \right)^2 \quad . \tag{149}$$

An example of such a rapid diffusion just behind a bellmouth is given in Figure 39, the diffusion taking place between pressure taps 8 and 10.

It follows that a discontinuity in curvature is undesirable in an inlet. Also, it is preferable to design for an approximately uniform wall pressure, minimizing the diffusion necessary at the bellmouth exit, assuming that it is distributed over a finite wall length. There is a real need for both theoretical and experimental

87

0.4" RADIUS

1/496"   1.434" - DIAMETER OF DUCT - 2.25"

WALL STATIC PRESSURE IN LB. /FT. ^{2}

(SUCKING AT OUTLET
WITH INLET OPEN)

DISTANCE ALONG WALL IN INCHES

Figure 39.   Static Pressure Along an Axisymmetric
Eductor - Payne, Inc. , Data.
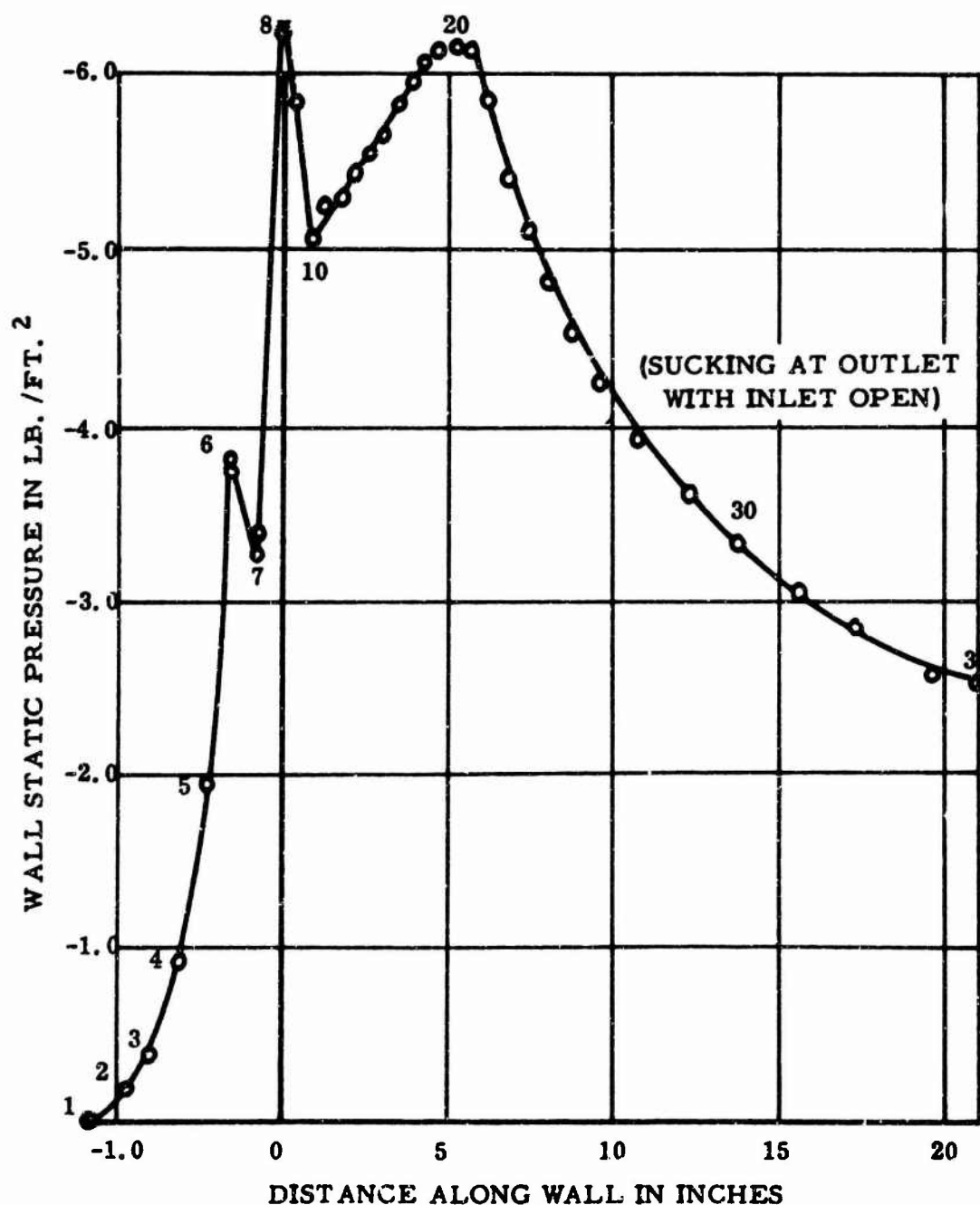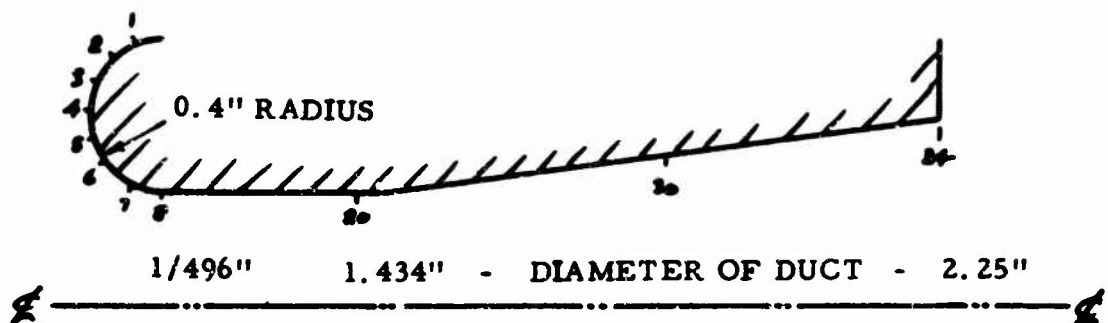
investigations of bellmouth inlets designed to such criteria. Almost all work to date has been ac hoc in nature. In particular, it should be noted that although an empirically designed bellmouth may have small losses by normal standards, these losses may still cause a major loss of thrust augmentation in an eductor application.

The smallest bellmouth is likely to be one with a constant wall pressure. Two-dimensional solutions exist for this case: the free-boundary Borda-mouthpiece solution, and the free-boundary solution for fluid issuing from a sharp-edged aperture. From Lamb (Reference 85, Art. 74), the solution for the Borda-mouthpiece is

$$x = (2b/\pi)(\sin^2 \tfrac{1}{2}\theta - \log \sec \tfrac{1}{2}\theta)$$

$$y = (b/\pi)(\theta - \sin \theta) \ ,$$

(150)

where $2b$ = final distance between walls .

Also from Lamb, Art. 75, the jet issuing from a <u>sharp-edged aperture</u> has a boundary defined by

$$x = (4b/\pi) \sin^2 \tfrac{1}{2}\theta$$

$$y = (2b/\pi)\{\log \tan \left[(\pi/4) + (\theta/2)\right] - \sin \theta\}$$

$$0 < \theta < \tfrac{1}{2}\pi \quad .$$

(151)

The first of these solutions is appropriate to the intake of a static eductor, where the entrained air can flow from any direction between 0 and 180° to the eductor axis. The second solution is appropriate for an intake mounted in a plane wall.

Since either curve is asymptotic only to a parallel duct, it might seem that at some point the theoretical curve must be empirically faired into the duct wall of the mixing chamber. However, in order to maintain constant static pressure, it

is necessary to progressively reduce the area of the mixing chamber moving downstream from the nozzles. This compromise can therefore be minimized by continuing part of the theoretical intake curve into the mixing chamber.

The free-streamline solutions given earlier in this section are for two-dimensional flow. A convenient method of applying them to the axisymmetric case is to assume that the ordinate y is proportional to the square of the radius. The accuracy of this method is not known. The only justification for its use is that it is frequently employed and often gives good results.

The axisymmetric Borda-mouthpiece streamline obtained in this way is given in Figure 40 and Table IV, together with the two-dimensional solution from which it was derived.

THE PRIMARY NOZZLE LOSS

The secondary air flowing past the primary nozzles suffers a total pressure loss which corresponds to the "drag" force which it develops on the nozzles. In terms of one-dimensional flow, the total pressure loss is given by

$$A_1 \Delta P_1 = (A_N C_{DN}) \tfrac{1}{2} \rho u_1^2 \qquad . \tag{152}$$

The nozzle drag coefficient C_{DN} will be higher than for a similar body in an infinite stream, for two reasons. In the first place, its proximity to the eductor walls will give rise to a "wind channel blockage" effect. Secondly, the "jet drag" effect identified by Payne and Anthony in Reference 30 will give rise to lower static pressures on the downstream faces of the primary nozzle array, further increasing its apparent drag in the surrounding secondary flow. The magnitude of both these effects depends upon the primary nozzle geometry.

By moving the primary nozzles out from the throat of the inlet bellmouth, they enter a region of lower primary flow velocity and hence reduce the magnitude of these losses. However, this now means that some of the mixing occurs at a greater static pressure than that prevailing in the mixing tube, so that the eductor efficiency is reduced. Thus, there is an optimum axial position for a given nozzle array and bellmouth, which will depend upon individual geometrical variables. Any simple generalization, such as some investigators have been tempted to make on the basis of isolated tests, is not necessarily applicable to new designs.
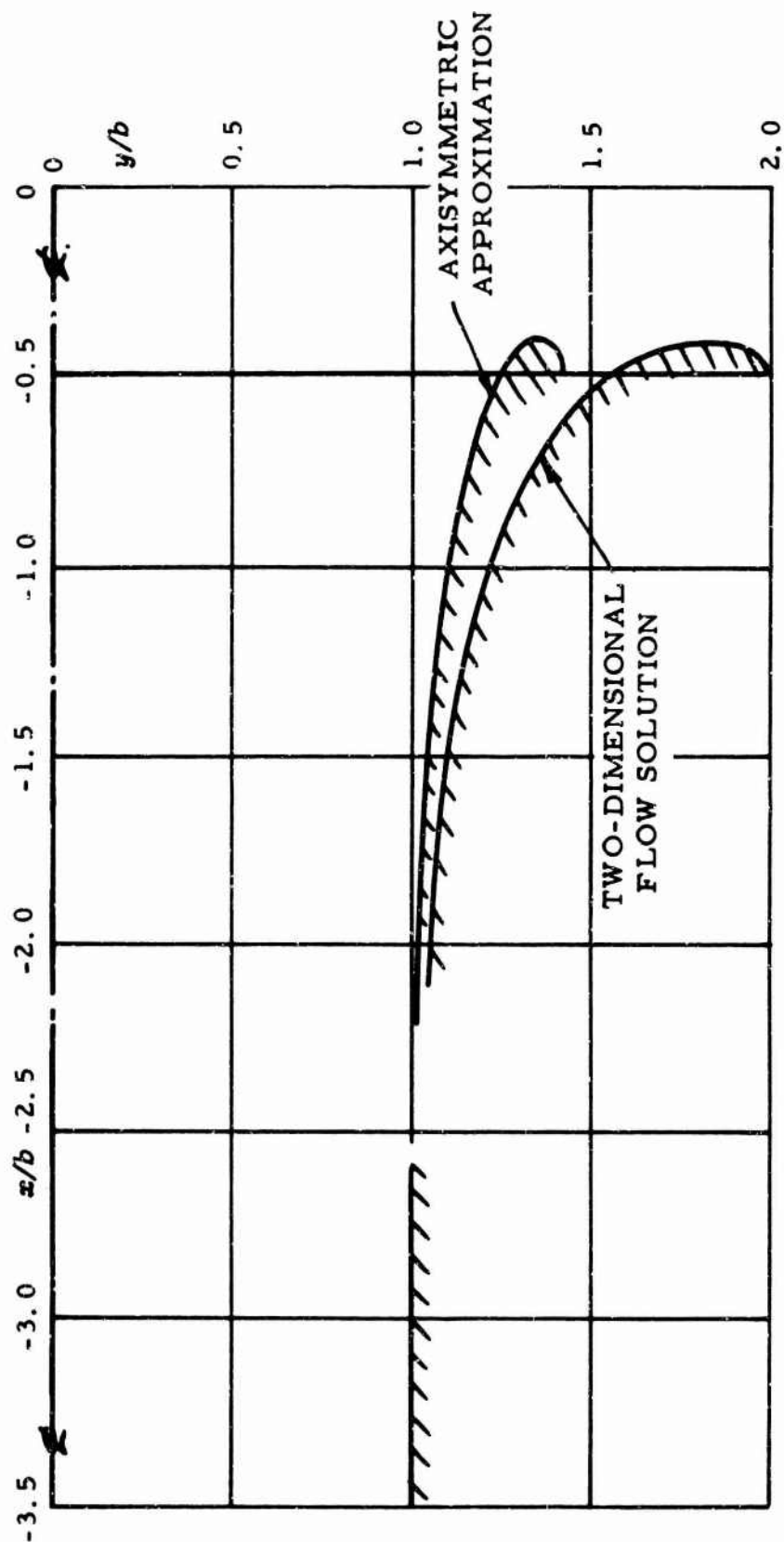
Figure 40. The Borda Mouthpiece Free Streamline Solution as an Intake Profile.

91

Table IV
THE "BORDA-MOUTHPIECE" SOLUTION

θ	x/b	y/b	$2-y/b$	$(2-y/b)^{\frac{1}{2}}$
20	0.0094	0.0022	1.9978	1.4140
40	0.0349	0.0175	1.9825	1.4070
60	0.0676	0.0579	1.9421	1.3930
80	0.0932	0.1312	1.8688	1.3670
100	0.0921	0.2420	1.7580	1.3250
120	0.0362	0.3910	1.6090	1.2680
140	-0.1210	0.5740	1.4260	1.1930
150	-0.2660	0.6750	1.3250	1.1500
160	-0.4970	0.7790	1.2210	1.1030
165	-0.6700	0.8340	1.1660	1.0800
170	-0.9200	0.8880	1.1120	1.0530
175	-1.3600	0.9430	1.0570	1.0285
180	$-\infty$	1.0000	1.0000	1.0000

THE MIXING CHAMBER WALL LOSS

A rough indication of the skin friction loss in the mixing chamber can be obtained by assuming that the secondary inlet velocity is applied over the entire surface. When the mixing section is properly designed for constant static pressure, this provides a reasonably accurate estimate, and we obtain

$$P_1 - P_m = \tfrac{1}{2}\rho\, u_1^2\, C_f\, (S_{WET}/A_m) \quad . \tag{153}$$

For the axisymmetric case, the theory developed in this report then gives

$$(P_1/P_m)/\tfrac{1}{2}\rho u_m^2 = C_f\, (x/d_m)\ \{(n+1)^2 n^2 (A_j/A_1)^2\}\ \left(8\,(\{A_1/A_m\}+1)\right)^{\frac{1}{2}} \tag{154}$$

$$/\ \left(1+n^2\, A_j/A_1\right)^2 ,$$

where x = the mixing chamber length

d_m = diameter of the diffuser throat .

Equation (154) is plotted in Figure 41. For a typical skin friction coefficient of 0.003, for example, and a mixing length ratio of x/d_m = 5.0, Figure 41 gives an equivalent diffuser loss of about 5 to 7 percent. Thus, the effective diffuser efficiency would only be about 93 to 95 percent, even if the diffuser itself were 100 percent efficient. Therefore, it is necessary to minimize the term C_f (x/d_m) as much as possible. C_f can be minimized by laminarization techniques designed to delay turbulent transition of the boundary layer as far downstream as possible. C_f may be minimized by using a multiplicity of primary nozzles. A circular mixing section is also desirable since it minimizes the wetted area.

THE DIFFUSER LOSS

The problem of minimizing diffuser loss has been studied exhaustively by many workers. A few references to this work are given in the bibliography; however, a detailed analysis of the problem would be inappropriate in this report. Figures 42 and 43 illustrate two unconventional ways of improving diffuser efficiency in the eductor application. They may be of value in indicating that the almost universally employed conventional configuration for eductors may not be optimum.
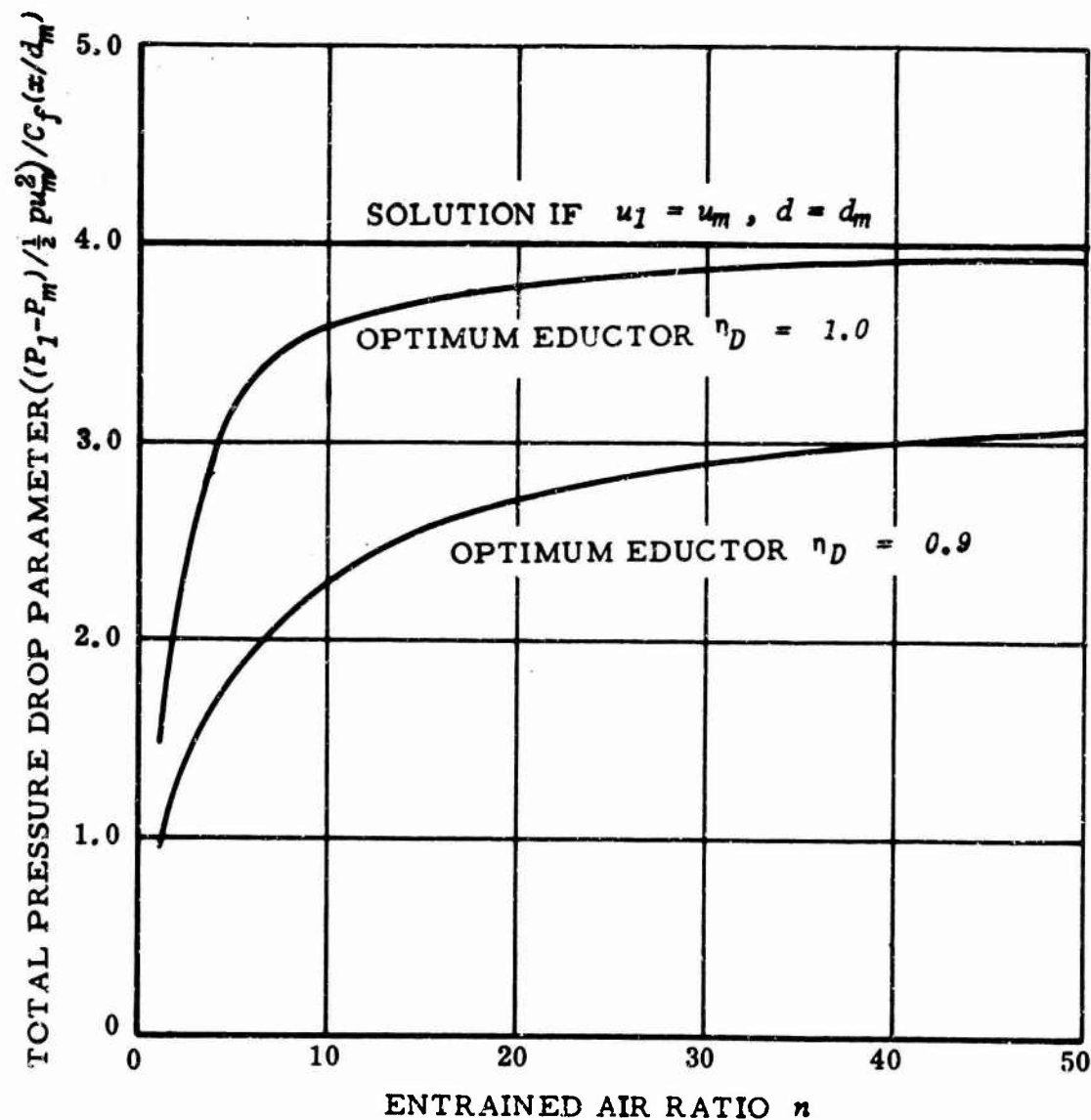
Figure 41. Effective Diffuser Loss Due to Skin Friction of Mixing Chamber Wall (Circular Section).
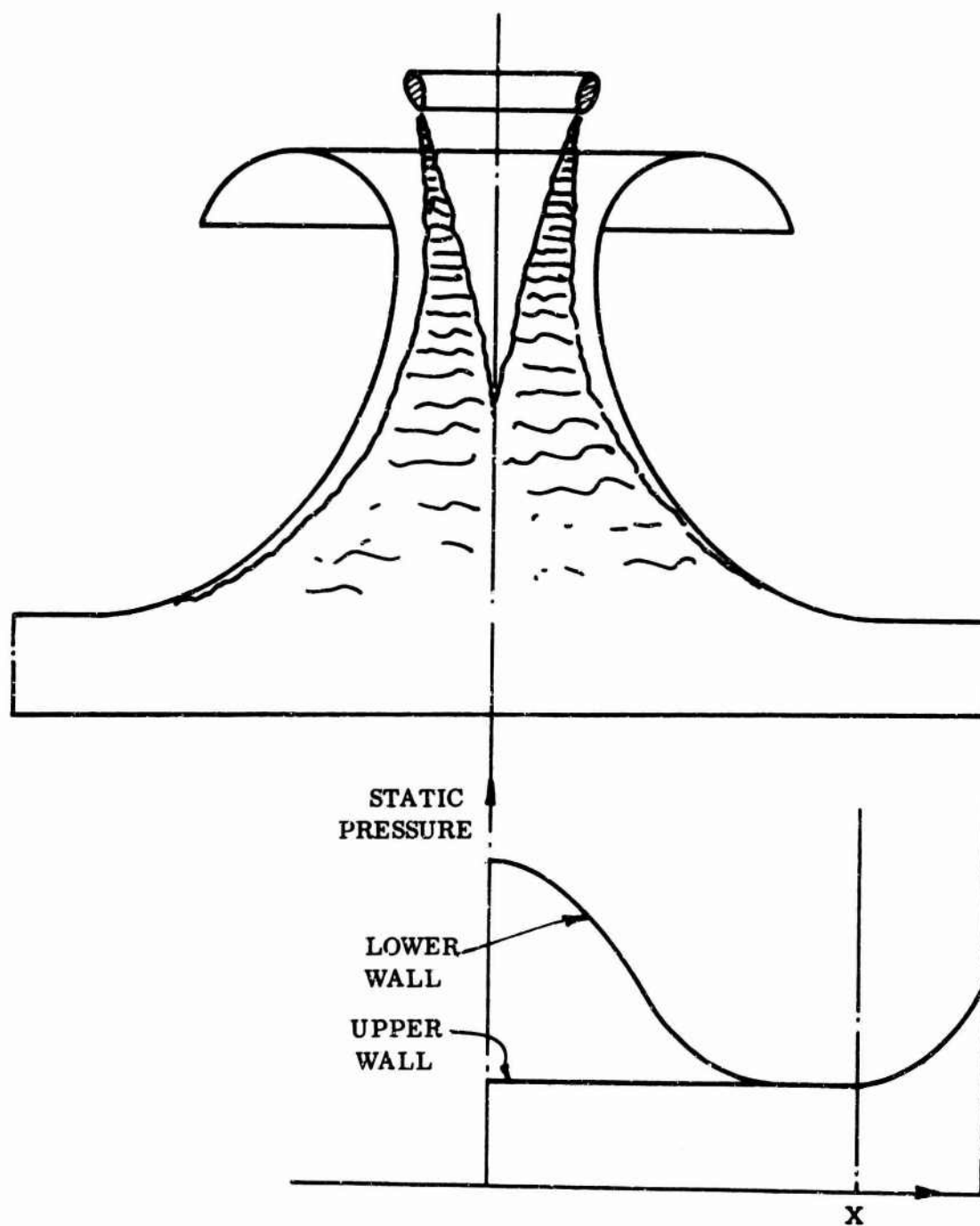
Figure 42.   Impinging Jet Diffuser With Mixing.

NOTE: Impinging jet diffuser has constant wall pressure during the
turn, so that mixing can continue efficiently in this region, so long as
it occurs near the wall.   The wall pressures are favorable to boundary
layer stability until final diffusion has commenced outboard of station X.

STATORS FOR
LARGE PRESSURE
RISES

BOUNDARY-LAYER
SUCTION AS AN AL-
TERNATIVE TO
STATORS
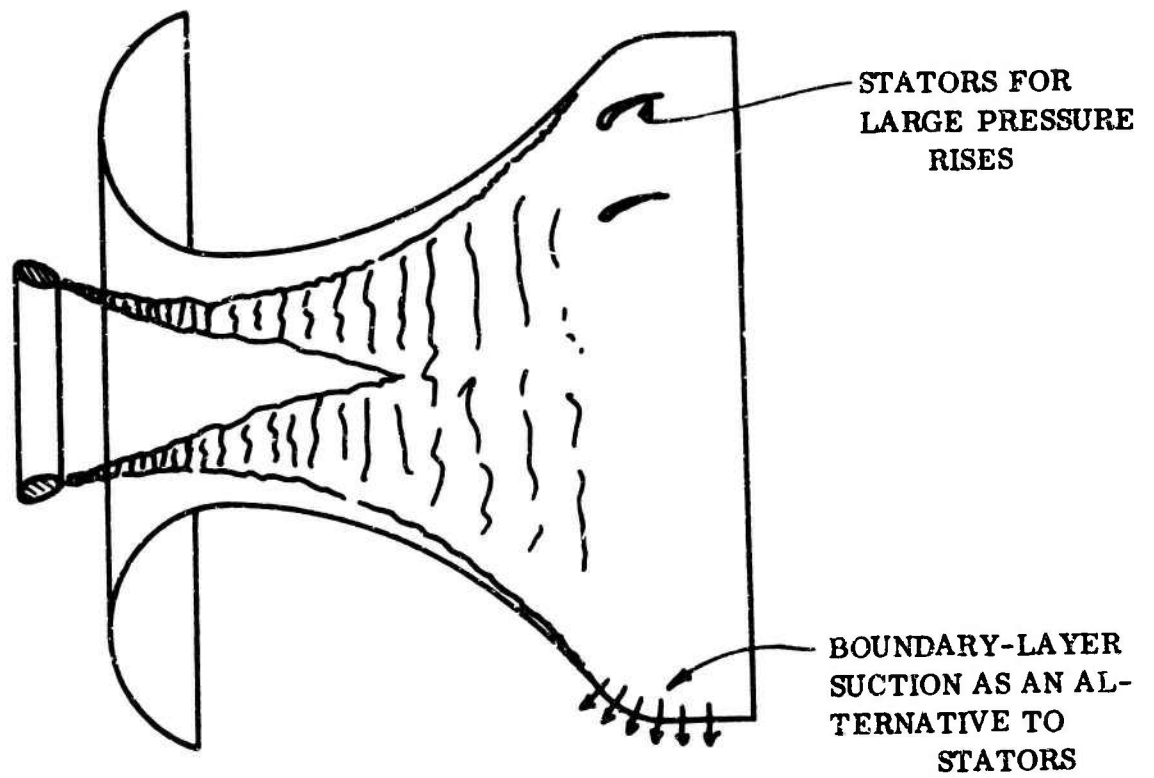
Figure 43.   Centrifugal Diffuser With Mixing.

NOTE: Centrifugal diffuser is designed for constant wall pressure, all the pressure rise occurring at the exit.   Hence, efficient mixing can take place in diffuser, provided it is close to the walls.

Chapter 10

SOME UNCONVENTIONAL EDUCTORS

MULTI-STAGE EDUCTORS

Figure 23 shows that eductor efficiency decreases as the entrainment ratio (n) increases for constant effective diffuser efficiency. Also, the optimum diffuser area ratio increases with (n), so that it is progressively more difficult to obtain satisfactory diffuser efficiency at the higher entrainment ratios needed to generate worthwhile augmentation ratios.

An obvious remedy is to divide an eductor into several "stages," the total efflux from each stage constituting the "primary" of the next, and larger, stage. This not only reduces the entrainment ratio per stage, but also reduces the diffuser area ratio requirement. The development of such a system has been associated chiefly with Melot and Bertin (Reference 17), although Morrison (Reference 2) has also reported some multi-stage experiments. As indicated in Table III and Figure 29, the multi-stage eductors tested have developed greater augmentation than the best single-stage units, as indeed should be expected from the considerations mentioned above.

It has been shown that even a single-stage eductor is far too complex a problem for "cut and try" engineering to be effective in obtaining high efficiency. Since multi-staging increases the number of variables by an order of magnitude, it is evident that the design of optimum staged eductors can only follow extensive theoretical analysis. However, the potential benefits, in terms of improved performance, are quite large. It underscores a requirement for initiation of appropriate research work in this area.

COANDA EDUCTORS

"Coanda flow" or "clinging flow" can occur when a fluid jet issues close to a solid surface. A typical example is illustrated in Figure 44.

Since the outside edge of the jet is at ambient static pressure throughout, the centrifugal forces generated around the curve must be balanced by a lower than ambient static pressure at the curved wall.
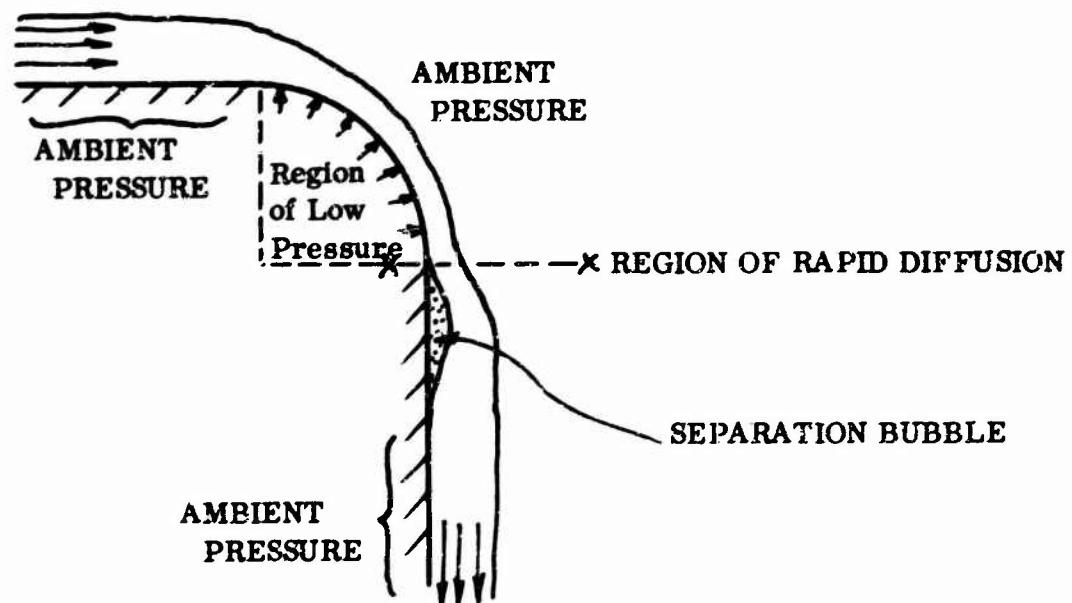
Figure 44. A Coanda Flow.

If the curve intersects with a tangential straight wall, then the sudden disappearance of the centrifugal forces in the flow must result in a sudden static pressure rise at the intersection. This effect is amenable to the rapid diffusion loss analysis mentioned earlier (Equation 149), and we find that quite large pressure losses are to be expected when the jet is thick. Coupled with the skin friction loss and the static pressure gradient across the jet, this diffusion loss explains why laboratory studies of the Coanda effect do not show any thrust augmentation effect, even though the inner portions of the jet entrains ambient air at a lower than ambient static pressure.

It has been shown that thrust augmentation occurs when a jet mixes with ambient air at a static pressure which is lower than ambient, and that there is an optimum static pressure for maximum augmentation; mixing at pressures away from this optimum results in less than the maximum possible augmentation.
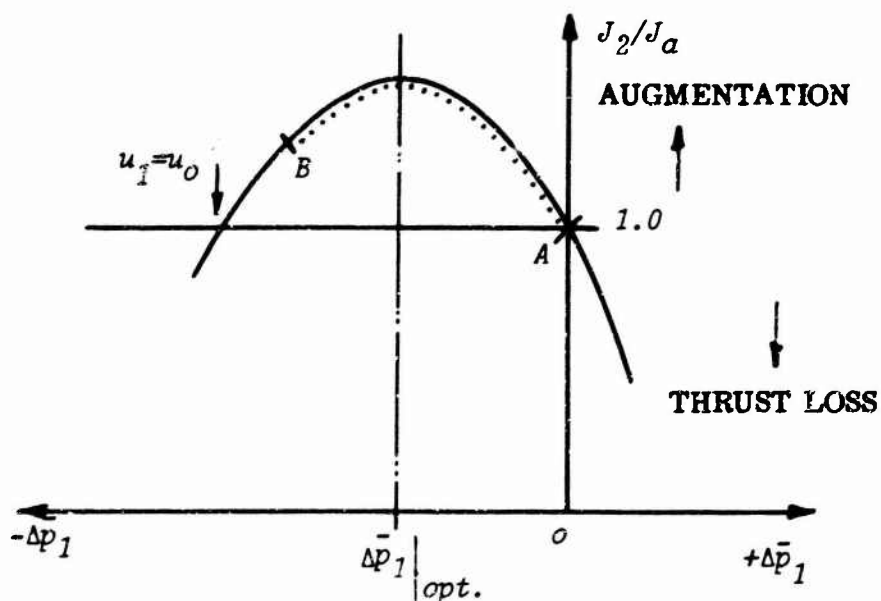
Figure 45. Variation of Augmentation Ratio J_2/J_a
With the Mixing Pressure Parameter $\Delta \bar{p}_1$.

In Coanda flow, the mixing pressure varies from ambient ($\Delta \bar{p}_1$ = 0, point A in Figure 45) at the outside of the jet to

$$\Delta \bar{p}_1 \bigg|_{WALL} = (-t/r_o)(2+t/r_o))/(1+t/r_o)^2 \tag{155}$$

at the wall (point B in Figure 45). Thus, the mixing pressure can be optimum at only one streamline, and thus the overall augmentation will be less than optimum.

The second factor determining augmentation is the efficiency at which the flow is diffused back to ambient from the mixing pressure Δp_1 .

It is obvious from Figure 18 that worthwhile thrust increases can be obtained only when the diffuser efficiency is high, 90 percent or greater. For relatively thick jets, the diffusion loss at the end of a Coanda curve can be quite large, with η_D as low as 0.5, so that high augmentation ratios can be obtained

99
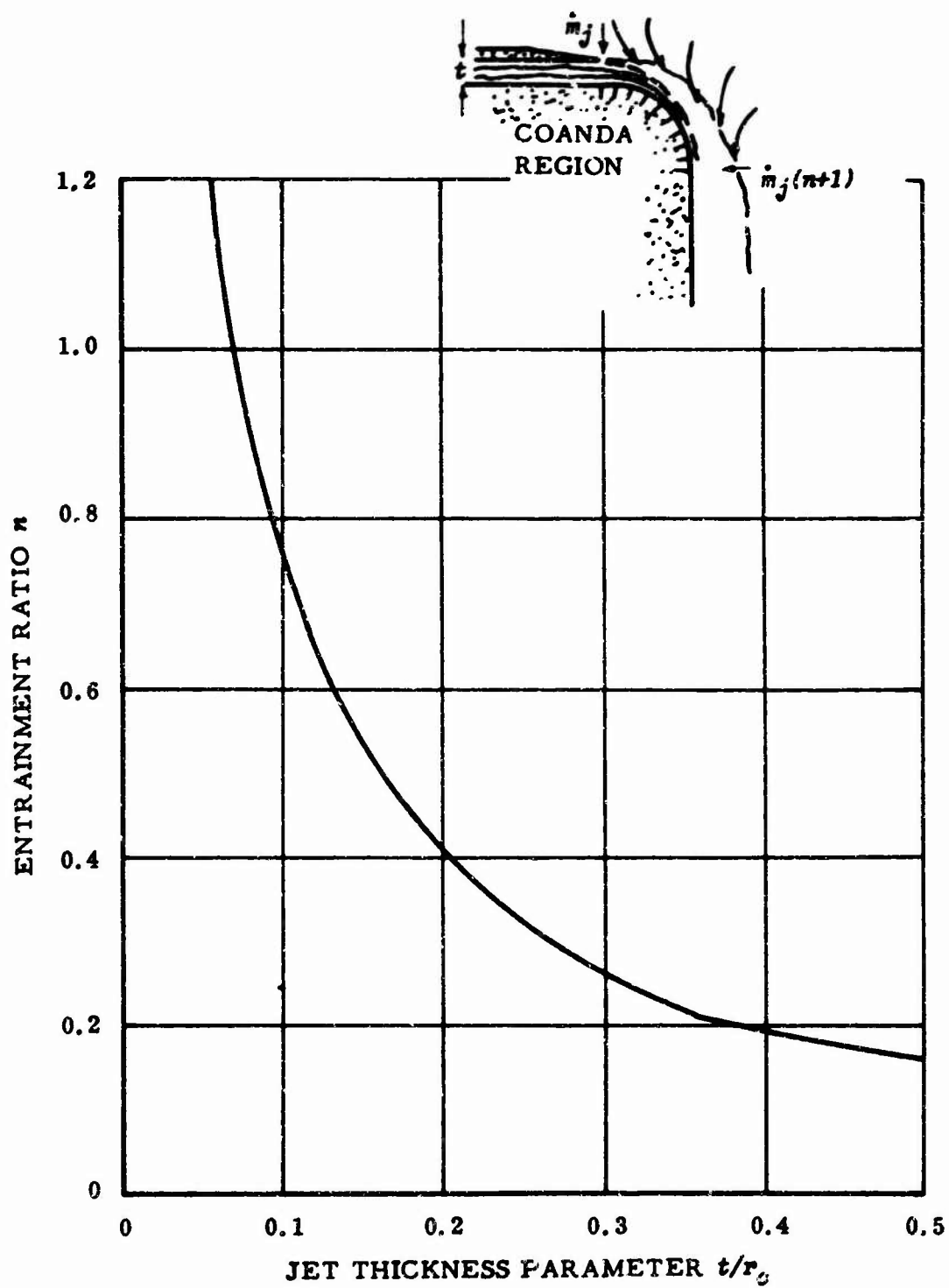
Figure 46.   Variation of Entrainment Ratio with Jet
Thickness for a Right-Angle Coanda Bend
(Based on Equation 58).

only by keeping the jet thin. However. the losses due to skin friction then become important.

The amount of ambient fluid entrained in the jet is another reason for using thin jets when augmentation is required. The attainable augmentation ratio naturally increases with the amount of fluid entrained and, as indicated in Figure 46, this becomes important only below t/r_o = 0.1. Very high entrainment ratios, therefore, require a jet thickness which is only a few percent of the radius of curvature; and in this case, boundary layer effects start to become important.

Although nothing can be done about Coanda mixing at nonoptimum pressures, we can avoid the efficiency loss due to diffusion, as indicated in Figure 47.

OTHER NOVEL EDUCTORS

Since a booster rocket operates mainly within the Earth's atmosphere, and is payload-limited by its static thrust, the possibility of air augmentation naturally arises. Work is proceeding on both static eductors for low speeds and "afterburning" with air at higher speeds, as indicated by Avery and Dugger in Reference 26.

Although this report is concerned with the traditional eductor concept involving steady-state viscous mixing between primary and secondary flows, it would be appropriate to notice a number of interesting new closely related developments in non-steady flow.

In addition to viscous shearing, a jet can be used to mechanically move the secondary fluid. By use of a pulsating jet, Lockwood and Patterson (References 14 and 22) have measured substantially higher augmentation ratios than those in steady-state operation. Conceptually, they generate a succession of "air pistons" which augments the effect of viscous shear in "driving" the secondary fluid along the eductor tube.

Foa (Reference 32) achieved an analogous effect by arranging for primary jets to issue from a rotating body, so that they describe a helical path, as illustrated in Figure 48. Thus, apart from the viscous mixing effects, the jet sheets tend to "mechanically" move the air as would a fan. In the words of Foa,

"Crypto-steady pressure exchange is a mode of direct energy transfer between flows, based on the principle that two adjacent streams which are both isoenergetic in the same frame of reference will, in general, exchange mechanical energy in any other frame. The efficiency of this process is potentially high,

ENTRAINED AIR

MIXING SECTION

DIFFUSER SECTION

SUPPLY DUCT

(RETRACTABLE) STATORS FOR LARGE PRESSURE-RISE DIFFUSERS. BOUNDARY-LAYER CONTROL BY SUCTION IS AN ALTERNATIVE.

STATIC PRESSURE

AMBIENT PRESSURE (p_a)

$p_w - p_a / \Delta P_j = -2(\delta/r_o)$

p_w

δ

WALL

EDGE OF JET

STATIC PRESSURE DISTRIBUTION ACROSS JET
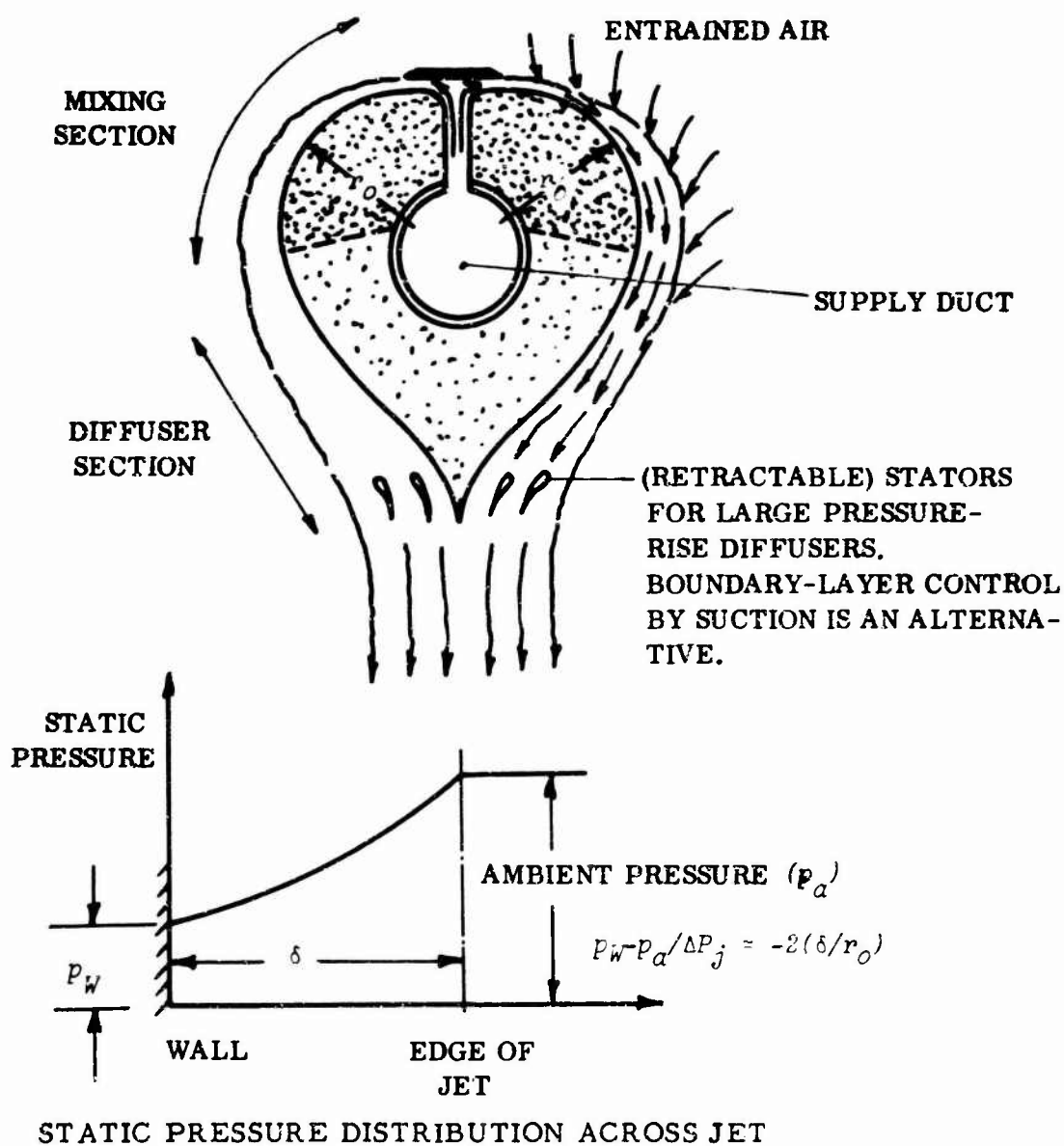
Figure 47.   A Coanda Thrust Augmentor.

NOTE: Due to the static pressure variation across the jet, the mixing pressure can be optimum at only one streamline. To offset this, diffusion losses can be half those for an equivalent (two-wall) diffuser. So far as is known, no Coanda devices so far tried has used a diffusion section, so that from eductor theory, we should not expect augmentation to be obtained.

102

(a) Path of Rotating Jets.

(b) Jets Rotating Through a Duct.
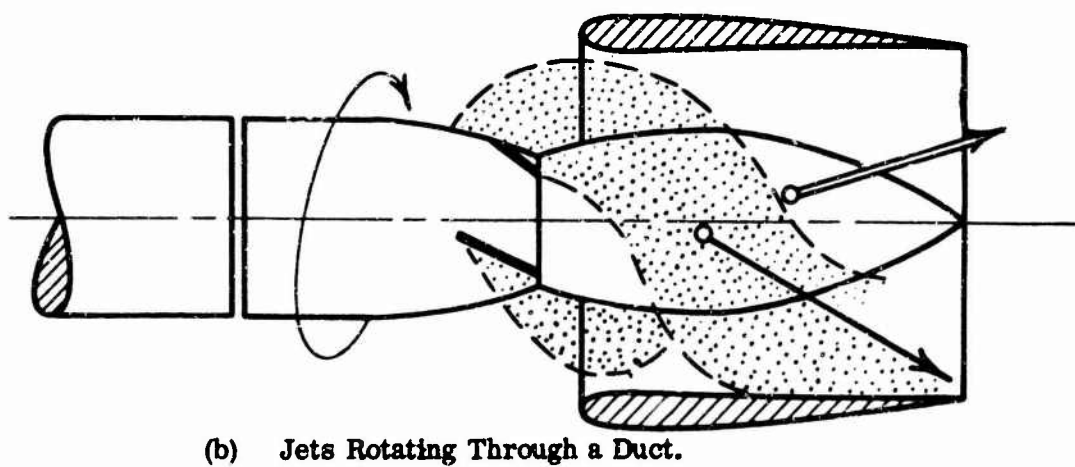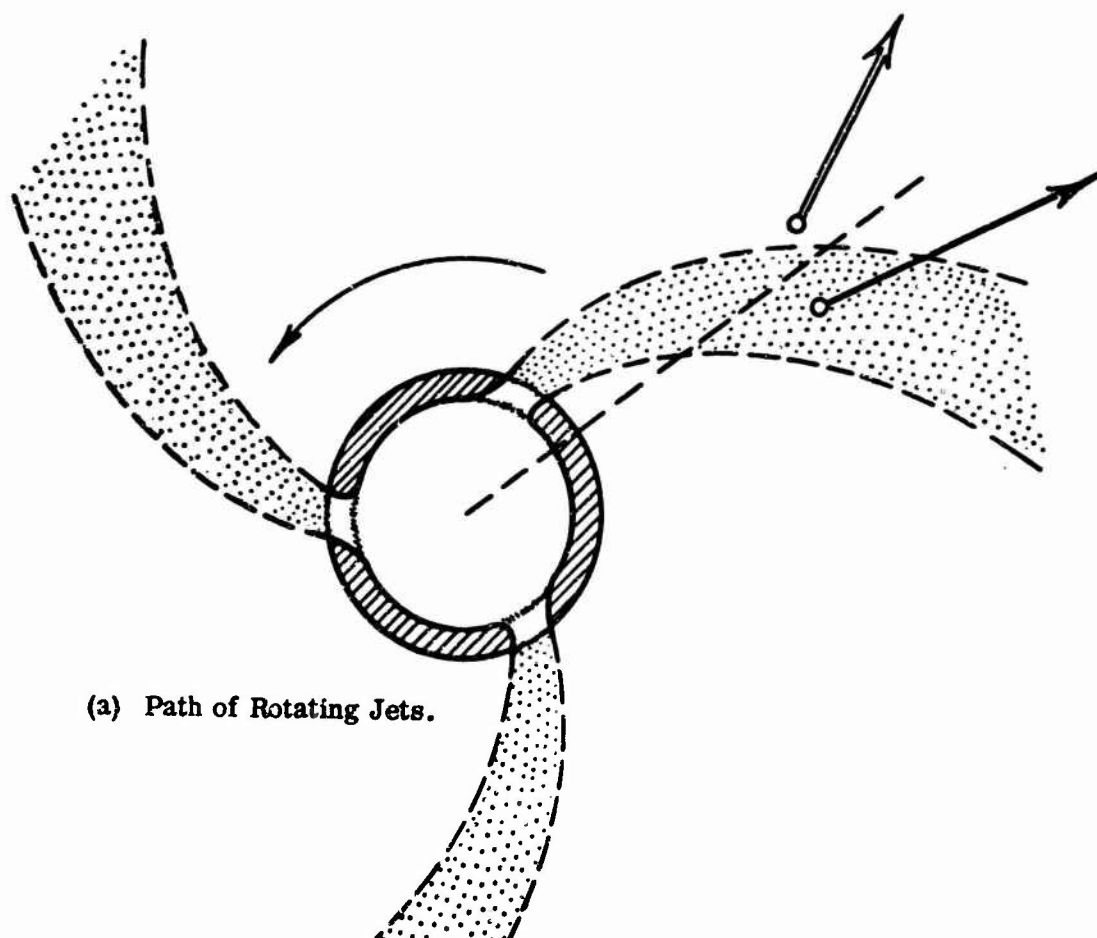
Figure 4C. Principle of the Foa Crypto-Steady Flow Eductor.

because a change of frame of reference is reversible, and the associated trans-
fer of energy is therefore nondissipative.

"An application of this principle to thrust or lift generation is discussed for the
purpose of illustration. In this application the interacting flows are steady and
isoenergetic in a rotating frame of reference but exchange energy in a stationary
frame. The exchange mechanism is essentially similar to that of a turbofan, but
the 'blades' are now patterns rather than bodies of abiding material. "

A system somewhere between those of Lockwood and Foa is the oscillating jet of
Saunders (Reference 33). Here the "mechanical" interaction between the jet and
the secondary fluid is similar to the propulsion obtained by a fish as it swims.
By using liquid amplifier techniques to oscillate the primary jet, Saunders avoids
the need for the moving mechanical parts required by the Foa system.

CONCLUSIONS

This report reviews the state of the art, so far as steady flow eductor technology is concerned, with particular reference to eductors which augment the thrust of a primary jet. Since the steady flow jet pump principle can be applied in a number of ways, and since non-steady flow systems are also of interest, the total field is much wider than that covered by this review.

So far as steady flow eductors are concerned, the following conclusions are drawn.

It seems clear from the review of the literature that a great deal of research work remains to be done before either adequate predictive ability is achieved or there is confidence in obtaining something near maximum efficiency.

It seems equally clear that hardware applications of the eductor principle have not profited to the extent made possible by existing research work, despite its limitations. Failure to profit from Helmbold's demonstration of the advantages of constant mixing pressure is a case in point.

The existing state of the art is given by

$$\frac{\text{Total Augmentor Thrust}}{\text{Primary Thrust}} = 0.995 + 0.565 \, log_{10} \, (A_2/A_j) \, ,$$

where A_2 and A_j are the eductor exit and primary jet areas respectively.

In the present report, a method of calculating eductor performance is presented and is shown to give good agreement with experiment. Significant improvements in eductor performance can therefore be expected from the application of this theory to the optimization of the new designs.

Multi-stage eductors have demonstrated significantly better performance loads than equivalent single-stage units. The existing state of the art is difficult to define, however, because of the relative porosity of experimental data. No theoretical analysis exists for the case of multi-stage units, so far as is known, although there would be no difficulty in extending the theory of the present report to this more complicated case.

BIBLIOGRAPHY

The following list of references is by no means intended as an exhaustive compilation, but is restricted to those publications with which the author is personally familiar. Nevertheless, that section of the bibliography dealing with eductors is believed to be fairly complete, since none of the earlier reports on the subject refer to other sources.

EDUCTORS

1.   Flugel, G., "The Design of Jet Pumps," NACA TM 982, July 1941.

2.   Morrison, Reaves, "Jet Ejectors and Augmentation," NACA Advanced Report, 1942.

3.   McClintock, Frank A., and Hood, J. Hall, "Aircraft Ejector Performance," Journal of the Aeronautical Sciences, Vol. 13, No. 1, November 1946.

4.   Huddleston, F. C., Wilsted, D. H., and Ellis, C. W., "Performance of Several Air Ejectors with Conical Mixing Sections and Small Secondary Flow Rates," NACA RM E8D23, 1948.

5.   Kennen, J. H., Neumann, E., P. and Lustwerk, F., "An Investigation of Ejector Design by Analysis and Experiment," MIT Guided Missiles Program, June 1948.

6.   Karman, Theodore von, "Theoretical Remarks on Thrust Augmentation," Reissner Anniversary Volume, 1949, page 461.

7.   Wagner, Friedrich, and McCune, Charles J., "A Progress Report on Jet Pump Research," Municiple University of Wichita Engineering Report No. 085, October 1952.

8.   Pai, S. I., "Fluid Dynamics of Jets," D. VanNostrand, New York, 1954.

9.   Helmbold, H. B., Luessen, G., and Heinrich, A. M., "An Experimental Comparison of Constant Pressure and Constant Diameter Jet Pumps," University of Wichita Engineering Report No. 147, July 1954.

10. Wood, R. D.. "Theoretical Ejector Performance in Comparison with Experimental Results," WADC TR 54-556, August 1954.

11. Payne, Peter R., "The Development of Ducted Rocket Power Unit Models," Proceedings of the First Model Aeronautics Conference, Royal Aeronautical Society, London, September 1954.

12. Szczeniowski, B. S., "Theory of the Jet Syphon," NACA TN 3385, 1955.

13. Helmbold, H. B., "Contributions to Jet Pump Theory," University of Wichita Engineering Report No. 294, September 1957.

14. Lockwood, R. M., "Investigation of the Process of Energy Transfer From an Intermittant Jet to an Ambient Fluid," Summary Report, Hiller Aircraft Corporation Report No. ARD-238, June 1959.

15. Wells, William Graham, "Theoretical and Experimental Investigation on a High Performance Jet Pump Utilizing Boundary Layer Control," Mississippi State University Research Report No. 30, June 1960.

16. Rabeneck, G. L., Shumpert, P. K., and Sutton, J. F., "Steady Flow Ejector Research Program," Lockheed Aircraft Corporation (Georgia Division) Final Report No. ER-470-8, December 1960.

17. Guienne, Paul, "Ejectors or the Ejector Wing, Applied to V/STOL Aircraft," Jahrbuch 1960 der Wissenschaftlichen Gesellschaft fuer Luftfahrt, September 1961.

18. Gates, M. F., and Fairbanks, J. W., "Summary Report - Phase III Program Annular Nozzle Ejector," Hiller Aircraft Corporation Report No. ADR-300, December 1961.

19. Recirculation Principles for Ground Effect Machines - Two-Dimensional Tests, USA TRECOM Technical Report 62-22, U. S. Army Transportation Research Command, Fort Eustis, Virginia, May 1962.

20. Reid, J., "The Effect of a Cylindrical Shroud on the Performance of a Stationary Convergent Nozzle," RAE Report Aero 2559, January 1962.

21. Hohenemser, K. H., "Preliminary Analysis of a New Type of Thrust Augmentor," Proceedings of the Fourth U. S. National Congress of Applied Mechanics, University of California, June 1962.

22. Lockwood, Raymond, and Patterson, W. G., "Interim Summary Report Covering the Period From 1 April 1961 to 30 June 1962 on Investigation of the Process of Energy Transfer from an Intermittent Jet to Secondary Fluid in an Ejector-Type Thrust Augmentor," Hiller Aircraft Company Report No. ADR-305, June 1962.

23. Recirculation Principle for Ground Effect Machine Two-Dimensional Tests, USA TRECOM Technical Report 62-66, U. S. Army Transportation Research Command, Fort Eustis, Virginia, June 1962.

24. Portnov, J. G. and Zotov, G. A., "Consecutive Operation of Gas Ejectors Under Steady-State Conditions," Air Force Systems Command, Foreign Technology Division FTD-TT-63-184, April 1963.

25. Payne, Peter R., "A Contribution to the Theory of Thrust (Momentum) Augmentors," Frost Engineering Report No. 197-2, August 1963.

26. Avery, William H., and Dugger, Gordon L., "Hypersonic Airbreathing Propulsion," Astronautics and Aeronautics, June 1964.

27. Payne, Peter R., and Anthony, Alastair, "Tests of Three Axisymmetric Model Eductors," Peter R. Payne Associates Report No. 57, November 1964.

28. Payne, Peter R., "Viscous Mixing Phenomena with Particular Reference to Thrust Augmentors," AIAA Paper No. 64-798, October 1964.

29. Wan, Chia-an, "A Study of Jet Ejector Phenomena," Mississippi State University Research Report No. 57, November 1964.

30. Payne, Peter R., and Anthony, Alastair, "An Exploratory Investigation of Mixing Losses in a Two-Dimensional Propulsive Jet," Payne, Inc. Working Paper No. 25-27, June 1965.

31. Vennos, S. L. N., "Experiments with Water-Water Bladeless Propellers," Summary Report No. TR AE 6106, Department of Aeronautical Engineering, Rensselaer Polytechnic Institute, May 1961.

32. Foa, J. V., "Crypto-Steady Pressure Exchange," Department of Aeronautical Engineering and Astronautics Report No. TR AE 6202, Rensselaer Polytechnic Institute, March 1962.

33. Saunders, W. A., "Beating Jet-Wing Aircraft," U. S. Patent 3,168,997, February 1965.

JET MIXING PHENOMENA

34. Forthmann, E., "Turbulent Jet Expansion," NACA TM 789, March 1936.

35. Tollmein, Walter, "Calculation of Turbulent Expansion Processes," NACA TM 1085, September 1945.

36. Liepmann, Hans Wolfgang, and Laufer, John, "Investigations of Free Turbulent Mixing," NACA TN 1257, August 1947.

37. Albertson, M. L., Dai, Y. B., Jensen, R. A., and Rouse, Hunter, "Diffusion of Submerged Jets," Transactions of the American Society of Civil Engineers, Vol. 115, 1950.

38. Helmbold, H. B., "Energy Transfer by Turbulent Mixing Under a Longitudinal Pressure Gradient," The Municipal University of Wichita Engineering Study 182, August 1955.

39. Rouse, Hunter, "Development of the Non-Circulatory Waterspout," Journal of the Hydraulics Division, Proceedings of the American Society of Civil Engineers, August 1956.

40. Schlichting, H., "Boundary Layer Theory," McGraw Hill, New York, 1960.

41. Davies, P.O.A.L., Barratt, M. J., and Fisher, M. J., "Turbulence in the Mixing Region of a Round Jet," Aeronautical Research Council, April, 1962.

42. Bhuta, P. G., and Page, R. H., Nonsteady Two-Dimensional Laminar and Turbulent Jet Mixing Theory," Proceedings of the Fourth U. S. National Congress of Applied Mechanics, University of California, June 1962.

43. General Dynamics/Convair, "Research on Coaxial Jet Mixing," November 1962.

44. Yakovlevskiy, O. V., "The Mixing of Jets in a Channel with Variable Cross-Section," Translation Services Branch, Foreign Technology Division, WP-AFB, Ohio, FTD-TT-62-1571, January 1963.

45. Faris, George Naim, "Some Entrainment Properties of a Turbulent Axi-Symmetric Jet," Aerophysics Mississippi State University Research Report No. 39, January 1963.

46. Heskestad, Gunnar, "Two Turbulent Shear Flows - I. A Plane Jet - II. A Radial Jet," Air Force Office of Scientific Research, Johns Hopkins University, June 1963.

47. Kruka, V., and Eskinazi, S., "The Wall-Jet in a Moving Stream," Syracuse University Research Institute, August 1963.

48. Ferri, Antonio, "Axially Symmetric Heterogeneous Mixing, rce Office of Scientific Research Report No. 5326, September 1963.

49. Mellor, G. L., "The Effects of Pressure Gradients on Turbulent Flow Near a Smooth Wall, "Department of Aerospace and Mechanical Sciences, Princeton University, January 1964.

50. Halleen, R. M., "A Literature Review on Subsonic Free Turbulent Shear Flow," Stanford University Report MD-11, April 1964.

51. Viscous Mixing of Two-Dimensional Jets with Particular Reference to Jets in Ground Proximity, USA TRECOM Technical Report 64-11, U. S. Army Transportation Research Command, Fort Eustis, Virginia, April 1964.

52. Zakkay, Victor, Krause, Egon, and Woo, Stephen D. L., "Turbulent Transport Properties for Axisymmetric Heterogeneous Mixing," Air Force Office of Scientific Research Report ARL 64-103, June, 1964.

53. Foss, J. F., and Jones, J. B., "A Study of Incompressible Turbulent Bounded Jets," Purdue Research Foundation, October 1964.

54. Timma, E., "Analytic Investigation of Turbulent Flat Jet, Developing in a Co-Stream," Translation Division, Foreign Technology Division, WP-AFB, Ohio, November 1964.

55. Chu, W. T., "Velocity Profile in the Half-Jet Mixing Region of Turbulent Jets," AIAA Journal, Vol. 3, No. 4, April 1965.

56. Hill, Philip G., "Turbulent Jets in Ducted Streams," Journal of Fluid Mechanics, Vol. 22, Part 1, 1965.

CONVENTIONAL CONICAL AND WEDGE DIFFUSERS

57. Gibson, A. H., "On the Flow of Water Through Pipes and Passages Having Converging or Diverging Boundaries," Proceedings of the Royal Society, Vol. A83, No. 563, 1910.

58. Patterson, G. N., "Modern Diffuser Design," Aircraft Engineering, Vol. 10, 1938.

59. Nikuradse, J., "Untersuchungen uber die Stromung des Wassers in Konvergenten und divergenten Kanalen," Ver. Deut. Ing. (Forschungsarb.) 289, 19, 20, 1939.

60. Copp, Martin R., "Effects of Inlet Wall Contour on the Pressure Recovery of a 10° 10-Inch-Inlet Diameter Conical Diffuser," NACA RM L51E11a, 1951.

61. Reid, Elliott G., "Performance Characteristics of Plane-Wall Two-Dimensional Diffusers," NACA TN 2888, February 1953.

62. Squire, H. B., "Experiments on Conical Diffusers," R and M 2751, Aeronautical Research Council, 1953.

63. Henry, John R., Wood, Charles C., and Wilbur, Stafford W., "Summany of Subsonic-Diffuser Data," NACA RM L56F05, October 1958.

64. Lieblein, S., "Loss and Stall Analysis of Compressor Cascades," Transactions of A.S.M.E., Journal of Basic Engineering, Series D, Vol. 81, No. 3, September 1959.

65. Paull, J. W., "Identification of Two Types of Separation," AIAA Journal, Vol. 2, No. 12, December 1964.

66. Goldschmied, Fabio R., "An Approach to Turbulent Incompressible Separation and the Determination of Skin-Friction Under Adverse Pressure Gradients," AIAA Journal of Aircraft, Vol. 2, No. 2, March-April 1965.

67. Payne, Peter R., "Some Aspects of Diffusion," Payne, Inc. Working Paper No. 25-28, June 1965 (To be published).

UNCONVENTIONAL DIFFUSERS

68. Migay, V. K., "Diffusers with Transverse Fins," AID Report T-63-8, January 1963.

69. Moiler, Paul S., "An Investigation of a Radial Diffuser Using Incompressible Flow Without Swirl," Report No. 63-9, McGill University, July 1963.

70. Migay, V. K., "The Aerodynamic Effectiveness of a Discontinuous Surface," WP-AFB Report No. FTD-MT-63-237, April 1964.

71. Polotsky, N. D., "Energy Characteristics of Curvi-Axial Diffusers," WP-AFB Report No. FTD-TT-64-711.

BELLMOUTH INTAKES

72. Blackaby, James R., and Watson, Earl C., "An Experimental Investigation at Low Speeds of the Effects of Lip Shape on the Drag and Pressure Recovery of a Nose Inlet in a Body of Revolution," NACA TN 3170, April 1954.

73. Claybourn, Henry Marshall, Sr., "Study of a Shrouded Propeller with Distributed Suction on the Inlet Profile," ONR Report No. 20, January 1959.

COANDA EFFECT

74. Coanda, Professor Henri, "Final Report of Contract No. AF 61 (514) 1409 between A. R. D. C. Brussels and SFERI-COANDA," Clichy (France), June 1957.

75. Glahn, Uwe H. von, "Use of the Coanda Effect for Obtaining Jet Deflection and Lift with a Single Flat-Plate Deflection Surface," NACA TN 4272, June 1958.

76. Bailey, A. B., and Roderick, W. E. B., "Use of the Coanda Effect for the Deflection of Jet Sheets Over Smoothly Curved Surfaces," Part I - Test Rig and Some Tests with Subsonic, Choked, and Overchoked Jet Sheets, Part II - Some Tests with Supersonic, Over and Under Expanded Jet Sheets, Part III - Application to the Lenticular Aerodyne, Institute of Aerophysics, University of Toronto, August - September 1961.

77. Korbacher, Dr. G. K., "The Coanda Effect at Deflection Surfaces Detached From the Jet Nozzle," Canadian Aeronautics and Space Journal, Vol. 8, No. 1, January 1962.

78. Investigation of Ventilated Clinging Flow Phenomenon, USA TRECOM Technical Report 63-38, U. S. Army Transportation Research Command, Fort Eustis, Virginia, August 1963.

79. Hope-Gill, C. D., "An Experimental Investigation into the Shape of Thrust Augmenting Surfaces in Conjunction with Coanda-Deflected Jet Sheets (Part I)," Institute for Aerospace Studies, University of Toronto, UTIAS Technical Note No. 70, July 1964.

80. Boyer, Luther J., "Preliminary Investigation and Evaluation of the Coanda Effect," Air Force Air Materiel Command, Technical Report No. F-TR-2207-ND, August 1964.

81. The Coanda Effect at Deflection Surfaces Widely Separated From the Jet Nozzle, USA TRECOM Technical Report 64-70, U. S. Army Transportation Research Command, Fort Eustis, Virginia, December 1964.

82. Mehus, T., "An Experimental Investigation into the Shape of Thrust Augmenting Surfaces in Conjunction with Coanda-Deflected Jet Sheets (Part II)," Institute for Aerospace Studies, University of Toronto, UTIAS Technical Note No. 79, January 1965.

GENERAL

83. Kuchemann, Deitrich, and Weber, Johanna, "Aerodynamics of Propulsion," McGraw Hill, London, 1953.

84. Viscous Mixing of Two-Dimensional Jets With Particular Reference to Jets in Ground Proximity, USA TRECOM Technical Report 64-11, U. S. Army Transportation Research Command, Fort Eustis, Virginia, April 1964.

85. Lamb, Sir Horace, "Hydrodynamics," Dover Publications, 1932.

DOCUMENT CONTROL DATA - R&D		
(Security classification of title, body of abstract and indexing annotation must be entered when the overall report is classified)		

1. ORIGINATING ACTIVITY (Corporate author) Peter R. Payne, Inc. 12221 Parklawn Drive Rockville, Maryland 20852	2a. REPORT SECURITY CLASSIFICATION Unclassified
	2b. GROUP

3. REPORT TITLE

"STEADY-STATE THRUST AUGMENTORS AND JET PUMPS"

4. DESCRIPTIVE NOTES (Type of report and inclusive dates)

Final Report   June 1965 – February 1966

5. AUTHOR(S) (Last name, first name, initial)

PAYNE, Peter R.

6. REPORT DATE March 1966	7a. TOTAL NO. OF PAGES 115	7b. NO. OF REFS 85
9a. CONTRACT OR GRANT NO. DA 44-177-AMC-337(T) b. PROJECT NO. c. Task No. 1P125901A01409 d.	9a. ORIGINATOR'S REPORT NUMBER(S) USAAVLABS Technical Report 66-18	
	9b. OTHER REPORT NO(S) (Any other numbers that may be assigned this report)	

10. AVAILABILITY/LIMITATION NOTICES

Distribution of this document is unlimited.

11. SUPPLEMENTARY NOTES	12. SPONSORING MILITARY ACTIVITY Department of the Army U.S. Army Aviation Materiel Laboratories Fort Eustis, Virginia

13. ABSTRACT

The state of the art in steady-state augmentors and jet pumps is briefly reviewed and a general performance theory developed. Generalized charts are presented giving the augmentation ratio obtainable from an optimized eductor, together with the associated geometrical and fluid-dynamic parameters. This theory is shown to give good agreement with experiment. Experimental measurements made by various investigators in the past do not achieve the predicted optimum performance, however, because of various deviations from optimum design in their test eductors.

The performance of eductors in an axial stream and the total head rise obtainable through an eductor are both investigated theoretically. The report concludes with a brief survey of various unconventional eductors, including multi-stage units, Coanda eductors and crypto-steady flow devices.

DD FORM JAN 64 **1473**

14. KEY WORDS	LINK A		LINK B		LINK C	
	ROLE	WT	ROLE	WT	ROLE	WT

INSTRUCTIONS

1. ORIGINATING ACTIVITY: Enter the name and address of the contractor, subcontractor, grantee, Department of Defense activity or other organization (corporate author) issuing the report.

2a. REPORT SECURITY CLASSIFICATION: Enter the overall security classification of the report. Indicate whether "Restricted Data" is included. Marking is to be in accordance with appropriate security regulations.

2b. GROUP: Automatic downgrading is specified in DoD Directive 5200.10 and Armed Forces Industrial Manual. Enter the group number. Also, when applicable, show that optional markings have been used for Group 3 and Group 4 as authorized.

3. REPORT TITLE: Enter the complete report title in all capital letters. Titles in all cases should be unclassified. If a meaningful title cannot be selected without classification, show title classification in all capitals in parenthesis immediately following the title.

4. DESCRIPTIVE NOTES: If appropriate, enter the type of report, e.g., interim, progress, summary, annual, or final. Give the inclusive dates when a specific reporting period is covered.

5. AUTHOR(S): Enter the name(s) of author(s) as shown on or in the report. Enter last name, first name, middle initial. If military, show rank and branch of service. The name of the principal author is an absolute minimum requirement.

6. REPORT DATE: Enter the date of the report as day, month, year; or month, year. If more than one date appears on the report, use date of publication.

7a. TOTAL NUMBER OF PAGES: The total page count should follow normal pagination procedures, i.e., enter the number of pages containing information.

7b. NUMBER OF REFERENCES: Enter the total number of references cited in the report.

8a. CONTRACT OR GRANT NUMBER: If appropriate, enter the applicable number of the contract or grant under which the report was written.

8b, 8c, & 8d. PROJECT NUMBER: Enter the appropriate military department identification, such as project number, subproject number, system numbers, task number, etc.

9a. ORIGINATOR'S REPORT NUMBER(S): Enter the official report number by which the document will be identified and controlled by the originating activity. This number must be unique to this report.

9b. OTHER REPORT NUMBER(S): If the report has been assigned any other report numbers (either by the originator or by the sponsor), also enter this number(s).

10. AVAILABILITY/LIMITATION NOTICES: Enter any limitations on further dissemination of the report, other than those imposed by security classification, using standard statements such as:

   (1) "Qualified requesters may obtain copies of this report from DDC."

   (2) "Foreign announcement and dissemination of this report by DDC is not authorized."

   (3) "U. S. Government agencies may obtain copies of this report directly from DDC. Other qualified DDC users shall request through
   _____."

   (4) "U. S. military agencies may obtain copies of this report directly from DDC. Other qualified users shall request through
   _____."

   (5) "All distribution of this report is controlled. Qualified DDC users shall request through
   _____."

If the report has been furnished to the Office of Technical Services, Department of Commerce, for sale to the public, indicate this fact and enter the price, if known.

11. SUPPLEMENTARY NOTES: Use for additional explanatory notes.

12. SPONSORING MILITARY ACTIVITY: Enter the name of the departmental project office or laboratory sponsoring (paying for) the research and development. Include address.

13. ABSTRACT: Enter an abstract giving a brief and factual summary of the document indicative of the report, even though it may also appear elsewhere in the body of the technical report. If additional space is required, a continuation sheet shall be attached.

It is highly desirable that the abstract of classified reports be unclassified. Each paragraph of the abstract shall end with an indication of the military security classification of the information in the paragraph, represented as (TS), (S), (C), or (U).

There is no limitation on the length of the abstract. However, the suggested length is from 150 to 225 words.

14. KEY WORDS: Key words are technically meaningful terms or short phrases that characterize a report and may be used as index entries for cataloging the report. Key words must be selected so that no security classification is required. Identifiers, such as equipment model designation, trade name, military project code name, geographic location, may be used as key words but will be followed by an indication of technical context. The assignment of links, rules, and weights is optional.